European Commission | Horizon 2020 European Union funding for Research & Innovation

Optimization tools and first applications in simulated environments

D 6.5

EU-SysFlex

This project has received funding from the European Union's Horizon 2020 research and innovation programme under grant agreement No 773505.

PROGRAMME	H2020 COMPETITIVE LOW CARBON ENERGY 2017-2-SMART-GRIDS
GRANT AGREEMENT NUMBER	773505
PROJECT ACRONYM	EU-SYSFLEX
DOCUMENT	**D 6.5**
TYPE (DISTRIBUTION LEVEL)	☒ Public ☐ Confidential ☐ Restricted
DATE OF DELIVERY	25.10.2019
STATUS AND VERSION	1.0
NUMBER OF PAGES	115
Work Package / TASK RELATED	WP6 Task 6.3
Work Package / TASK RESPONSIBLE	Carmen Calpe, innogy /Sebastian Wende – von Berg, IEE
AUTHOR (S)	Lothar Löwer – Fraunhofer IEE Sebastian Wende-von Berg – Fraunhofer IEE/ Uni-Kassel "e2n" Wiebke Albers, Carmen Calpe – innogy Maik Staudt – MITNETZ STROM Zhenqi Wang – Uni-Kassel "e2n" Carla Marino, Alessio Pastore – e-distribuzione Daniele Clerici, Giacomo Viganò – RSE Suvi Takala, Antti Hyttinen – Helen Pirjo Heine – Helen Electricity Network João Vieira Silva, Bernardo Silva – Inesctec Corentin Evens, Poria Divshali – VTT

DOCUMENT HISTORY

VERS	ISSUE DATE	CONTENT AND CHANGES
0.1	14/06/2019	First draft version
0.2	04/09/2019/	Second draft version
0.3	17/10/2019	Third draft version
0.4	25/10/2019	Fourth draft version
1.0	12/11/2019	Final document

DOCUMENT APPROVERS

PARTNER	APPROVER
innogy	Carmen Calpe/ WP leader
EDF	Marie-Ann Evans / Project Technical Manager
EIRGRID	John Lowry / Project Coordinator, with PMB review

TABLE OF CONTENTS

LIST OF FIGURES

LIST OF TABLES

ABBREVIATIONS AND ACRONYMS

AMR	Automatic Meter Reading
BESS	Battery Energy Storage System
BUC	Business Use Cases
CDF	Cumulative Density Function
D	Deliverable
DER	Distributed Energy Resource
DSO	Distribution System Operator
EC	European Commission
EPSO	Evolutionary Particle Swarm Optimization
EU-SYSFLEX	Pan-European System with an efficient coordinated use of flexibilities for the integration of a large share of Renewable Energy Sources (RES)
EHV	Extra High Voltage (e.g. 380 kV)
EV	Electric Vehicles
EVCS	Electric Vehicle Charging Stations
FCR-D	Frequency Containment Reserves for Disturbances
FCR-N	Frequency Containment Reserves for Normal operation
HV	High Voltage (e.g. 110 kV)
IED	Intelligent Electronic Devices
LV	Low Voltage (e.g. 0.4 kV)
MINLP	Mixed Integer Non-Linear Programming
MO	Management Office
NCAS	Network Calculation Algorithm System
MV	Medium Voltage (e.g. 20 kV)
NG	Network Group
OLTC	On-Load Tap Changer
OPF	Optimal Power Flow
P	Active Power
PDF	Probability Density Function
PMB	Project Management Board
PV	Photovoltaic
Q	Reactive Power
RES	Renewable Energy Sources
SoC	State of Charge
STATCOM	Static Synchronous Compensators
SUC	System Use Cases
TM	Technical Manager
TSO	Transmission System Operator
WP	Work Package

EXECUTIVE SUMMARY

The EU-SysFlex H2020 project aims at a large-scale deployment of solutions, including technical options, system control and a novel market design to integrate a large share of renewable electricity, maintaining the security and reliability of the European power system. The project results will contribute to enhance system flexibility, resorting to both existing assets and new technologies in an integrated manner, based on seven European large scale demonstrators. Three of these demonstrators, which are in the focus of this report, have the overall objective of analyzing and demonstrating the exploitation of decentralized flexibility resources connected to the distribution grid for system services provision to the TSOs, by the means of three physical demonstrators located in Germany, Italy and Finland, using different assets located at complementary voltage levels (high, medium and low voltage) of the distribution grid. These demonstrations showcase innovative approaches in flexibility management targeted to support transmission system operators' (TSO) and distribution system operators' (DSO) needs and their related services, identified within the EU-SysFlex H2020 funded project. These approaches are followed by the means of suitable system processes, which have been described beforehand in terms of System Use Cases (SUC) that are related to previously described Business Use Cases (BUC). The functionalities identified within the SUC modelling have been mapped into four main software tools groups, namely communication tools, forecast tools, simulation tools and optimization tools. These tools are described in four corresponding deliverables[1]: this deliverable, D6.5 "Optimization Tools and First Applications in Simulated Environments" is a part of this set and addresses the optimization tools and preliminary tests of demonstrators set-ups carried out with these tools.

Optimization can be interpreted in a general way, as finding the best fitting solution for a given problem. Due to the rising number of renewable generating units, which are mainly connected to the distribution grids and hence are not at central positions from a grid perspective, the complexity of the electric energy system is increasing extensively. Current control strategies of such units do not take into account the large and increasing number of distributed generating sources in an optimal way for the system. The units are still predominantly operated using a fixed operation mode disregarding the available feed-in flexibilities of such generating units. However, these units could also be used to provide several valuable services to the system operators, DSO as well as TSO.

Therefore, one goal is to provide new tools to support the system operators calculating the flexibility of those fluctuating units relating their active and reactive power generation at a single or several grid connection points between DSO and TSO and taking several individual boundaries into account in order to enable ancillary services provision to the TSO, which have to comply with the requirements of both: DSO and TSO. Additional tools have

[1] D6.2: Forecaset: Data, Methods and Processing. A common description
D6.3: Grid simulations and simulation tools. Preliminary results
D6.4: General description of processes and data transfer within three EU-SysFlex demonstrators
D6.5: Optimization Tools and First Applications in Simulated Environments

been developed within the Finish demonstrator, which focus on assisting an aggregator in determining correct bidding times and size of the bids to TSO ancillary markets for reserves and balancing power.

From the preliminary simulated results of the different optimization approaches in three different voltage levels we can conclude, that there is a large potential, and the possibility to use it in order to support DSO and TSO in operating the grid. The techniques used for this and first results are presented in this deliverable.

In the German Demonstrator, dealing with meshed high and extra-high voltage grids, two optimization approaches are being tested: On the one hand, the NETOPT optimization tool for online calculation of generator based operational set-points and on the other hand the PQ Maps tool which provides PQ-flexibility at the TSO-DSO interfaces in a graphical way. NETOPT will be used in a national environment taking into account actual legal grid regulations whereas PQ-Maps provide theoretical PQ areas, so far independent of current national restrictions. The simulative results make evident that both tools lead to accurate and realistic results and returned valuable knowledge for the field tests of Task 6.4. Whereby, on the one hand, the NETOPT tool is capable to calculate active as well as reactive power flexibilities taking into account several presently existing conditions like actual feed-in and the operation modes of the flexible units. Using NETOPT, various constraints like (n-1) security, voltage limits, load angle restrictions are taken into account. Additional limitations could be defined easily. Different set points relating the TSO-DSO connection point/points have been computed, leading to optimized, individual set points for the controllable flexible units in the DSO grid. Even in the case where a desired request (set point) relating the TSO-DSO connection point/points cannot be realized, the optimization algorithm of NETOPT ensures optimal system operation. On the other hand, the PQ Maps tool is capable to enhance the exchange of information between TSO and DSO. The key behind this enhancement is the ability to show how flexibility exploitation can impact on the TSO-DSO interfaces without disclosing confidential information e.g., topology data. The German demonstrator set-up is applied in a part of the German 110kV high voltage distribution network that has more than one grid connection point to the extra-high voltage level. Therefore, the new version of the PQ Maps is suitable for this type of networks since it has the capability to compute transmission network equivalents. With them, it is possible to empower both TSO and DSO with the knowledge of how the active and reactive power flows are redistributed throughout their several interfaces.

In the Italian Demonstrator, which operates in radial medium voltage grids, reactive power capability versus tap shifting ranges of transformers are inspected and a tool for the provision of either P or Q flexibilities with regards to grid operation as well as market aspects is being presented. From the analysis and the corresponding simulative tests, multiple conclusion can be drawn. The optimization tools showed that the full exploitation of theoretical reactive capability requires a specific management of the OLTCs, which may be quite demanding in terms of tap shifting, compared to a limited gain in capability area; The reactive power request modelled through the realistic set-point profile does not require to reach the limits of the available capability, even with a small amount of flexible resources (case 3 scenario); Higher shares of flexible resources (i.e. case 5 scenario) allow to address better both the needs of DSOs (efficient management of distribution network) and the needs of TSOs (support of transmission network management); Flexible resources close to primary substation are better suited for flexibility provision versus the transmission network, since dispersed resources cannot be exploited fully due to network constraints and their better capability to support local voltage control; Assets like STATCOMs can

provide an essential contribution, in presence of flexibility provision versus the transmission network, since they can virtually separate distribution and transmission networks in terms of reactive power fluxes, leading to an efficient management of distribution network and a better fulfilment of TSO requests; Suitable management of the STATCOMs may relieve the OLTCs operation, allowing a better voltage and losses control by the means of reactive power modulation.

Next, the Finnish Demonstrator deals with the optimization of selling active power flexibility, generated in low voltage grids by active prosumer households, battery systems (BESS) and e-mobility (EV). The optimization of the BESS and of the EV charging station gives bids to be placed on the markets for FCR-N (and FCR-D for the EV charging stations). Only active power of these assets has been optimized. The optimization in the Finnish demonstrator is based on the historical behavior of the markets, i.e. “How would the assets have performed over the past considered time period if it had been given these specific settings?” and then attempt to optimize the settings. Using battery systems, the optimization shows about 7% increased income compared to a system without it. The optimization of the EVs shows little profit, with the existing stations and EV users, when participating to the FCR markets.

1. INTRODUCTION

System operation is facing enormous challenges today. With the transformation of the European power systems towards electrical generation based on renewable, increasingly variable, energy sources such as wind, photovoltaic and hydropower, the technological coupling of the heat and power sectors as well as the unbundling of the energy markets, all tasks and responsibilities related to system operation face significant changes. Today, energy trading takes into account bottlenecks between market areas (cross-border exchanges), but it does not consider the technical restrictions encountered by the electrical grids within a single market area. This can lead to various technical problems, such as line overloading or voltage violation. Additionally, generation has become more and more decentralized, due to the connection of a large number of generators to the distribution grid, e.g. rooftop mounted PV-plants to the lower voltage level. This creates new challenges like reverse power flows resulting in voltage problems. Furthermore, units with high power feed-in, like offshore wind farms, are often installed far away from the energy consumption centers, leading to e.g. high load flows over a long distance in case of high wind situations. Contrary to the raised complexity of the whole energy system, the increasing number of distributed generation units offers also the possibility to use the feed-in flexibilities coming along with these units to provide several valuable services to the system operators, DSO as well as TSO. Therefore, there is an increased demand in assisting functionalities to prepare and substantiate decisions as well as in functionalities that optimize the system operation and determine more fitting and effective set-points for the individual generators.

This increasing penetration of Distributed Renewable Energy Sources in the distribution grids has lead to new operational and planning challenges for TSO and DSO. Both, quality of service and security of supply might be affected by the technical challenges caused by this continuous growth. TSO and DSO are responsible for managing their systems and need to adapt to this new environment so that they can continue to ensure the security and reliability of the system operation.

Therefore, the changing structure of the energy supply – from large dispatchable generation plants in the transmission grid to smaller decentralized and inverter based variable generation plants in the distribution grids – is a clear sign that mechanisms capable to promote a strong collaboration between TSO and DSO will be essential [1]. Services such as the estimation of power and flexibility from distributed resources and its technical validation are among those mechanisms. Coordination between all the involved parties and the development of optimization methodologies are crucial to support this process.

The EU-SysFlex project aims to enable the European energy system to use efficient, coordinated active as well as reactive power flexibilities in order to integrate high levels of Renewable Energy Sources (RES). One of the main objectives of the project is to examine the European power system with at least 50% of electricity coming from RES, an increasing part of which from variable, distributed and Power Electronic Interfaced sources, i.e. wind and solar. Therefore, the project aims at a comprehensive deployment of solutions, including technical options, system control and a novel market design to integrate a large share of renewable electricity, maintaining the security and reliability of the European power system.

In order to achieve the project objectives, data management analysis, the identification of technical shortfalls requiring innovative solutions, innovative tool development and integration and testing of new system services in the control centers of the system operators are included in the project approach. The project results will help to improve system flexibility by using already existing assets and new technologies in an integrated way, based on seven European large scale demonstrators in Germany, Italy, Finland, Portugal (2 demos), France, and the Baltic states (Work Package (WP) 6, 7, 8 and 9).

It is the project's goal to increase the flexibility of the future European system by developing the capability to provide not only the energy, but also the reliability and stability, through system services, required to integrate high RES. Therefore Work Package (WP) 6 *"Demonstration of flexibility services from resources connected to the distribution network"* analyses the opportunities arising from decentralized flexibility resources connected to the distribution grid to serve the needs of the overall power system, in coordination between DSOs and TSOs, by means of three demonstrators located in Germany, Italy and Finland.

1.1 WP6 OBJECTIVES AND RELATIONSHIPS BETWEEN TASKS

One of the main objectives of WP6 is to analyze and test the use of distributed flexibility resources, with a focus on enabling provision of system services from resources connected to the distribution grids in accordance with the requirements of DSOs and TSOs. This process poses major challenges to DSOs since they are obliged to connect renewable energy to their distribution networks, but these networks were initially not designed to handle large volumes of power generation units. Here are two main requirements: First is to follow the current policies for the decarbonization of the energy systems in integrating large amount of RES in the grid structure. On the other hand, the DSOs must ensure the security and resilience of their networks. For this, the DSOs need adequate "freedom" in the operation of their networks to avoid overloads and restrictions, which can be currently "superimposed" in certain operating conditions by requirements of TSOs, which have to take care about the problems in their grids like frequency stability or reverse power flows caused by the increase penetration of RES. These partly contradictory requirements can be met by an improved cooperation between TSOs and DSOs using RES's active and reactive power flexibilities.

In detail, three sub-objectives can be identified:

- Improve TSO-DSO coordination;
- Provide ancillary services to TSOs from distribution system flexibilities;
- Investigate how these flexibilities could meet the needs of both TSOs and DSOs.

WP6 addresses these objectives through five interlinked tasks. Task 6.1 refers to the required coordination of the work package. Task 6.2 focuses on the definition of System Use Cases (SUC) based on the Business Use Cases (BUC) coming from WP 3. Within Task 6.3, systems and tools are being developed in order to set up the SUC. In Task 6.4, field tests are carried out in the three demonstrators. In addition, the results of these field tests will be analyzed and common conclusions will be drawn in Task 6.5. A schematic overview of all the relationships described above is depicted in Figure 1.

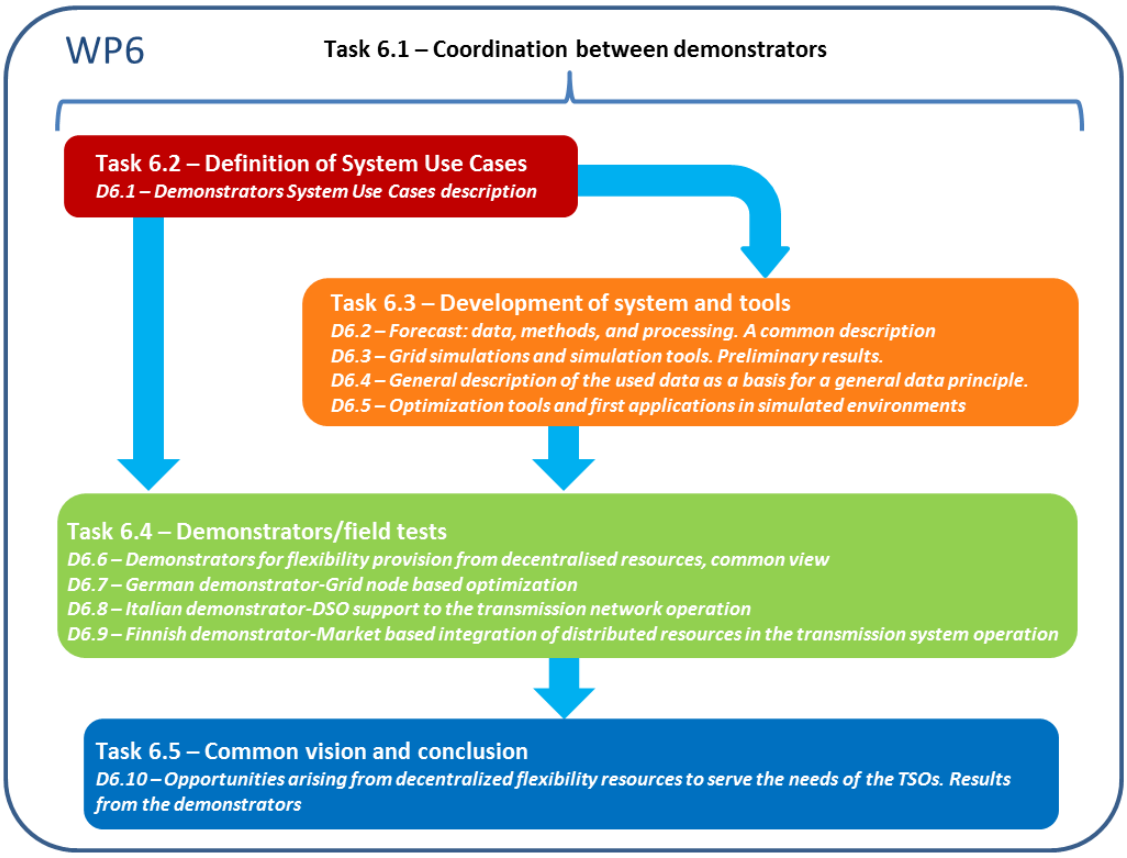

FIGURE 1 – WP6 OVERVIEW AND RELATIONSHIPS WITHIN TASKS

The activities and achievements of each Task, and of the whole Work Package itself, is presented through a comprehensive set of Deliverables[2]. In the following, they are shortly described, divided by Task:

- Task 6.2 "Definition of System Use Cases":
    - Deliverable 6.1 *"Demonstrators Use Cases description"* presents the "translation" of Business Use Cases from WP3 into System Use Cases
- Task 6.3 "Development of systems and tools":
    - Deliverable 6.2 *"Forecast: Data, Methods and Processing. A common description"* presents the description of requirements of the DSO/TSO interface, in order to harmonize the data formats and models for all the trials;
    - Deliverable 6.3 *"Grid simulations and simulation tools"* presents the first results about network models and simulations from the demonstrators;
    - Deliverable 6.4 *"General description of the used data as a basis for a general data principle"* presents the description of communication interfaces between the actors involved in the demonstrators;

[2] At the moment of the publication of this Deliverable D6.5, the following deliverables have already been finalized and can be found at the EU-SysFlex website (www.eusysflex.com): D6.1, D6.3, D6.4 and D6.6.

- Deliverable 6.5 *"Optimization tools and first applications in simulated environments"* presents the description of the optimization tools and the range of flexibilities used in the demonstrators;

- Task 6.4 "Demonstrators/field tests":
  - Deliverable 6.6 *"Demonstrators for flexibility provision from decentralized resources, common view"* presents the deployment plan, including technical specifications, procurement procedures for technical equipment, timeline for installations, and monitoring procedures;
  - Deliverable 6.7 *"German demonstrator - Grid node based optimization"* presents the information about the German demonstrator results, including the description of the working framework;
  - Deliverable 6.8 *"Italian demonstrator - DSO support to the transmission network operations"* presents the information about the Italian demonstrator results, including the description of the working framework;
  - Deliverable 6.9 *"Finnish demonstrator – Market based integration of distributed resources in the transmission system operations"* presents the information about the Finnish demonstrator results, including the description of the working framework;
- Task 6.5 "Common vision and conclusion":
  - Deliverable 6.10 "Opportunities arising from the decentralized flexibility resources to serve the needs of the TSOs. Results from the demonstrators" presents common conclusions and recommendations from the demonstrators' activities, in order to contribute to the WP objectives and overall Project results.

The scope of Task 6.3, to which this deliverable belongs, is to develop the algorithms and the software tools, which embed the innovative functionalities and the corresponding requirements defined in the System Use Cases, presented in Deliverable 6.1. Task 6.3 deals with four groups of tools, divided by the type of application (forecast, simulation, communication and optimization). They are presented and described in four corresponding Deliverables (D6.2 to D6.5). This group of tools will be integrated in the demonstrator set-ups in order to carry out the field tests, which are the scope of Task 6.4 and will be described in a dedicated set of deliverables (D6.7, D6.8 and D6.9 respectively). This Deliverable (D6.5) deals with the description of the developed optimization tools and some exemplarily results from the different demonstrators.

1.2 SCOPE AND OBJECTIVE OF THIS DELIVERABLE

As briefly explained in the previous section, this deliverable is part of a set of four deliverables designed to introduce and describe the activities and preliminary results of Task 6.3 and the corresponding software tools and algorithms used in the three demonstrators.

Each Deliverable deals with a specific type of tools and algorithms, which are shortly described in the following:

- Observation and forecasting tools: These tools are designed to improve forecasts of variable resource, market, grid requirements, and the behavior of distributed resources in case of pricing and control signals. They are introduced and described in D6.2 *"Forecast: Data, Methods and Processing. A common description"* and developed to meet the specific needs of the different demonstrators. However, it is necessary to achieve a higher observability of the system and thus more accurate network conditions.
- Grid Simulation tools: These tools as well as simulation tests using the tools are used to investigate different handling and operations of the demonstrator networks. Appropriate scenarios modeling a novel flexibility management within the actual demonstrator networks are simulated to assess different goals. Additionally, simulations serve as a test and validation environment for the other tools to prepare for their use in the physical demonstration set-ups. This is being described and presented in D6.3 *"Grid Simulations and simulations tools. Preliminary results"*
- Communication tools: These tools are intended to support the communication interfaces between the actors involved in the demonstrators. The existing communication platforms will be improved and new interfaces will be defined to enable interactions between the involved actors based on the processes described in the use cases. These tools are presented and described in D6.4 *"General description of the used data as a basis for a general data principle"*
- Optimization tools: These tools aim to identify and utilize the best and optimized flexibility potential of decentralized resources in subordinated DSO grids in order to achieve a better coordination and grid integration, providing various services and products to the TSO grid in compliance with given network constraints under various operating conditions. The tools, described in Deliverable D6.5 *"Optimization tools and first applications in simulated environments",* enhance existing demonstrator infrastructures and systems and allow for optimal use of the tested controllable assets (i.e. RES, Battery Energy Storage System (BESS), Static Synchronous Compensators (STATCOM), Electric Vehicles (EV)).

The scope of this deliverable is to describe the optimization approaches and methods adopted within WP6 and to explore the new operating conditions demonstrator networks have to face, in presence of distributed assets as well as to use the flexibilities of these assets in order to provide ancillary services to the TSO. With the successful implementation and application of the optimization tools within each demonstrator and under usage of forecast and communication systems, the benefits can be achieved, representing the main objectives of WP6.

1.3 STRUCTURE OF THIS DELIVERABLE

As already mentioned above, this deliverable is part of a series of deliverables in Task 6.3 but also within the whole work package. It should stand for itself in form and content in general, but has always to be considered as one part of a larger series, as explained in chapter 1.1. Besides this introduction, within the next chapters, the different optimization approaches and tools in each demonstrator are described in detail including some first results on simulated environments. The general objectives of each optimization within its specific environment and the innovations, which come along with these new approaches, are described.

The document structure is as follows:

- Chapter 2 gives a short overview about the optimization approaches within WP6;
- Chapter 3 deals with the German demonstrator optimizing flexibilities in meshed extra-high and high voltage grids;
- Chapter 4 presents the Italian demonstrator, which optimizing flexibilities in radial medium voltage grid structures;
- Chapter 0 describes the work performed in the Finnish demonstrator, developing methods to increase the value generated by the operation of flexible units;
- Chapter 6, as a conclusive chapter, provides a summary and an outlook with ongoing research and open questions.

2. OVERVIEW OF OPTIMIZATION APPROACHES WITHIN WP6

Optimization is beneficial when a system or situation can be solved in different ways and is dependent on numerous variables. In power system operation, the main objective is usually a stable and secure provision of electric energy, but it is also important to achieve this in a cost efficient manner. Conventionally, a classical optimal power flow (OPF) computation is applied to manage dispatching of generators in the transmission grid in order to ensure the distribution of energy to the consumers.

However, more and more generation units are installed within lower voltage grids and such an optimization performed by a Transmission System Operator (TSO) is either neglecting the potential of many distributed resources or too complex, with too many embedded resources, and with not enough observability of the distributed network constraints, to provide adequate results. The flexible resources in the high, medium and low voltage grids as well as each technology used for these resources come with different characteristics and hence require a different approach in order to manage and use the different kinds of assets, e.g. in low voltage grids there are small prosumers with rooftop photovoltaic (PV) installations, electric vehicles (EV) or home storage systems. In the medium voltage grids, there are many installed generation units, varying in size and characteristics such as medium-sized or large PV plants or wind parks which can be controlled by aggregators, or activated automatically by Distribution System Operators (DSOs) in case of events threatening the safe and secure grid operation. There can be also small generating units, which act almost autonomously using a fixed operation mode and cannot be remotely operated. In addition, larger storage systems can be found with the potential to store and deliver fast and flexible power and reactive power. In high voltage grids, besides the traditional fuel-based power plants, very large PV and wind parks are connected. Their influence on the grid status is important and they can cause congestion (e.g. overloading of lines) or voltage problems in high generation and low consumption phases, but could at the same time help and solve problems when they are operated in a coordinated way between the system and asset operators. Of course, congestion can also occur in lower voltage levels, where at the moment, predominantly voltage problems occur. The latter might change with uprising electro mobility penetration, if EV can be efficiently managed for demand response and storage.

For different aspects coming with these flexibilities, optimization tools are necessary. In order to tackle those, OPF computation can also be successfully and efficiently applied to manage distributed resources focusing on different objectives, like the provision of system services to both TSO and DSO, without shifting constraints from one system to the other, or to decide on the possibilities an aggregator has on using assets in the TSO markets (FCR-N, FCR-D). However, the realization of such tools opens new insights on the usage of asset flexibilities and can lead to great innovations within current system operation strategies. To achieve that, challenges have to be overcome. E.g. Current operation strategies will be influenced and new ways of running the system will be applied. New processes have to be set up and security strategies have to evolve. Furthermore, current regulatory barriers have to be taken into account. Within the EU-SysFlex demonstrators, new techniques and ways of operating the system are not only meant to be simulated. They are applied in real world systems to assist and improve current system operation. For this, requirements of the system operators (DSO and TSO) have to be respected and implemented. From a technical point of view, in order to achieve high availability, the resources

require adequate ways to handle unexpected situations as well as errors and faults in the incoming data or uncertainties in the measurements and forecasts.

Developing optimization tools, based on new or already existing mathematical approaches, and make them ready for the usage in high-end environment is one of the big challenges in this task and will lead to new innovations within these three demonstrators. How these approaches will look like and how they compare to each other and what questions and challenges can be solved by them, will be shown in the following sections and chapters of this deliverable. The following table gives a brief overview of the scope of each optimization within each of the three demonstrators

TABLE 1 – BRIEF OVERVIEW OF THE SCOPE OF THE OPTIMIZATION WITHIN THE THREE DEMONSTRATORS

DEMONSTRATOR	SCOPE AND CHALLENGES OF OPTIMIZATION
German	Determination of grid secure active and reactive power flexibility from distributed energy sources within 110kV distribution grids and provision of such information to the DSO-TSO interface at 110kV/400kV.
Italian	Determination of grid secure active and reactive power flexibilities in 10/20kV radial distribution grids from MV assets and provision of them to the DSO-TSO interface at 20kV/110kV.
Finnish	Aggregation of low voltage grid flexibilities from distributed assets and provision to the flexibility markets.

However, by inspecting the grid structure with a comprehensive grid layout, it is obvious that there are different network configurations as depicted in Figure 2 and thus, different kind of problems for the system operators arise, which are directly related to the voltage level. Dealing with a meshed grid structure of high and extra high voltage grids with a certain amount of redundancy also means it is necessary to avoid incorrect grid conditions like congestion problems taking into account a disturbed system operation such as (n-1) events. Looking at medium or low voltage grids, which are mainly operated as radial grids or open loops, voltage problems play a more important role. As a matter of fact, these grids are not (n-1) secure.

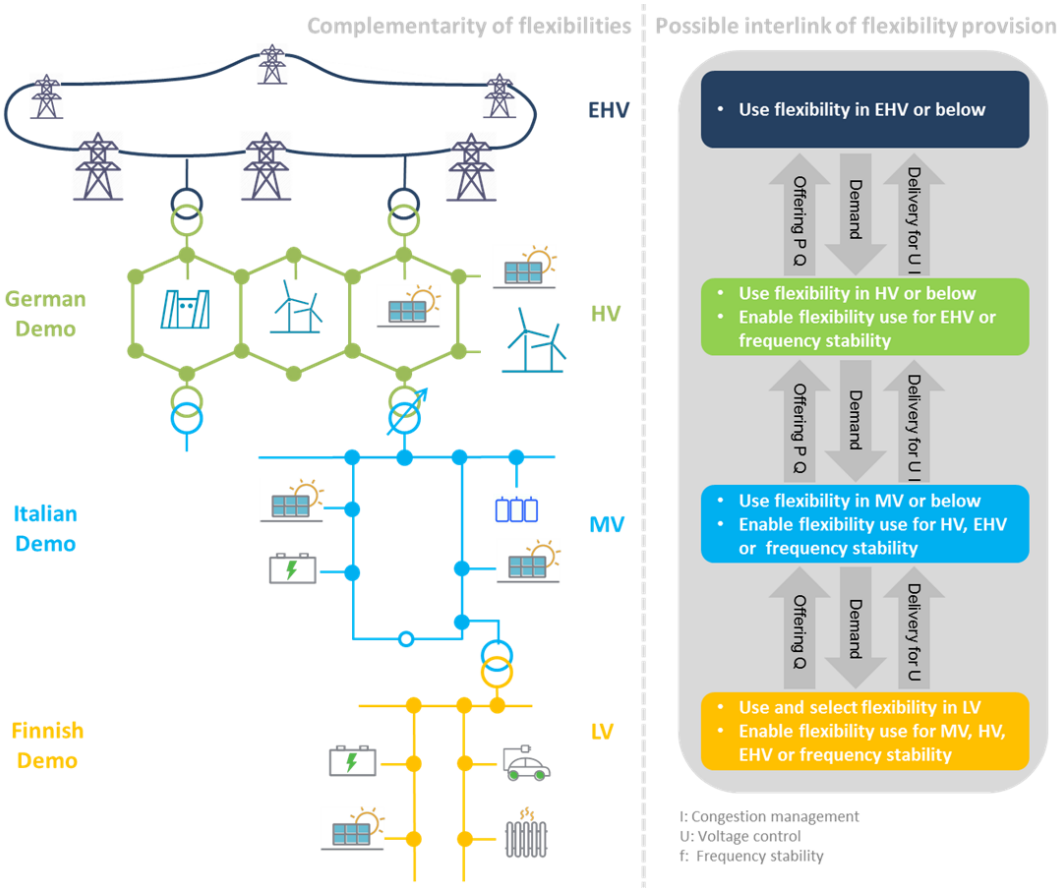

FIGURE 2 – POSSIBLE THEORETICAL INTERLINK BETWEEN DEMONSTRATIONS FOR FLEXIBILITY PROVISION

Thus, different optimization algorithms have been developed and tested within the scope of the EU-SysFlex project taking into account the specific needs of TSOs as well as DSOs operating their extra high, high, medium and low voltage levels independently. Hence, the techniques and methods applied and evaluated here are in some aspects of utterly difference.

2.1 GERMAN DEMONSTRATOR

The German demonstrator set-up is located in a part of the German 110 kV high-voltage distribution network. Here, the focus is on coordinating distributed energy resources (DER) connected to high-voltage (HV) grids in order to provide suitable active and reactive power (P-Q) flexibilities to the high-voltage grids of a DSO themselves as wells as to the extra-high-voltage (EHV) grids of a TSO. Additionally, possible measures shall be provided in case of foreseen congestion or voltage problems. The goal is to show that exploiting the flexibility of decentralized energy resources as well as improving the communication between DSO and TSO, both grids can be operated more reliable and efficient compared to an uncoordinated use of only flexibilities connected to the own grid. This goal is addressed by enabling the provision of congestion-free P and Q flexibilities, or PQ Maps to TSOs as well as by improving communication between DSOs and TSOs and improve information exchange.

With regard to the presented problems, two optimization tools with different application functionalities were developed within the German demonstrator complementarily aiming at determining available flexibilities for enabling the provision of active and reactive power to the TSO and for the DSO's own use. Both tools contribute to the objective of optimizing available flexibility resources connected to meshed distribution grids with multiple grid connection points to the transmission grid.

One optimization tool, named NETOPT, has the goal of providing (n-1)-secure specific set-points to the online control center of the DSO for individual generation units taking a few well-defined objective functions into account like the calculation of the currently possible reactive power flexibilities or the minimum possible active power feed-in at several TSO-DSO grid connection points, taking the present active power values as well as the actual operation modes of the generators into account. The functionality of the developed algorithms of this optimization tool can and therefore will be evaluated and investigated by means of a live field test.

The other optimization tool, named PQ Maps, estimates the theoretical entire range of active and reactive power operating points that can be exchanged at TSO-DSO connection points considering the flexibility in upwards and downwards power available in the distribution grid. This tool provides the flexibility information graphically to the TSO and the dependencies between active and reactive power flows without calculating generator specific set-points. The approach of the PQ Maps is developed to show a simplified data exchange between DSO and TSO with all needed data available, assuring that no sensitive network data is shared between TSO and DSO. The PQ Maps thus act on the decision support field by providing to the network operator all the possibilities of active and reactive power that can be exchanged at the TSO-DSO interfaces. This is done while only focusing on ensuring the technical feasibility of the grid. The PQ Maps solution goes beyond the limitations of the current regulatory framework in Germany. It therefore aims at providing additional beneficial results for thought-provoking impulses in the discussion for future regulatory framework.

With both approaches, one can theoretically calculate power exchange limits between transmission and distribution grids as well as specific set-points for operational purposes. While the set-points take into account current operation modes and schedules from energy resources, the PQ Maps provide maximum possible flexibility areas. Within future works (not within this project) including the scheduled field test, the goal is to show that both approaches are able to calculate realistic flexibilities including all operational constraints like (n-1) calculation as well as voltage and loading limits.

2.2 ITALIAN DEMONSTRATOR

The Italian demonstrator set-up is located in a part of the Italian medium voltage distribution grid. Its main scope is to use the controllable assets connected to distribution network for supporting ancillary service provision to the high voltage (transmission) grid. Its goal is to demonstrate that the already connected DERs and some dedicated, partially newly installed assets (BESS, STATCOM) can be managed and optimized locally by the DSO in order to provide a suitable and congestion free PQ flexibility range at the primary substation of a TSO. This goal is pursued through the provision of aggregated reactive power capability and a cumulative parameter curve (energy/cost) for active power. In this context, an improved optimization tool is necessary to efficiently manage the distribution network in presence of a higher share (compared to the present scenario) of power flexibilities from distributed resources, in order to address the specific requests from TSO (and also DSO) while guaranteeing secure and efficient system operations. The optimization tool further developed for the Italian demonstrator, besides its base solver (OPF), is capable of aggregating reactive and active flexibilities and addressing power exchange constraints at primary substation node (slack node): these functionalities are embedded in a single algorithm for fast and efficient calculations.

2.3 FINNISH DEMONSTRATOR

In the Finnish demonstrator, the purpose of the optimization is to determine how to bid and operate resources distributed in the low and medium voltage grid. The resources considered are a set of public electric vehicle charging stations and an industrial-scale battery system. For each of them, a strategy has been determined and the optimization process helps in fixing the bidding price on the selected markets. Its main scope is to manage the low and medium voltage flexible resources in order to allow active power to be exploited in the TSO ancillary service market. The aim is to increase the revenue generated by the operation of flexible units, which is pursued through innovative aggregation approaches. Thus, main objectives are the investigation of different operating conditions in the presence of various flexibilities as well as market optimization services. Due to the fact that the Finnish demonstrator is focused on market mechanisms and pricing of services, the data used and the concepts implemented (cost or revenue optimization) are in essence very different from the ones used in the German and Italian demonstrators (optimization of the power flows).

3. OPTIMIZATION IN THE GERMAN DEMONSTRATOR

The German demonstrator deals with several 110 kV high-voltage grids (network groups, NG), of the same distribution system operator (DSO, MITNETZ), which are connected to a 380 kV extra high-voltage grid of a transmission system operator (TSO, 50 Hertz). Each network group is connected to the overlaying transmission grid via more than one grid connection point (GCP). The network groups, as well as the simulated areas of the extra-high voltage grid (first loops of the overlaying grid), are strongly meshed and contain various renewable and conventional generators. About 70% of these renewable generators (predominantly Wind and PV installed since 2014) can be controlled regarding their active and reactive power feed-in.

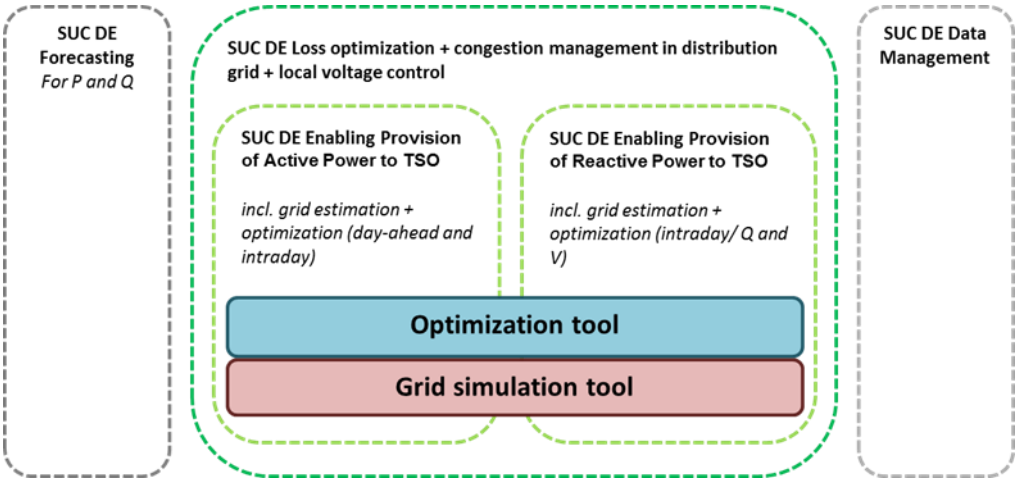

FIGURE 3: USE CASES, FUNCTIONALITIES AND TOOLS RELATIONSHIPS SCHEME

The objective of the German demonstrator is to examine the potentials of these flexible generators by determining available flexibilities for enabling the provision of active and reactive power to the TSO and for the DSO's own use. Furthermore, it supports TSO or DSO operation taking into account specified set-points (active power, reactive power and voltage set-points) at e.g. the grid connection points, calculating optimized set-points for the flexible generators in the DSO network. These processes were modelled in Task 3.3 and are presented in Deliverable 3.3 through two Business Use Cases: the first one (DE-AP) describes a business process focused on provision of active power flexibilities from distribution grid for congestion management in the transmission grid and the second one (DE-RP) describes a business process focused on the management and optimization of reactive power exchange at TSO/DSO interface, for supporting voltage control and congestion management services.

The technical realizations of the Business Use Cases were modelled in Task 6.2 and are presented in Deliverable 6.1 [31] in two System Use Cases (see Figure 3).

As explained in chapter 2.1, two optimization tools (NETOPT and PQ Maps) with different complementary application functionalities were developed within the German demonstrator in order to fulfill the specifications of the use cases.

NETOPT has the goal of providing specific set-points to the online control center of the DSO for individual generation units considering a specific objective function like loss minimization, calculation of reactive power flexibilities based on the actual active power feed-in and operation modes of the available generators. Another benefit is the ability to predict (n-1)-secure set-points in active and reactive power for each connected power plant and so to realize support for the congestion management and voltage control of the TSO. This approach enables efficient grid operation with its integrated loss optimization under consideration of the current German regulatory framework.

The second optimization tool, named PQ Maps, determines areas of feasible active and reactive power operating points at TSO-DSO interfaces. In order to provide flexibility areas for several grid connection points, this optimization tool needs the modelling and integration of a network equivalent for the transmission network so that it can resemble its behavior. To exploit successfully the full theoretical flexibility potential available in the DSO grid, TSO must know beforehand its impact at each TSO-DSO interface. The calculated PQ Maps determine the maximum/minimum of active and reactive power that can be exchanged at the TSO-DSO interfaces and provides the flexibility information graphically to the TSO without calculating generator specific set-points. This approach goes beyond the limitations of the regulatory current framework.

Both tools will be tested in a field test within the EU-SysFlex project. The PQ Maps will run in parallel to demonstrate and test a simplified data exchange procedure between DSO and TSO. But the full PQ-flexibility range cannot be realized in the field, due to current German regulatory aspects . Such process provides valuable inputs of utmost importance for both system operators without disclosing confidential information. With the help of such a parallel running approach the demonstrator aims at providing beneficiary results for thought-provoking impulses in the discussion how to evolve the regulatory framework.

The NETOPT tool will be tested within the field test as an active decision maker. A bi-directional communication between the NETOPT tool in the Demonstrator and the control center of MITNETZ Strom will be set up, in order to process the results of NETOPT in the operational decisions.

Although with different goals, the developed approaches are complementary. The PQ Maps is a decision-support tool that exploits the flexibility available in the distribution side at their maximum/minimum levels to graphically show how this impact on the TSO-DSO interfaces. Therefore, areas of feasible PQ points at these interfaces are presented to the user. However, the PQ Maps do not provide insights on the combination of set-points to reach a specific PQ point available on the flexibility areas. The algorithm only ensures that there is at least one combination of flexibility activations that allow to reach that PQ point. The current operating point is of course encompassed by the set of PQ points provided by the PQ Maps. The NETOPT tool also developed in the scope of the German demonstrator works exactly on this part. It computes the resources set-points that optimize the current network operation considering a specific objective function.

Within the chapters 3.1 – 3.5, the need of the NETOPT optimization tool for the online control center is being described (Chapter 3.1) as well as a short overview about the optimization functionalities is being given (Chapter 3.2). Next, a detailed description about the internal program and data structures as well as some implemented functionalities and equations of this optimization tool are presented (Chapter 3.3). In Chapter 3.4 the grid, which is used to calculate active and reactive power flexibilities as well as generator set-points to achieve an overall active power, reactive power or voltage set-point, are being described (Chapter 3.5).

In Chapter 3.6, the PQ Maps tool is presented. It also paves the way for an increased cooperation between TSO and DSO. The approach of this PQ Maps tool was first developed within the scope of a previous project, called FP7 evolvDSO. The PQ Maps is a method to estimate the active and reactive power flexibility ranges at the TSO-DSO interfaces by exploiting the available flexible resources while not jeopardizing with the distribution network operation. In case of meshed distribution networks with more than one interconnection to the transmission network, the previous version of the PQ Maps could only be applied to an individual primary substation if the active and reactive power flows remain unchanged in the remaining ones. Within EU-SysFlex, an innovative upgrade to overcome this drawback based on the development of transmission network equivalents is presented.

Finally, a conclusion and outlook for both tools are given in Chapter 3.7.

3.1 NEED FOR THE NETOPT OPTIMIZATION TOOL

One objective of the online control center optimization tool within the German Demonstrator is to find optimal set-points for numerous generating units within several 110 kV grids. For this, the individual and specific needs of system operators (TSO as well as DSO) are taken into account and a universal, freely configurable Optimal Power Flow (OPF) algorithm is necessary. In general, the goal of an OPF is the derivation of parameters, in this case set-points, in order to optimize a given (grid) scenario to achieve goals like the maximization of reactive power capability. Another aim of the OPF can be the minimization of total generation costs, system losses, voltage deviations, total CO_2 emissions of the generating units or the number of network interventions. This must be done in compliance with two general requirements: On the one hand - quite generic - boundary conditions like keeping the maximum permissible utilization of the equipment have to be taken into account as well as operating the grid within accepted voltage limits. On the other hand, there are system operator individual requirements like the consideration of special protection settings, which represent the main challenge of the development of the online control center optimization tool.

Additionally, in the optimization process several grid scenarios have to be taken into account inspecting the grid layout without any fault as well as with a single out-of-service component ((n-1)-case) at the same time so that the computed set-points are valid for all scenarios.

3.2 OVERVIEW OF THE NETOPT OPTIMIZATION FUNCTIONALITIES FOR P AND Q SET-POINT FLEXIBILITIES

A short overview about the main features and grid constraints, to be taken into account for the online grid control center optimization tool for the German demonstrator, is given in the following table:

TABLE 2 – BRIEF OVERVIEW OF THE OPTIMIZATION FUNCTIONALITIES OF THE ONLINE CONTROL CENTER OPTIMIZATION TOOL

Optimization	German Demonstrator
Voltage Level of Considered Flexibilities	110 kV
Interconnection between:	DSO and TSO (110 kV and 220/380 kV)
Objective	Active and reactive power management
Boundaries	DER P and Q boundaries
Constraints	Grid Constraints: • Bus Voltage 108 kV – 121 kV (n-0) • Bus Voltage 99 kV – 123 kV (n-1) • Line Loading 50% (n-0) • Line Loading 100% (n-1) • Load angle ≤ 30° in case Line Current > 300 A
Solver / Methods	Non-linear optimization of extended load flow problem
Algorithms	Interior Point
Programming Language	AMPL, PYTHON
Data Model	Based on mpc-format (Matpower case file)
Aimed Accuracy	10^{-4}
Risks	Long optimization time in case of several (n-1) problems which have to be considered

3.3 TECHNICAL DESCRIPTION OF THE NETOPT OPTIMIZATION TOOL

This section briefly explains the programs used for the optimization environment as well as basic methods and functions of the NETOPT optimization tool. Subsequently, the implemented objective functions, boundaries and constraints are presented in detail.

Here, it has to be explicitly pointed-out that the optimization tool uses the generator reference system for all generator-based values. This is common practice having a look at various grid calculation programs like e.g. Powerfactory [2], Integral [3], Matpower [4] (a power flow calculation program based on Matlab® [5]) or pandapower [6]. Thus, generator feed-in results into positive values for active power (P). In the same manner, a positive reactive power value means an over-exited operation, which results in an increase of voltage magnitude. Correspondingly, the presented figures use this reference system too, which might be confusing having reports and figures in mind that use the consumer reference system.

3.3.1 OPTIMIZATION TOOL AND ENVIRONMENT

The optimization environment consists of different programs and applications modelling, solving and verifying non-linear optimization problems within electric power systems. Main components and programs of the developed environment are listed below. The selected optimization tool, so called AMPL ("A Mathematical Modelling Language" [7]) is a state-of-the-art modelling environment especially for non-linear optimization problems. The optimization process was mainly performed to allocate distributed reactive power provision optimally by wind power plants. The main program is being written in Python [8] in combination with the simulation and power system calculation software pandapower. An overview about the data processing as well as the different optimization capabilities of the main program NETOPT, the grid optimization tool which is being developed by Fraunhofer IEE, is depicted in Figure 4 and explained in more detail in the next section. pandapower is also being used in order to verify the optimized set-points and to perform (n-0) as well as (n-1) calculations in order to detect problems like congestion or node voltages outside the defined limits.

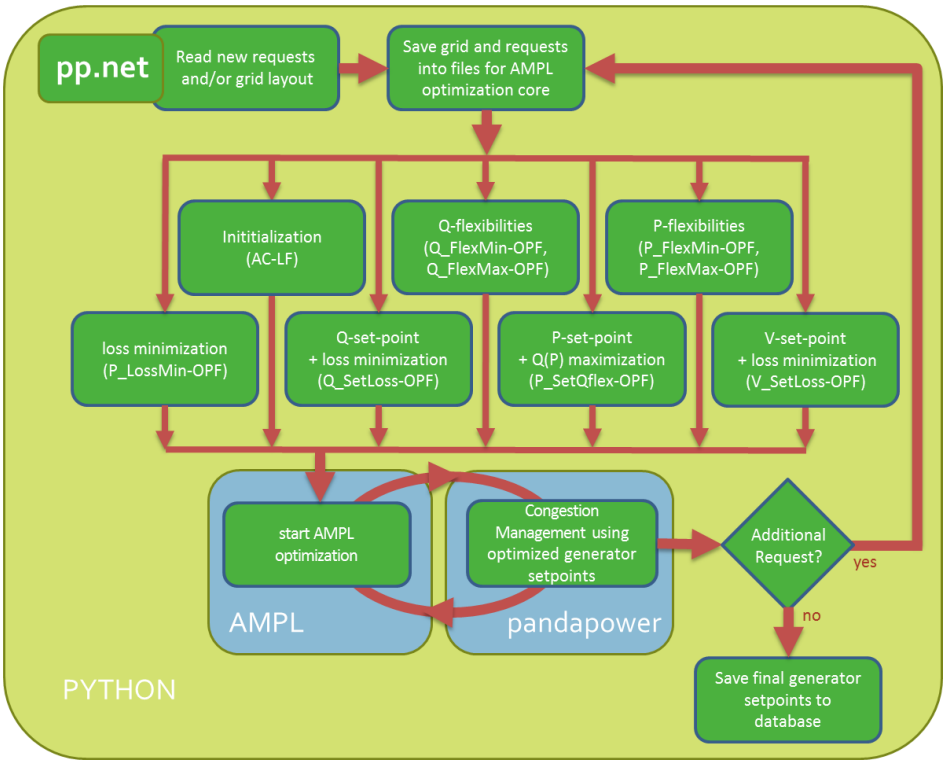

FIGURE 4 – STRUCTURE OF THE OPTIMIZATION TOOL "NETOPT"

The optimization kernel used for the development of the optimization tool is an AMPL-developed environment for complex power flow calculation and optimization. An easy handling and "direct" implementation of the mathematical problems in program code represent the strengths of such an algebraic high-level language. Different interior point solvers such as e.g. "KNITRO" [9]can be used and is explained in more detail in the subsection 3.3.1.4 below. The specific feature of the approach chosen here is to realize a load flow target, which

can be outside the focus of standard OPF procedures. Furthermore, the implementation as a mathematical method (in contrast to heuristic methods) ensures that the results are reproducible for the same input variables.

The developed optimization algorithm is able to process different scenarios simultaneously. This implies, that e.g. (n-1)-problems have to be identified in advance and passed to the optimizer as scenarios to be considered. The objective functions of the optimization process consist primarily in a reduction of the network losses in compliance with various secondary conditions (mathematical constraints) to be derived from the individual investigation objective, like a fixed value at GCP. The flexible units in the network serve to achieve these goals. The complex load flow equations, technical equipment limits and all additionally defined requirements represent boundary conditions to be strictly adhered [10].

3.3.1.1 NETOPT – MAIN PROGRAM (DATA PROCESSING)

This part of the program, written in PYTHON, contains the main functions of the optimization tool. It converts the description of the grid layout from pandapower into AMPL format and calls AMPL using the solver KNITRO to solve the described problem, which has been setup before. Additionally, it checks the proposed set-points based on (n-0 / n-1)-calculations using functions of pandapower. Thus, finding optimal generator set-points is in iterative procedure, which partly needs a sequential optimization process, performed by this instance. Finally, the results are written in a database. Figure 5 shows the data exchange between the different program components.

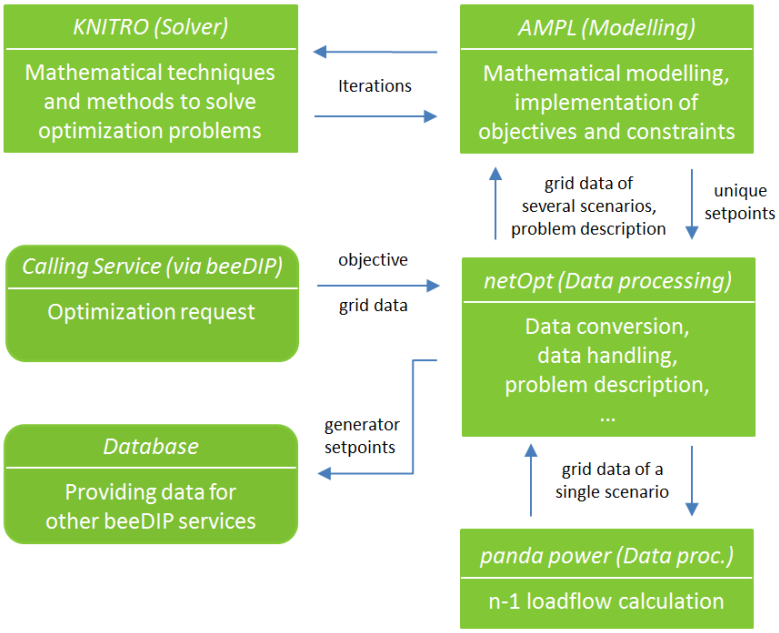

FIGURE 5 – OPTIMIZATION AND SIMULATION ENVIRONMENT.

3.3.1.2 PANDAPOWER (DATA PROCESSING)

pandapower, also written in PYTHON, is a joint development of the research group Energy Management and Power System Operation of University of Kassel and the Department for Distribution System Operation at the Fraunhofer Institute for Energy Economics and Energy System Technology (IEE) in Kassel. It combines the python data analysis library, named pandas, and the power flow solver PYPOWER to create an easy to use, element based

network calculation program aimed at automation of analysis and optimization in power systems. pandapower is also open source available and being further developed by this community[3].

3.3.1.3 AMPL (MODELLING)

This mathematical model is the core of the optimization tool, being composed of sets, variables and parameters, from which objectives and constraints are built describing the real world behavior and technical dependencies of the modelled system(s). All equations shown in this chapter are realized directly in the AMPL language. AMPL converts the model into a matrix-based formulation that is passed to the solver.

In the field of non-linear optimization, the functionality of the automatic differentiation (AD) supported by AMPL must be mentioned here. In order to solve the present non-linear problems, the first derivation of the problems is needed. Since their formation is essential in order to find the solution, AD support of AMPL is an enormous relief. Thus, setting up the problem description, the differentiability of the model descriptions have to be taken into account.

3.3.1.4 KNITRO (SOLVER)

A solver is a software technical implementation of methods and procedures to solve optimization models. The following part describes the commercial solver KNITRO used in this work. KNITRO has solution methods for continuous and (partly) discrete optimization models with integer and/or binary variables. Solving nonlinear problems is of particular complexity and difficulty. Ensuring that an optimal solution is found as well as keeping computation time reasonable, has led to a variety of algorithms and approaches [11]. The current version 11 of KNITRO results in the following four concrete algorithms / procedures:

- Interior-Point / Direct ([12])
- Interior-Point / Conjugate-Gradient ([13])
- Sequential Linear Quadratic Programming (SLQP, [14] [15])
- Sequential Quadratic Programming (SQP)

KNITRO has an automatic mode that analyses the problem structure and then selects the appropriate algorithm. Nevertheless, the algorithm can also be specified besides numerous other options by the user directly. The automatic mode examines the problem and its characteristics and selects the most suitable algorithm (and other settings) accordingly. Manual tests with the algorithms also showed that the first algorithm is the most appropriate one. Thus, the first algorithm (“interior point / direct") has been chosen for the models created in this work.

[3] https://pandapower.readthedocs.io/en/v2.0.1/index.html

3.3.2 METHODS AND FUNCTIONS OF THE OPTIMIZATION TOOL

The following sub-chapters give some detailed information about some program internals like the modelling of the passive grid model, loads and generators, the data management as well as some special demands based – on the one hand – on a demand of partner MITNETZ ("load angle" investigation) and – on the other hand – on grid safety issues ((n-1)-criteria). Additionally, the sequential approach within the optimization process is being described.

MODELLING OF THE PASSIVE GRID MODEL

The modelling of the network is essentially based on the node admittance matrix, referring (3.1).

$$\underbrace{\begin{bmatrix} \underline{y}_{11} & \underline{y}_{12} & \cdots & \underline{y}_{1i} & \cdots & \underline{y}_{1N} \\ \underline{y}_{21} & \underline{y}_{22} & \cdots & \underline{y}_{2i} & \cdots & \underline{y}_{2N} \\ \vdots & \vdots & \ddots & \vdots & \ddots & \vdots \\ \underline{y}_{i1} & \underline{y}_{i2} & \cdots & \underline{y}_{ii} & \cdots & \underline{y}_{iN} \\ \vdots & \vdots & \ddots & \vdots & \ddots & \vdots \\ \underline{y}_{N1} & \underline{y}_{N2} & \cdots & \underline{y}_{Ni} & \cdots & \underline{y}_{NN} \end{bmatrix}}_{\underline{Y}_{KK}} \begin{bmatrix} \underline{U}_1 \\ \underline{U}_2 \\ \vdots \\ \underline{U}_i \\ \vdots \\ \underline{U}_N \end{bmatrix} = \begin{bmatrix} \underline{I}_1 \\ \underline{I}_2 \\ \vdots \\ \underline{I}_i \\ \vdots \\ \underline{I}_N \end{bmatrix} \tag{3.1}$$

Using mathematical optimization software, it is very important to taken into account that such software usually cannot handle complex numbers. Therefore, all the described admittance matrices must be separated into a real and an imaginary part. Thus, the node admittance matrix program-internally is described via a conductance as well as a susceptance matrix as presented in (3.2).

$$\begin{bmatrix} \underline{y}_{11} & \underline{y}_{12} & \cdots & \underline{y}_{1N} \\ \underline{y}_{21} & \underline{y}_{22} & \cdots & \underline{y}_{2N} \\ \vdots & \vdots & \ddots & \vdots \\ \underline{y}_{N1} & \underline{y}_{N2} & \cdots & \underline{y}_{NN} \end{bmatrix} = \begin{bmatrix} g_{11} & g_{12} & \cdots & g_{1N} \\ g_{21} & g_{22} & \cdots & g_{2N} \\ \vdots & \vdots & \ddots & \vdots \\ g_{N1} & g_{N2} & \cdots & g_{NN} \end{bmatrix} + \mathrm{j} \begin{bmatrix} b_{11} & b_{12} & \cdots & b_{1N} \\ b_{21} & b_{22} & \cdots & b_{2N} \\ \vdots & \vdots & \ddots & \vdots \\ b_{N1} & b_{N2} & \cdots & b_{NN} \end{bmatrix} \tag{3.2}$$

MODELLING OF LOADS AND GENERATORS

All loads are taken into account as grid components with a fixed active and reactive power demand. Thus, their active as well as reactive power data are implemented in AMPL as a parameter and not as a variable. In AMPL, parameters hold "hard" values. These values can be defined and changed in AMPL, but a solver (KNITRO) will not change them while looking for an optimal solution. In contrast, variables are quantities that a solver is allowed to change as it looks for a solution to the mathematical program.

Thus, contrary to the loads, the power data of all generators are generally considered as variables with individual active as well as reactive power limits.

In case a generator is in SLACK operating mode, the voltage magnitude at the corresponding grid node is being set and fixed (held constant) to the voltage magnitude set-point of this generator, whereas the voltage angle of this node is set to "0°" and also fixed. If a generator operates in PV mode, again the voltage magnitude at the corresponding grid node is being set and fixed (held constant) to the voltage magnitude set-point of this

generator. Additionally, the active power value of this generator is fixed and thus cannot be modified by AMPL and KNITRO.

In general, generators are simply modelled in the OPF as PQ nodes. Active as well as reactive power data of generators are modelled in each case considering the initial value and a variable value, referring to (3.3). Of course, the resulting value has to be within defined limits.

$$P_{\mathrm{G}} = \Delta P_{\mathrm{G}} + P_{\mathrm{G,init}} \tag{3.3}$$

Within prior versions of the optimization tool, these limits were considered as parameters. In the framework of the project, they are modelled here as variables in order to be able to calculate them based on the specific optimization demands, e.g. computing individual reactive power limits based on an (maybe modified) active power value. Of course, both limits can be set to the same value to receive a constant behavior.

Based on the needs of the project, three possible control modes for generators are considered and modelled in the OPF for dealing with reactive power provision:

- *Q*(*P*)-characteristic based on MITNETZ
- cos(φ)
- *Q*(*V*)-characteristic; droop control

Each control mode is static with fixed set-points at least relating a single optimization. Thus, in just reactive power optimization, the OPF can simply work with the generators using the *Q*(*P*)-characteristic. Nevertheless, all modes are implemented in the same way, as follows: defining variable reactive power limits based on actual active power value set-point (redispatch optimization) or an actual voltage magnitude value (droop control).

As already mentioned, most generators are modelled in the OPF as grid elements in PQ operating mode which reactive power output can vary in the range $Q_{range,g} = [Q_g^{min}, Q_g^{max}]$. Reactive limits are updated depending on the considered active power value (in relation to its rated power value P_r) or to the actual voltage magnitude and the control mode of the generator. Regarding the control modes cos(φ) and droop control, Q_g^{min} and Q_g^{max} are set to identical values. Thus, no flexibility is being provided.

As already mentioned, for setting up the problem description, the differentiability of the model descriptions has to be taken into account in order to ensure good convergence. Thus, discontinuities (different gradients for a unique active power value) have to be avoided calculating e.g. reactive power limits/flexibilities. Due to this, the values of Q_g^{min} as well as Q_g^{max} are calculated using continuously differentiable functions as described in below.

Based on the quite simple dependency between active as well as reactive power taking cos(φ) control mode into account, which is a linear behavior by definition, is not presented in this document. However, inspecting some measurements, the reactive power limits are calculated taking into account a second order polynomial relationship, as depicted in Figure 6.

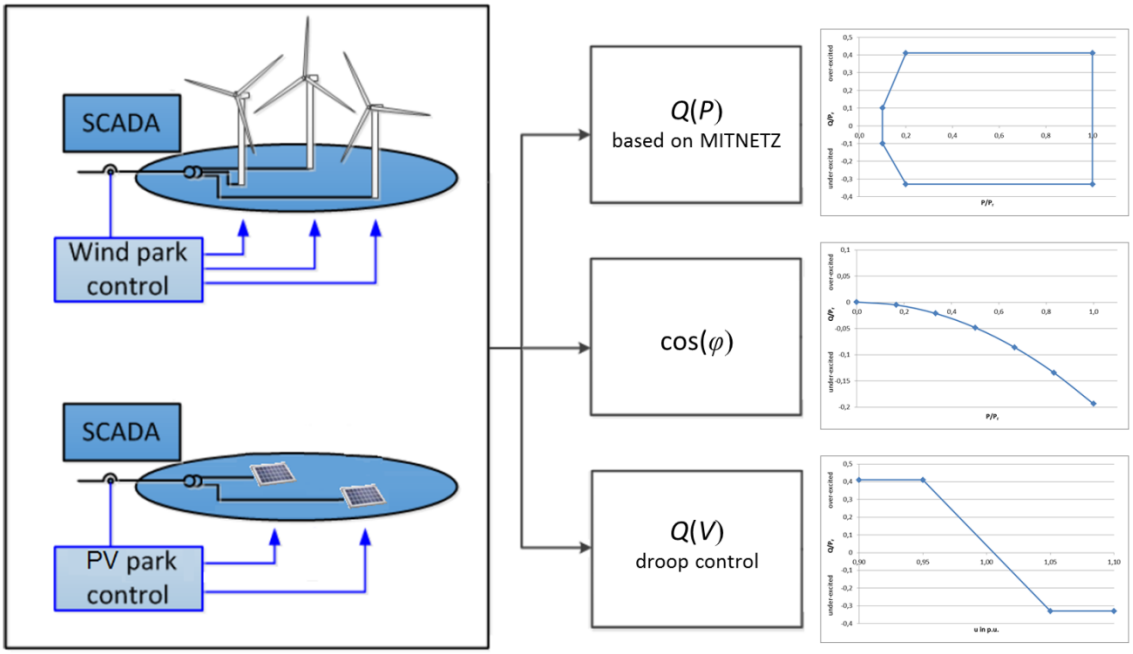

FIGURE 6 – DIFFERENT GENERATOR CONTROL MODES

The reactive power range based on the $Q(P)$-characteristic is modelled using an exponential function (3.4). Here, P_r is the rated (maximum) active power output of the generator. This method intrinsically represents reactive power limits in the load flow, whilst ensuring fast convergence due to the derivability of such a function.

$$Q = c \cdot P_r \cdot (1 - e^{-(a \cdot \frac{P}{P_r})^b}) \qquad \begin{array}{ll} c = 0.41,\ a = 6.966;\ b = 3.525 & \text{for } Q_g^{max} \text{ (over-excited)} \\ c = -0.33,\ a = 7.241;\ b = 3.156 & \text{for } Q_g^{min} \text{ (under-excited)} \end{array} \qquad (3.4)$$

The parameters of these equations are calculated taking sampling points (0.1|0.1) and (0.2|96% · limit value) into account, resulting in the characteristic (minimum requirement for reactive power provision of generators), depicted in Figure 7.

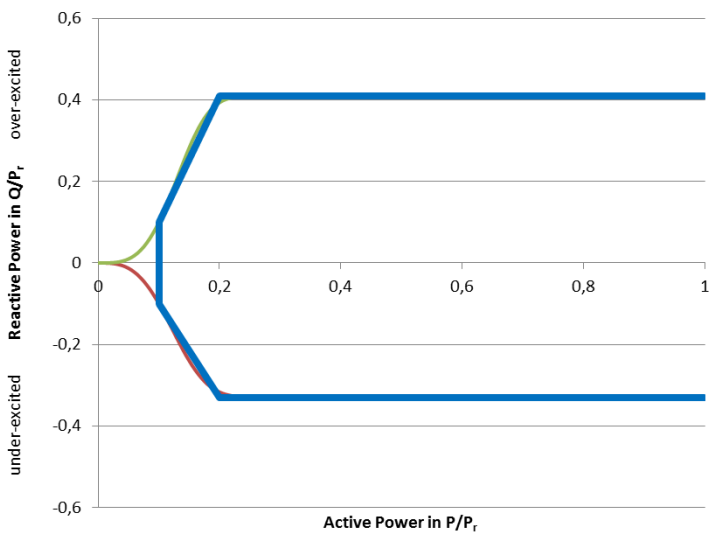

FIGURE 7 – CONTROL MODE BASED ON MITNETZ

The $Q(V)$ characteristic is simply implemented as a linear dependency between reactive power and voltage magnitude (3.5) taking boundaries into account as presented in Figure 8. This ensures that the desired shape is achieved while ensuring good convergence. The factors m, Δv as well as both boundary values can be defined individually for each single generator.

$$\frac{Q}{P_{\mathrm{r}}} = m \cdot (v + \Delta v) - m = m \cdot ((v + \Delta v) - 1) \tag{3.5}$$

Based on the parameter Δv the characteristic can be easily adapted to other voltage set-points (voltage value with neutral reactive power behavior) with shifting the characteristic slightly to lower or higher voltage values.

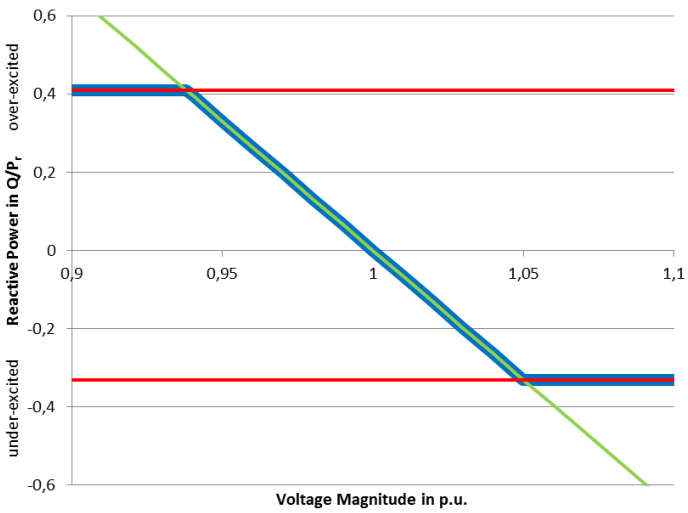

$m = -6.6$
$\Delta v = 0$

FIGURE 8 – CONTROL MODE "Q(V)"

INTERNAL GRID DATA MANAGEMENT

The grid data itself, which have to be considered in the optimization process simultaneously and thus, sent to and processed by AMPL simultaneously, is being stored in an (in general) two-dimensional data set as depicted in Figure 9. This structure has been established to contain on the one hand several grid descriptions (scenarios) of nearly the same grid layout in order to calculate e.g. identical valid generator set-points for all those scenarios and on the other hand to store different, time dependent feed-in situations (maybe forecast information) to decrease e.g. the number of tap changer modifications of transformers. According to the demands of the project, only the first column of this structure is needed and used.

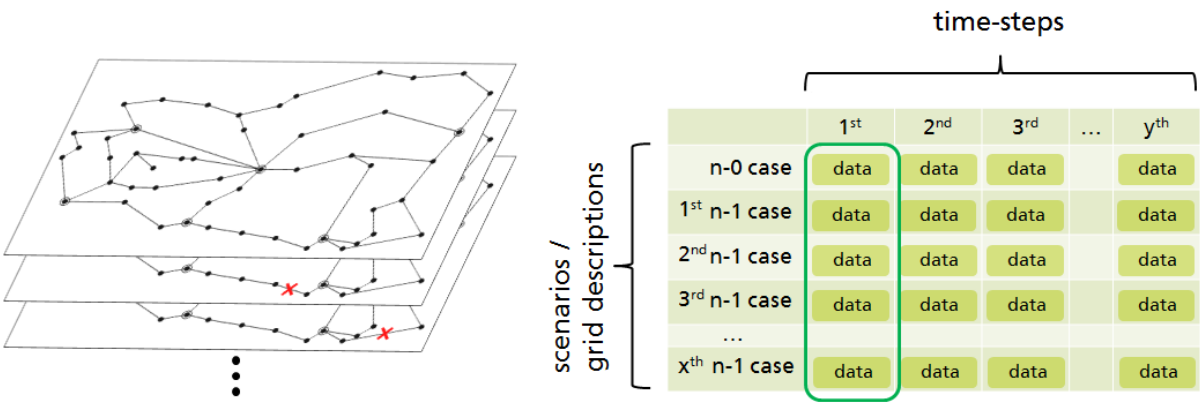

FIGURE 9 – INTERNAL GRID DATA MANAGEMENT

"LOAD ANGLE" INVESTIGATION

The protection concept of the considered networks envisages that the phase angle for the power flows in the network (within the frame of the demonstrator only regarding the 110 kV lines) does not exceed an angle of 30° ((3.6), (3.7)) which would mean a too high ratio of reactive power to active power which can cause voltage problems in cases of line faults.

$$-30° \leq \varphi \leq 30° \tag{3.6}$$

This results to:

$$\frac{|Q|}{|P|} \leq \tan 30° = \frac{1}{\sqrt{3}} \quad \Leftrightarrow \quad |Q| \leq \frac{|P|}{\sqrt{3}} \quad \Leftrightarrow \quad Q^2 \leq \frac{P^2}{3} \tag{3.7}$$

Within the project there is the specific demand to inspect the "load angle" at both sides of the 110 kV lines and to ensure that it is smaller 30° in case of a current flow higher than 300 A like depicted in Figure 10. The protection functions are released in case of a current value of 300 A. Below this value, no evaluation of the load angle or power ratio has to be performed. Nevertheless, the optimization tool has to find a generator set-point while ensuring that this problem does not occur.

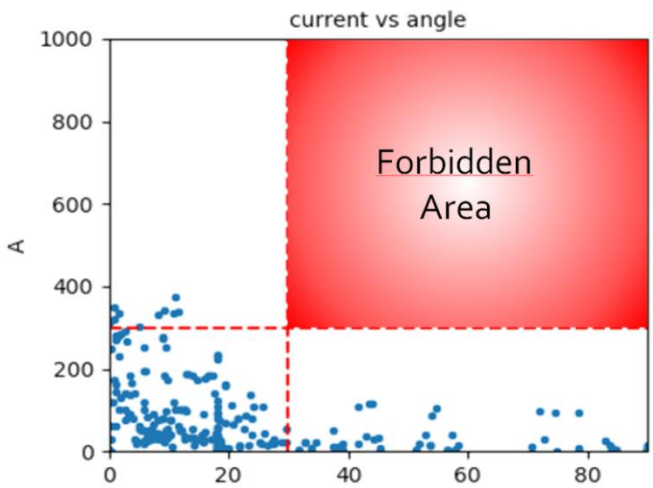

FIGURE 10 – "LOAD ANGLE" PROBLEM

DETERMINISTIC (N-1) CRITERIA

The (n-1) criterion states that no single failure of a network element caused by a short circuit, ground fault or interruption may result in a supply interruption. This is called the structural and operational (n-1) criterion [16] and is one of the technical evaluation criteria, which results in limits for resource utilization and operating voltages both in network operation and network planning [17], [18], [19]. The (n-1) criterion is considered to be met if there is no permanent limit value violation of network operating variables such as operating voltages or inadmissible equipment loads (current loads) due to a failure of a network device caused by a fault. In general, only selected resources are included in the (n-1) analysis. Due to a lack of redundancy, lines operated as a radial feeder cannot be included in the test, since an interruption of such a connection leads to an unavailable network section. From this systematics, it is obvious that an (n-1) problem can already exist long before the nominal current carrying capacity of a line is being reached. For example, a circuit loaded at 70% may be overloaded to 105% if a parallel circuit fails, thereby violating the (n-1) criterion in the initial state. Therefore, the limit values for the equipment utilization and the operating voltages for the initial state have to be checked. Calculating the equipment utilization, the maximum thermally permissible current has to be taken into account. Mainly due to the thermal inertia of the equipment, short-term overloads can be accepted. For example, this limit can be 110% for cables and overhead lines and 120% for transformers [18].

SEQUENTIAL OPTIMIZATION

The optimization process starts with the optimization of the (n-0) case. In the next step, all possible (n-1) cases are evaluated using the calculated optimal generator set-points. If there is any problem with a single (n-1) case, a marker is being set, indicating that the grid layout containing the (n-1) case has to be taken into account by the optimizer (send to AMPL) in general.

Since, especially detecting set-points just taking into account the (n-0) case, there can be several (n-1) problems, e.g. voltage problems at numerous nodes located in a single feeder connecting a controlled generator providing a lot of reactive power. Solving only one of those (n-1) problems reducing the reactive power provision of the generator can directly result into solving several or all of the (n-1) problems. Thus, in order to decrease the number of grid description being sent to AMPL at the same time, the number of grids is only increased by a certain number (default number is 3).

There is nearly the same issue dealing with the “load angle” condition: due to the fact, considering the “load angle” constraint leads to a relatively large number of additionally conditions (six conditions for each inspected line) which make the optimization more difficult and time-consuming. The optimization is divided into two parts. First, generator set-points are evaluated while considering all other problems like voltage problems – except the “load angle”. Taking into account the optimized generator set-points, the grid is being inspected and optimized considering the “load angle” conditions in a next step. Hence, in cases where an (n-1) problem leads to both under-voltage as well as “load angle” problems based on an extreme reactive power feed-in of the generators a hierarchical approach is applied. At first, the voltage problem is considered which solution may lead to decreased reactive power feed-in and thus maybe automatically to an elimination of the “grid angle” violation problem.

Furthermore, the algorithm dealing with an active power set-point in combination with the calculation of possible reactive power limits is being divided into two optimizations basing on each other. This means that the second

calculation uses the result of the first calculation for initialization. Here, active as well as reactive power set-points have to be computed which in general leads to a nearly infinite number of possibilities. Such an uncorrelated problem description results into the problem that the optimization algorithm cannot detect any direction to find optimized set-points. Consequently, the active power set-point is adjusted first taking into account a maximum reactive power capability of the generators. Only after this optimization, the reactive power range relating a single or a combination of grid conjunction points are inspected.

Figure 11 gives an overview about the structure of the main calculation routine. As already described, in order to reduce the number of grids, which are sent to the AMPL optimization tool, the optimization process only starts optimizing the normal grid layout (n-0). Once new optimized set-points for the generators are detected, these set-points are evaluated regarding possible (n-1) problems. This is being done replacing the old generator settings within the pandapower grid description, performing several load flow calculations using pandapower and evaluating voltage values, line utilization ratios and so-called “load angles” (exceeded Q/P ratio in case of a pre-defined exceeded current value). (n-1) problems are sent to the optimization tool (AMPL) as scenarios/grid descriptions as depicted in Figure 9.

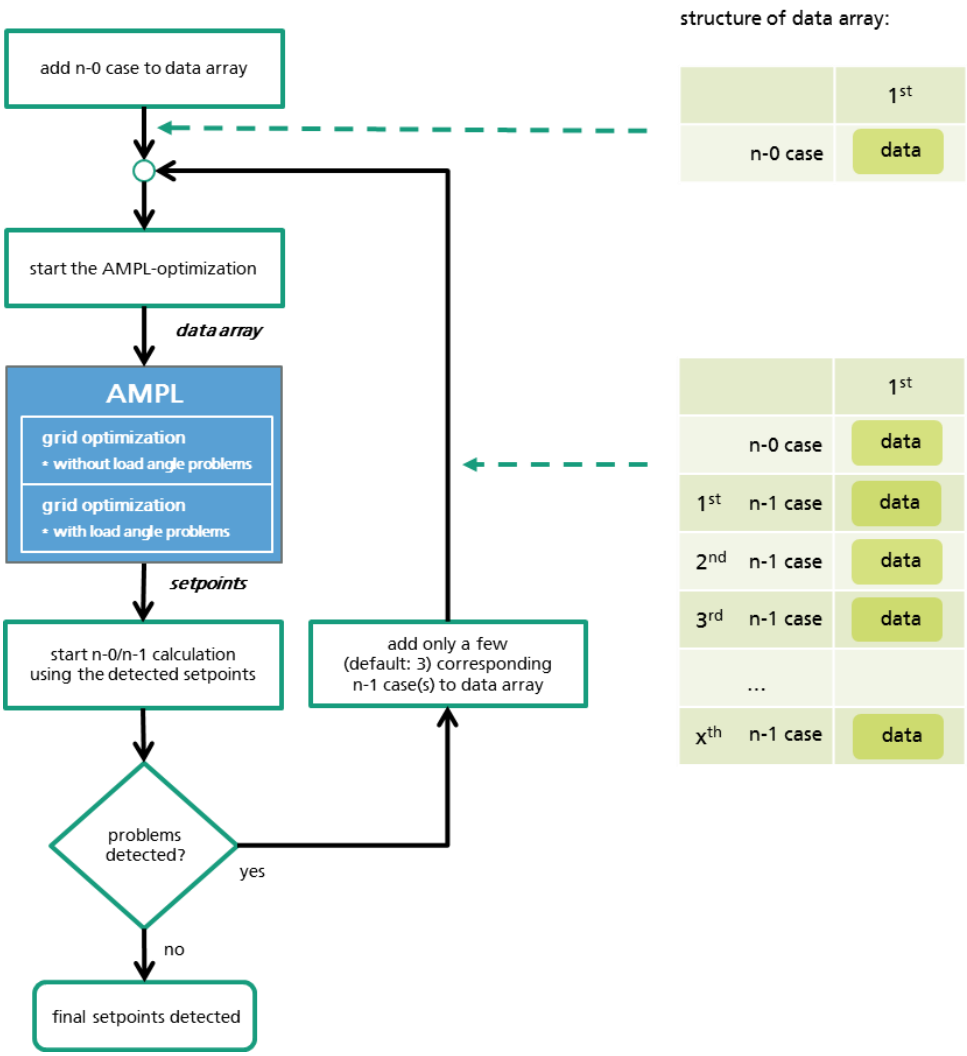

FIGURE 11 – ITERATIVE, SEQUENTIAL OPTIMIZATION

3.3.3 OBJECTIVE FUNCTIONS, BOUNDARIES AND CONSTRAINTS

The following sub-chapters give some detailed information about the implemented objective functions as well as some boundaries and constraints, taken into account by the optimization procedure.

OBJECTIVE FUNCTIONS

In the scope of optimization tool for the German demonstrator, all optimizations generally take into account the (n-0) case (scenario 0: s_0) only - of course ensuring (n-1) safety, referring to (3.8)-(3.12). Nevertheless, performing e.g. a loss-optimization, the losses within possible (n-1) cases are not considered computing generator set-points to reduce active power losses within the 110 kV grid level.

In order to solve different, maybe combined objectives, the description of the problem, to be solved by the optimizer in general can be performed using a multi-objective formulation using weighting factors μ_i like:

$$\min\{\mu_{\text{losses}} \cdot f_{\text{losses},s_0} + \mu_{\Delta Q_{GCP}} \cdot f_{\Delta Q_{GCP},s_0} + \mu_{V_{set}} \cdot f_{\Delta V_{set},s_0}\} \tag{3.8}$$

Minimization of grid losses:

$$f_{\text{losses},s_0} = \sum_{i\in A}\sum_{j\in A} g_{ij,s_0}\left[V_{i,s_0}^2 + V_{j,s_0}^2 - 2V_{i,s_0}V_{j,s_0}\cos(\theta_{i,s_0} - \theta\right. \tag{3.9}$$

Minimization of quadratic deviation from global reactive power exchange target:

$$f_{\Delta Q_{set},s_0} = \left(\sum_{i\in M}\sum_{j\in K} V_{i,s_0}V_{j,s_0} \cdot \left[g_{ij,s_0}\sin(\theta_{i,s_0} - \theta_{j,s_0}) - b_{ij,s_0}\cos(\theta_{i,s_0} - \theta_{j,s_0})\right] - Q_{set,s_0}\right)^2 \tag{3.10}$$

Minimization of sum of quadratic deviations from reactive power targets at each grid conjunction point:

$$f_{\Delta Q_{GCP},s_0} = \sum_{GCP}\left(\sum_{i\in M_{GCP}}\sum_{j\in K_{GCP}} V_{i,s_0}V_{j,s_0} \cdot \left[g_{ij,s_0}\sin(\theta_{i,s_0} - \theta_{j,s_0}) - b_{ij,s_0}\cos(\theta_{i,s_0} - \theta_{j,s_0})\right] - Q_{GCP,s_0}\right)^2 \tag{3.11}$$

Minimization of sum of quadratic deviations from voltage targets at selected grid nodes:

$$f_{V_{set},s_0} = \sum_{i\in A}\left(V_{i,s_0} - V_{set,i,s_0}\right)^2 \tag{3.12}$$

Active power losses in the system are described by f_{losses}. $f_{\Delta\text{Qset}}$ describes the quadratic deviation from a global reactive power exchange set-point Q_{set} with the transmission grid. The function f_{Vset} represents the quadratic deviation of voltages at several selected grid nodes from the set-points. $f_{\Delta\text{QGCP}}$ is used to penalize quadratic deviations from individual reactive power exchange set-points Q_{cp} at each grid conjunction point. The factors μ_i in (3.8) denote the objective weights.

As depicted in (3.13), a desired set-point value itself is also included into the optimization objective to ensure solvability. Considering a set-point as a constraint would directly lead to insolubility in case the set-point cannot be reached. Adding the set-point to the objective function using a description like

$$\min\{(Q - Q_{\text{set}})^2\} \tag{3.13}$$

will ensure solvability, weakening the problem description. Nevertheless, in case the set-point can be totally reached, it will find the best result.

BOUNDARIES AND CONSTRAINTS

The state and control variables are bounded by the following equality and inequality constraints. Within the description of the power flow optimization, the AC power flow can be described as constraints to ensure a technical valid solution of the optimization problem. The basic power flow itself therefore has no objective and therefore is no optimization in the classical meaning. It can be described by bus-based constraints for the active powers being valid for the set $N_{\text{PQ,PV}}$ of all PQ- and PV-nodes (3.14) and for reactive powers for the set N_{PQ} of all PQ-nodes in the grid as given in (3.15). The index j represents all buses in the system besides the current bus i. Equality constraints comprise the power balance at each node expressed by power flow equations.

$$0 = \sum_{a=1}^{A} P_{\text{G},i,a} - \sum_{b=1}^{B} P_{\text{L},i,b} - V_i \cdot \sum_{j=1}^{n} V_j \cdot \left[\, g_{ij} \cos(\theta_i - \theta_j) - b_{ij} \sin(\theta_i - \theta_j)\right] \;, \quad \forall \text{i} \in N_{PQ,PV} \tag{3.14}$$

$$0 = \sum_{a=1}^{A} Q_{\text{G},i,a} - \sum_{b=1}^{B} Q_{\text{L},i,b} - V_i \cdot \sum_{j=1}^{n} V_j \cdot \left[\, g_{ij} \sin(\theta_i - \theta_j) - b_{ij} \cos(\theta_i - \theta_j)\right] \;, \quad \forall \text{i} \in N_{PQ} \tag{3.15}$$

In order to realize an optimization problem, flexibilities have to be implemented in the description. Depending on the technical problem to be optimized, these flexibilities may occur on generation or load side as well as on the branch elements. The following equations (3.16), (3.17) describe the real and reactive power limits for each generator in the network. Set G describes the number of generators in the network.

$$P_{\text{G},g}^{\min} \leq \Delta P_{\text{G},g} + P_{\text{G},g} \leq P_{\text{G},g}^{\max} \;, \qquad \forall g \in \text{G} \tag{3.16}$$

$$Q_{\text{G},g}^{\min} \leq \Delta Q_{\text{G},g} + Q_{\text{G},g} \leq Q_{\text{G},g}^{\max} \;, \qquad \forall g \in \text{G} \tag{3.17}$$

In the project, only the generators within the grid are intended to provide flexibilities due to possible changes in their (active as well as) reactive power set-points. Furthermore, there are limits to the magnitude and angle of the voltage at the network node (3.18), (3.19). Set N describes the number of nodes in the network.

$$V_i^{\min} \leq V_i \leq V_i^{\max} , \qquad \forall i \in \mathrm{N} \tag{3.18}$$

$$\delta_i^{\min} \leq \delta_i \leq \delta_i^{\max} , \qquad \forall i \in \mathrm{N} \tag{3.19}$$

In order not to lead to overloading of branch elements such as cables and transformers, the permissible current carrying capacity must also be complied with (3.20). Set Z describes the number of branch elements in the network.

$$\left(|I_{ij}|, |I_{ji}|\right) \leq I_{ij,ji}^{\max} , \qquad \forall (i,j) \in Z \tag{3.20}$$

Furthermore, there is the specific demand to limit the "load angle", i.e. the ratio between reactive and active power flow via a line in case of a current flow increases 0.3 kA. This conditional demand requires complementary constraints as well as the introduction of additional "slack" variables S^{I} and S^{Q2P}. Complementary in this context means that the product of two variables must be zero (3.21)-(3.26).

$$0 \leq S_{i,j}^{\mathrm{I}} \perp S_{i,j}^{\mathrm{Q2P}} \geq 0, \qquad \forall (i,j) \in Z \tag{3.21}$$

$$0 \leq S_{j,i}^{\mathrm{I}} \perp S_{j,i}^{\mathrm{Q2P}} \geq 0, \qquad \forall (i,j) \in Z \tag{3.22}$$

with

$$|I_{ij}| \leq 0.3\ \mathrm{kA} + S_{i,j}^{\mathrm{I}} , \qquad \forall (i,j) \in Z \tag{3.23}$$

$$|I_{ji}| \leq 0.3\ \mathrm{kA} + S_{j,i}^{\mathrm{I}} , \qquad \forall (i,j) \in Z \tag{3.24}$$

$$Q_{i,j} \leq \frac{P_{i,j}}{3} + S_{i,j}^{\mathrm{Q2P}} , \qquad \forall (i,j) \in Z \tag{3.25}$$

$$Q_{j,i} \leq \frac{P_{j,i}}{3} + S_{j,i}^{\mathrm{Q2P}} , \qquad \forall (i,j) \in Z \tag{3.26}$$

3.4 TEST CASES FOR THE NETOPT-OPTIMIZATION TOOL

The following chapter presents the calculation results taking into account a real existing 110 kV grid of the distribution system operator MITNETZ. This grid, which schematically is being presented in Figure 12, consists of

- 379 grid nodes – thereof 16 within the 380 kV and 176 within the 110 kV grid
- 41 generators– thereof 29 controllable generators
- 211 lines – thereof 207 within the 110 kV grid (based on the fact that e.g. 20 kV loads are directly connected to an 110 kV/20 kV transformer, there are a lot of grid nodes higher or lower 110 kV level compared to the number of lines
- 2 network groups (separate 110 kV areas connected to the 380 kV grid)
- 5 grid connection points
- 10 EHV/HV transformers (between 380 kV and 110 kV)

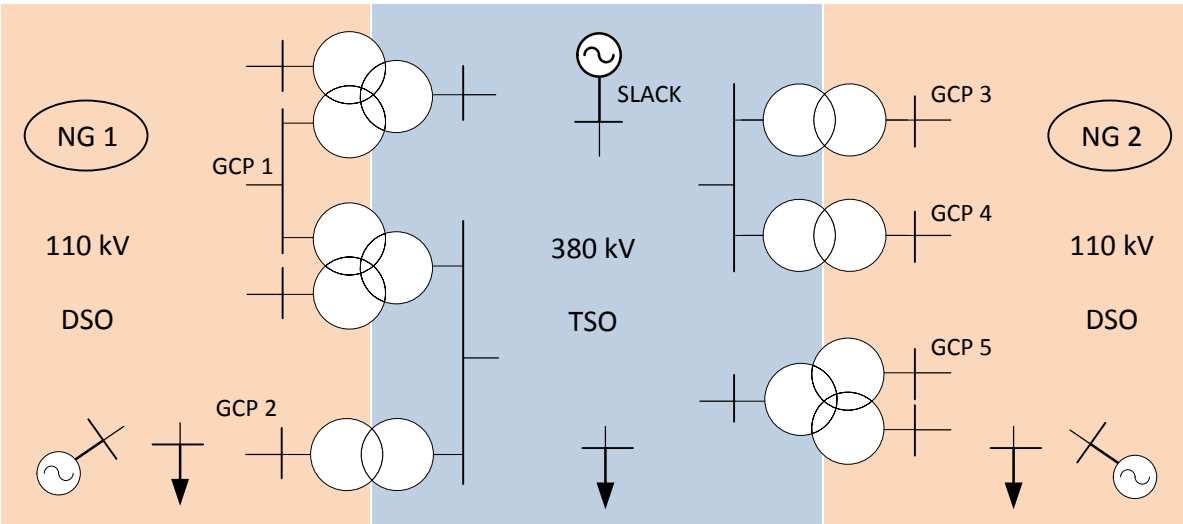

FIGURE 12 – SCHEMATIC GRID LAYOUT OF THE INSPECTED, REAL EXISTING GRID

In general, in order to present optimized results, the calculation procedure has been divided into two sections. First, an optimization result shall be calculated taking given constraints like current limits, voltage boundaries and load angles etc. as unalterable into account (3.27). Nevertheless, this can lead to the situation that no result can be found in case of maybe already existing problems in the grid which in general should not occur like line overloading in case of an (n-1) event. If so, in a second step, those constraints are weaken and shifted to the objective function. Now, the problem is relaxed which means that out-of-limit conditions are possible. Of course, each out-of-limit condition leads to a penalty value to be reduced by the optimization algorithm (3.28), (3.29).

Objective function of the first section (loss minimization) taking hard boundaries into account:

$$\min\{f_{\text{losses},s_0}\}, \quad \text{several constraints like } V_i^{\min} \leq V_i \leq V_i^{\max}, \ \forall i \in \mathrm{N} \tag{3.27}$$

Objective function of the second section (loss minimization) taking weak boundaries into account:

$$\min\{\mu_{\text{losses}} \cdot f_{\text{losses},s_0} + \mu_{\Delta\text{V}} \cdot f_{\Delta\text{V},s_0,s_1} + \mu_{\Delta\text{I}} \cdot f_{\Delta\text{I},s_0,s_1} + \cdots\} \tag{3.28}$$

or, dealing with a reactive power set-point:

$$\min\{\mu_{\text{losses}} \cdot f_{\text{losses},s_0} + \mu_{\Delta\text{V}} \cdot f_{\Delta\text{V},s_0,s_1} + \mu_{\Delta\text{I}} \cdot f_{\Delta\text{I},s_0,s_1} + \cdots + \mu_{\text{set}} \cdot (Q - \text{Q}_{\text{set}})^2\} \tag{3.29}$$

Here, the penalty term are always positive values. In order to identify easily that penalty terms have to be used to receive an optimization result, an accuracy variable has been introduced (3.30).

$$\text{accuracy} = \frac{\text{abs}(\mu_{\text{losses}} \cdot f_{\text{losses},s_0})}{\text{abs}(\mu_{\text{losses}} \cdot f_{\text{losses},s_0}) + \mu_{\Delta\text{V}} \cdot f_{\Delta\text{V},s_0,s_1} + \mu_{\Delta\text{I}} \cdot f_{\Delta\text{I},s_0,s_1} + \cdots} \tag{3.30}$$

Of course, this variable simply indicates that penalty terms are used. Its value itself does not indicate if a solution is quite good or bad. In case no penalty term has to be used, the accuracy calculates to “1”.

3.5 EXAMPLARY SIMULATIVE RESULTS FROM THE NETOPT OPTIMIZATION TOOL

In the following calculation and optimization results of a 110 kV grid operated as two network groups are shown for time-frame of about five hours (time series calculation). First, the calculated reactive and active power flexibilities relating an exchange between TSO and DSO are presented. Next, in order to show the power of the optimization tool, the following set-points/demands – which partly could not be reached at any single time-step – are set, so far without any real request of the TSO:

- Loss minimization in the 110 kV grid (aim of the optimization if no set-point requirements received)
- Reactive power set-point: Requirement of reactive power exchange between the 380 kV and the 110 kV grid to be -170 Mvar (under-excited operation)
- Active power set-point: Requirement of active power exchange between the 380 kV and the 110 kV grid to be +600 MW (feed-in)
- Voltage set-point: Requirement at 380 kV grid node of transformer station Lauchstädt to be controlled to 1.06 p.u. (402.8 kV).

Here, all figures contain the results of four different calculations/optimizations:

- normal AC-load flow calculation (AC_LF, red color)
- optimal power-flow calculation taking individual optimization request into account (e.g. P_LossMin-OPF, Q_SetLoss-OPF, P_SetLoss-OPF, U_SetLoss-OPF, … , green color)
- optimal power-flow calculation taking minimum reactive power provision into account (Q_FlexMin-OPF, blue color)

- optimal power-flow calculation taking maximum reactive power provision into account (Q_FlexMax-OPF, again in blue color in order to show the possible range with the same color)

These four calculations are performed independent from each other on the same grid situation for each time step, i.e. the reactive power range (minimum as well as maximum reactive power provision) is being calculated based on the actual feed-in of the generators coming with the grid description itself (time series data without taking any previous set-points from the optimizer into account). In case the calculated generator set-points would be sent to the units and processed, the grid description, taken into account by the optimization tool, would be directly affected leading to different flexibilities relating later time steps. Nevertheless, so far the set-points are simply calculated and not sent to the units.

Please consider that the lines partly overlap within the presented diagrams, especially performing calculations dealing with reactive power set-points only. Here, the active power operation of the generators is not modified and thus, except active power losses, the presented curves are nearly identical.

Please also note that the generator reference system is being used within the following figures. Thus, an active power feed-in is depicted with positive values as well as an over-exited operation of the generators, relating reactive power values.

3.5.1 REACTIVE POWER FLEXIBILITY

The reactive power outputs of the controllable generators within both 110 kV network groups are optimized to minimize as well as maximize the reactive power exchange between the TSO and the DSO grid. The active power outputs of the generators are not modified in both optimizations. The band of the possible reactive power flexibility is depicted as the area between the two curves in Figure 13.

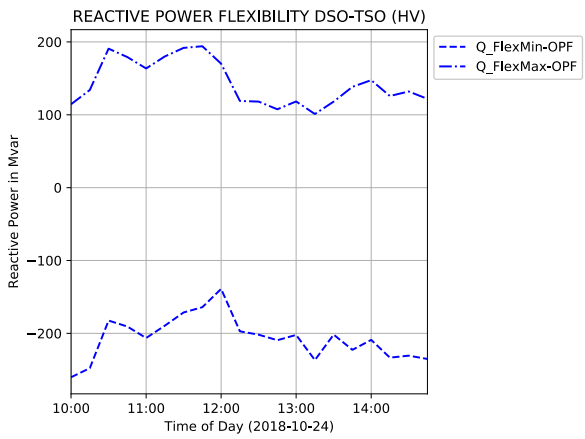

FIGURE 13 – RESULTS "REACTIVE POWER FLEXIBILITY"

This flexibility information could be sent to the TSO, which then is able to ask about a certain operation point within this range e.g. in order to support voltage stability in the EHV grid.

3.5.2 ACTIVE POWER FLEXIBILITY

The active power outputs of the controllable generators within both 110 kV network groups are set to minimize as well as maximize the active power exchange between the TSO and the DSO grid. Within the investigated grid, the active power-feed of the controllable generators can be reduced to "0" without getting any grid problems. Furthermore, there have not been any grid restrictions leading to the need to reduce active power feed-in. Due to this, the actual feed-in of these generators is the maximum possible feed-in based on current wind conditions or present solar radiation (= maximum active power flexibility). Thus, the presented time series of an "AC-LF" (AC load flow calculation) which takes the actual feed-in into account equally shows the curve of the maximum active power flexibility (P-FlexMax-OPF). The minimum active power flexibility (P_FlexMin-OPF) is not being presented in most of the following figures. Of course, it is being calculated and could be presented as shown in Figure 14.

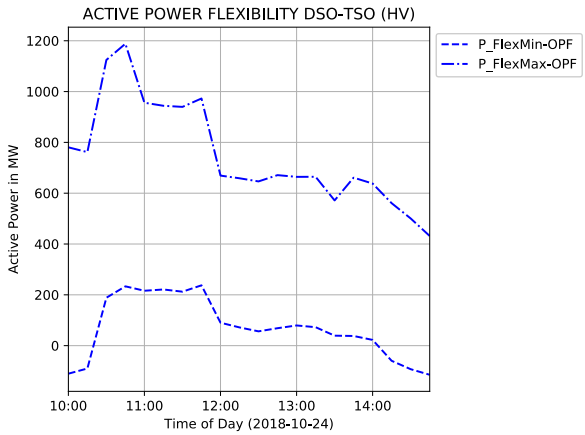

FIGURE 14 – RESULTS "ACTIVE POWER FLEXIBILITY"

Even in the case when all controllable generators are completely shut down, most of the investigated time-steps still show a feed-in into the TSO grid due to the existing non-controllable generators. Like in the case of reactive power flexibilities, TSO and DSO can use such information for improved operational planning, which results in a more effective use of resources and hence reduced operational costs. This active power flexibility information can be taken into account by the TSO dealing with e.g. corrective congestion management.

3.5.3 LOSS MINIMIZATION

The reactive power outputs of the controllable generators are set to minimize active power losses within both 110 kV network groups. At a first glance the results depicted in Figure 15 show an unexpected behavior: the loss optimized feed-in of the generators partly leads to lower values than inspecting the maximum reactive power provision of the generators (Q-FlexMax-OPF) which leads to high voltages and thus, into reduced losses generally.

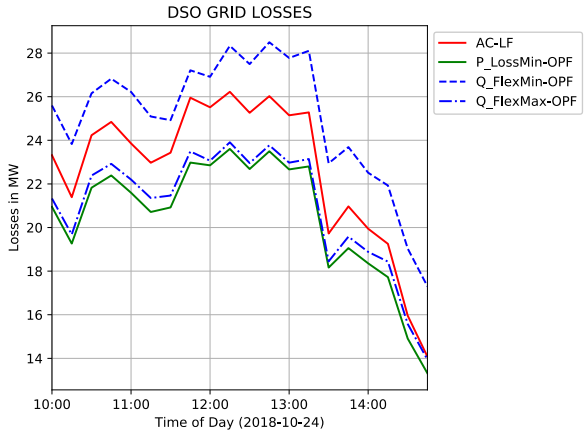

FIGURE 15 – RESULTS "LOSS MINIMIZATION"

Nevertheless, it has to be taken into account that the objective functions of both calculations, depicted in the same diagram, are different. Loss minimization deals with finding reactive power set-points in order to minimize active power losses within the 110 kV branches whereas reactive power provision deals with minimizing or maximizing reactive power directly without taking care about active power data. However, the optimizer found minimum values, which are even better than simply operating the grid with increased node voltages (over-exited operation of generators in order to provide maximum reactive power). The results are therefore plausible and show the capability of the optimization tool.

3.5.4 REACTIVE POWER SET-POINT

This optimization deals with a reactive power set-point relating both 110 kV network groups. The reactive power outputs of the controllable generators are set to receive a reactive power exchange with the 380 kV grid of -170 Mvar (here, a negative value means under-excited operation). The results are presented in the following Figure 16.

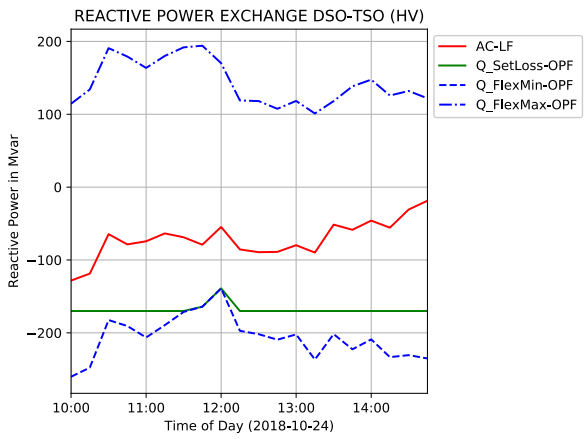

FIGURE 16 – RESULTS "REACTIVE POWER SET-POINT"

Inspecting the calculated "accuracy" values, it can be seen that penalty terms are used in two time steps. Thus, an optimal solution could not be reached. Having a look at the reactive power capability of both network groups, it becomes evident that there is no possibility to provide the requested amount of reactive power. Nevertheless, the generator set-points are calculated to their minimum possible values even when not fulfilling the set-point completely.

Looking at the reactive power contribution of both net-groups (Figure 17), it is obvious that the optimizer does not operate the generators of both network groups in a similar way, e.g. and simply reducing the reactive power of all generators using a percentage value to receive the demand. Instead of this, induvial, optimized set-points are calculated.

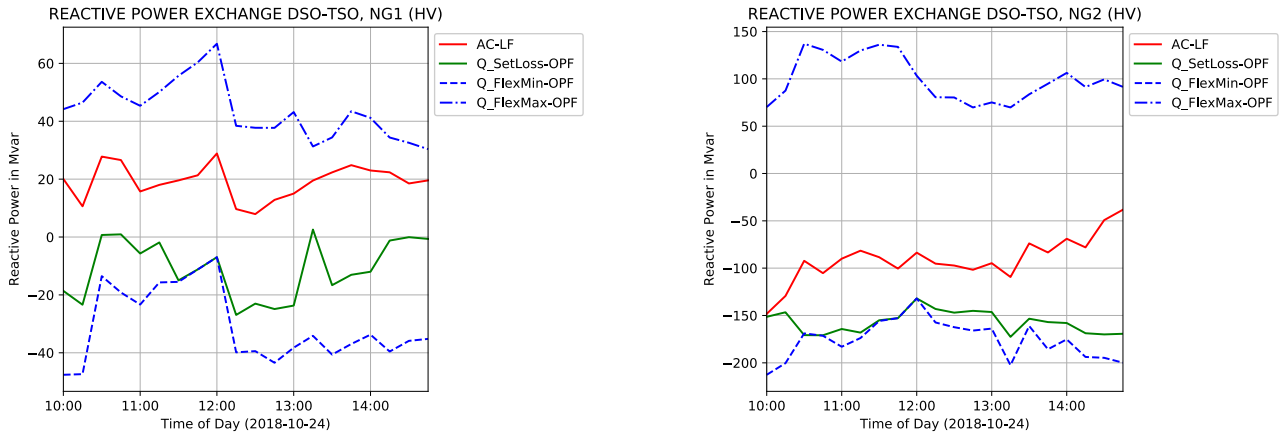

FIGURE 17 – RESULTS "REACTIVE POWER SETPOINT", CONTRIBUTION OF THE NET-GROUPS

3.5.5 ACTIVE POWER SET-POINT

This optimization takes into account an active power set-point. Here, the active power outputs of the controllable generators are limited to receive an active power feed-in of both 110 kV network groups of 600 MW ensuring maximum reactive power flexibility at the same time.

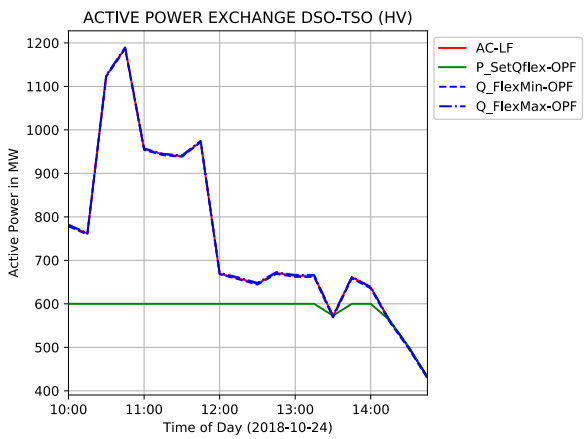

FIGURE 18 – RESULTS "ACTIVE POWER SET-POINT"

Having a look at the active power capability of both network groups, the generators cannot feed-in the requested active power demand of the set-point. Of course, the generator set-points are calculated to provide the maximum possible values – refer to Figure 19, which shows the feed-in of both network groups. Again, it is obvious that the optimizer does not operate the generators of both network groups in a similar way. It is calculating induvial, optimized set-points.

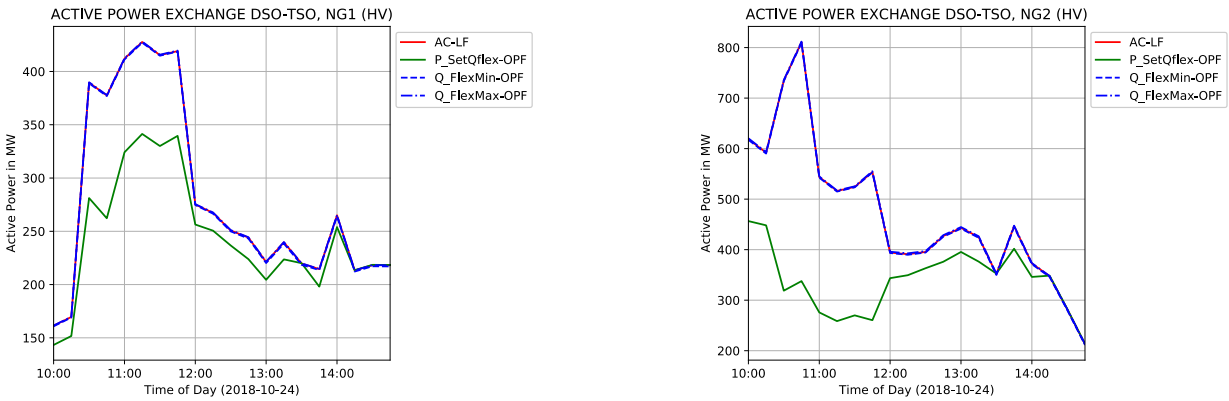

FIGURE 19 – RESULTS "ACTIVE POWER SET-POINT", CONTRIBUTION OF THE NET-GROUPS

3.5.6 VOLTAGE SET-POINT

Finally, this optimization deals with voltage control of an 380 kV conjunction point of a 110 kV network group (Lauchstädt) as well as taking loss minimization into account, again finding optimized reactive power set-points for the controllable generators in the 110 kV grid. In detail, a 380 kV grid node of transformer station Lauchstädt is controlled to 1.06 p.u. (402.8 kV). This set-point can be reached at any time as depicted in Figure 20 the lower right graphic dealing with the voltage magnitude of the corresponding grid node.

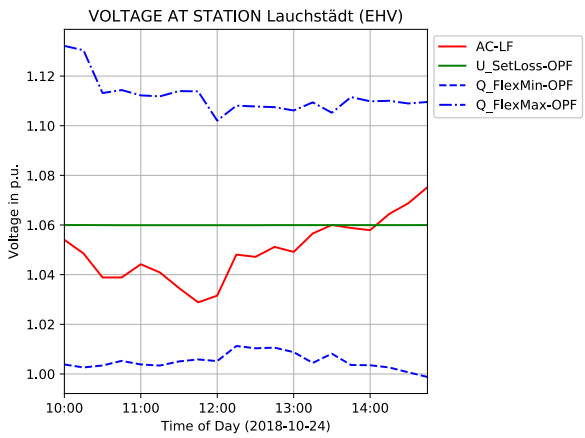

FIGURE 20 – RESULTS VOLTAGE SETPOINT"

Inspecting the reactive power contribution of both net-groups as depicted in Figure 21, the reactive power capabilities of the generators of net-group 1 are used to control the voltage at the inspected node.

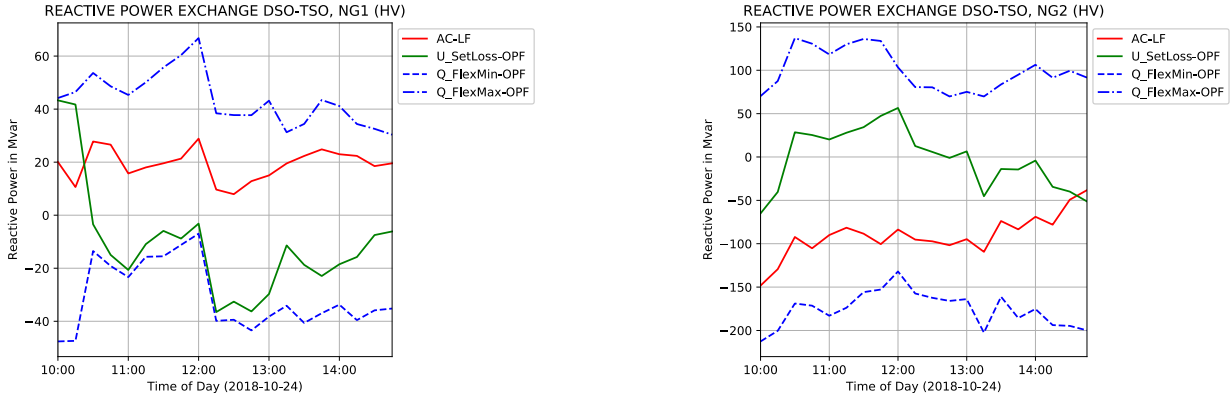

FIGURE 21 – RESULTS "VOLTAGE SET-POINT", USED REACTIVE POWER RELATING EACH NET-GROUP

Having a look at the different optimization results, the power and capability of the optimization tool becomes visible. Set-points for the distributed units have been calculated even in case the demand could not be reached based on different reasons like to low active power feed-in and thus, to less reactive power capability to reach a voltage set-point. In such a case, the units are operated to reach the demand as close as possible instead of simply aborting the optimization procedure with a message "request cannot be reached".

3.6 NEED FOR THE PQ MAPS OPTIMIZATION TOOL AND TRANSMISSION NETWORK EQUIVALENTS

Besides the above described techniques of calculating operational set-points for flexibilities under current grid constraints and power supply schedules, the determination of the maximum/minimum approachable PQ-flexibilities will now be considered. Due to a variety of reasons e.g. reactive power support actions, both TSO and DSO might be interested in changing the current operating set-points at their interfaces. The exploitation of the flexibility available in distribution grid is one way to fulfill this goal. However, such exploitation needs to be carried without jeopardizing the distribution network operation. The PQ Maps thus provides to both system operators the full range of possible operating points at their interfaces while complying with voltage and branch capacity limits. It is ensured by the algorithm that there is at least one combination of flexibility activations that allow to achieve each one of the estimated PQ possibilities. The flexibility information is graphically provided to both the TSO and DSO without disclosing sensitive information such as the flexibility provider as well as the DSO network data. Furthermore, an additional feature has been developed, considering TSO loops among DSO grids i.e. TSO has several DSO grid interconnection substations – meshed grids. This PQ Maps upgrade allows not only to estimate the power limits that can be exchanged as well as illustrates how they are redistributed throughout the different TSO-DSO interconnections.

3.6.1 PQ MAPS

Within the scope of a previous FP7 project, called evolvDSO, an optimization tool – PQ Maps – capable to empower both TSO and DSO with the knowledge of the active and reactive power ranges that can be exchanged at their interface while using the available flexibility resources and without jeopardizing the distribution network operation (e.g. voltage problems, branch congestions) was developed. The PQ Maps are only able to provide a flexibility area for a single primary substation. Because of that, in case of meshed distribution networks with more than one interconnection to the transmission network, this methodology can be applied to an individual primary substation only if the active and reactive power flows remain unchanged in the remaining stations To overcome this limitation, the optimization tool needs the modelling and integration of a network equivalent for the transmission network so that the existent mutual dependencies between different connection points can be considered.

The visual information provided by the PQ Maps gives a significant support for both planning and operational domains. It guides DSO in order to avoid penalizations due to possible violations of power exchange rules defined by the TSO as well as enhances the accuracy in the definition of contractual values of electrical energy exchange between transmission and distribution systems. In addition, the network planner can exploit these maps to assess the impact of additional flexible resources to the system flexibility.

The above mentioned potentialities of the PQ Maps can only be achieved if a robust and accurate algorithm is available. To do so, the path of including the impact of the transmission network is being followed in EU-SysFlex project.

OVERVIEW OF THE OPTIMIZATION FUNCTIONALITIES

A short overview about the main features and grid constraints, to be taken into account in the project, is given in the following table:

TABLE 3 – BRIEF OVERVIEW OF THE OPTIMIZATION FUNCTIONALITIES OF THE PQ MAPS AND NETWORK EQUIVALENTS

Optimization	German Demo – PQ Maps
Voltage Level	110 kV
Interconnection between	DSO and TSO (110 kV and 220/380 kV)
Objective	Estimate the P and Q Limits that can be exchanged between Transmission and Distribution Networks exploiting the available flexibility, while not jeopardizing the Distribution Network Operation
Equivalent Boundaries	Embedding Potential Constraints Arising in the Transmission Network Operation (e.g., Voltage or Overloading Problems)
Constraints	Grid Constraints: • Bus Voltage 99kV – 123 kV (n-1) • Line and Transformer Loading 100% (n-1) • Technical Limits of Generators, Capacitor Banks, On-Load Tap Changers • Flexibility Limits Imposed By Each Der
PQ Maps Solver/Methods	Non-Commercial Solver based on the Primal-Dual Interior Point Method
Equivalent Solver/Methods	Matpower Standard Solver based on A Newton's Method to Run Power Flow Studies
	Non-Commercial Solver for the Evolutionary Particle Swarm Optimization (Epso)
PQ Maps Programming Language	C++
Equivalent Programming Language	Matlab
Data Model	Network Topology - ENTSO-E CIM Derived Model CGMES Forecasts And Flexibilities – Json Structures
Risks	Related with the above mentioned boundaries, but only having a neglectable impact on the project goals

OPTIMIZATION OBJECTIVES:

The PQ Maps algorithm is based on the mathematical formulation and concepts of an Optimal Power Flow (OPF) problem. However, and since the main goal is not the classical one (i.e. minimization of generation fuel costs), the objective function needs to be automatically adapted to find the perimeter of the flexibility area.

$$\boldsymbol{\alpha} * P_{DSO \to TSO} + \boldsymbol{\beta} * Q_{DSO \to TSO} \tag{3.31}$$

The $\boldsymbol{\alpha}$ and $\boldsymbol{\beta}$ coefficients will therefore be responsible to minimize or maximize the $P_{DSO \to TSO}$ and $Q_{DSO \to TSO}$ injections (active and reactive power flows at the TSO-DSO interface nodes). Geometrically, this objective function represents a group of straight lines whose slope (**φ**) is defined by the relation between the above mentioned coefficients (tan **φ** = $\boldsymbol{\alpha}/\boldsymbol{\beta}$). Thus, different values of **φ** will lead to different points on the perimeter of the flexibility area.

BOUNDARIES AND CONSTRAINTS:

Being an optimization problem that aims to estimate the active and reactive power flexibility ranges at the TSO-DSO interfaces, its decision variables are naturally associated with the activated flexibilities as well as with slack bus voltage magnitude:

- Activated generation flexibility ($\Delta P_k^G, \Delta Q_k^G \ \forall k \in N_G$)
- Activated demand flexibility ($\Delta P_h^D, \Delta Q_h^D \ \forall \ h \in N_D$)
- Reactive Power Compensators variation ($\Delta Q_{rc}^{cond} \ \forall rc \in N_{rc}$)
- TAP changing ($\Delta tap_{ij}^t \ \forall t \in N_{OLTC}$)

where N_G, N_D, N_{rc} and N_{OLTC} correspond to the number of generators, loads, reactive power compensators and OLTCs presented on the distribution network. The aforementioned activated flexibilities i.e. decision variables are bounded by limits – flexibility bands – that can be technical (e.g., reactive power compensation capacity) or not technical (e.g., flexibility bids offered by aggregators or other market players).

$$\Delta P_{k,min}^G \leq \Delta P_k^G \leq \Delta P_{k,max}^G, \forall k \in N_G \tag{3.32}$$

$$\Delta Q_{k,min}^G \leq \Delta Q_k^G \leq \Delta Q_{k,max}^G, \forall k \in N_G \tag{3.33}$$

$$\Delta P_{h,min}^D \leq \Delta P_h^D \leq \Delta P_{h,max}^D, \forall h \in N_D \tag{3.34}$$

$$\Delta Q_{h,min}^D \leq \Delta Q_h^D \leq \Delta Q_{h,max}^D, \forall h \in N_D \tag{3.35}$$

$$\Delta Q_{rc,min}^{cond} \leq \Delta Q_{rc}^{cond} \leq \Delta Q_{rc,max}^{cond}, \forall rc \in N_{rc} \tag{3.36}$$

In addition to these constraints and since the PQ Maps algorithm is based on the OPF concepts, it also inherits the typical OPF restrictions: active and reactive power balance (3.37) and (3.38), voltage magnitude limits (3.39),

voltage angle at the slack bus (3.40), discrete sets concerning tap positions and capacitor banks steps (3.41) and (3.42), direct and inverse branch flows limits (3.43) and (3.44).

$$(\Delta P_n^G + P_n^G) - (\Delta P_n^D + P_n^D) - P_n = 0, \forall n \in N \tag{3.37}$$

$$(\Delta Q_n^G + Q_n^G) + (\Delta Q_n^{cond} + Q_n^{cond}) - (\Delta Q_n^D + Q_n^D) - Q_n = 0, \forall n \in N \tag{3.38}$$

$$V_{n,min} \leq |V_n| \leq V_{n,max}, \forall n \in N \tag{3.39}$$

$$\phi_{ref} = 0 \tag{3.40}$$

$$Q_n^{cond} \in \{Q_n^{cond}\}, \forall n \in N_{rc} \tag{3.41}$$

$$tap_{ij}^t \in \{tap_{ij}^t\}, \forall t \in N_{OLTC} \tag{3.42}$$

$$|S_{ij}^b|^2 \leq (S_{max}^b)^2, \forall b \in B \tag{3.43}$$

$$|S_{ji}^b|^2 \leq (S_{max}^b)^2, \forall b \in B \tag{3.44}$$

where

$$P_n = |V_n| \sum_{k=1}^{N} [|V_k|(G_{nk} * cos\,\theta_{nk} + B_{nk} * sin\,\theta_{nk})] \tag{3.45}$$

$$Q_n = |V_n| \sum_{k=1}^{N} [|V_k|(G_{nk} * sin\,\theta_{nk} - B_{nk} * cos\,\theta_{nk})] \tag{3.46}$$

The activated active and reactive power flexibility in each bus n are illustrated by ΔP_n^G, ΔQ_n^G, ΔP_n^D, ΔQ_n^D ,ΔQ_n^{cond}. In addition, P_n^G, Q_n^G, P_n^D, Q_n^D, Q_n^{cond} state the operating point resulting from the market-clearing mechanism, the DSO Distributed Renewable Energy Sources (DRES) and the net-load forecasts. P_n (3.45) and Q_n (3.46) are the active and reactive flows from the network branches to each bus n.

The mathematical formulation of the optimization problem here described details how it is possible to explore the flexibility perimeter of a PQ map i.e. estimate the active and reactive power limits that can be exchanged at the TSO-DSO interface. However, the update of the objective function parameters ($\boldsymbol{\alpha}$ and $\boldsymbol{\beta}$) together with the constraints above mentioned are only capable to estimate convex flexibility areas. In order to capture the existence of non-convexities a new constraint need to be included in the mathematical formulation, as it will be described in the following.

OPTIMIZATION SOLVER AND ALGORITHMS:

The procedure to identify the flexibility area at the TSO-DSO connection points is composed by several steps:

1. Determine the minimum and maximum values of active power at TSO-DSO connections points as well as the corresponding reactive power - $\varphi = 0°$ and $\varphi = 180°$, so $\alpha = \pm 1$ and $\beta = 0$

2. Determine the minimum and maximum values of reactive power at TSO-DSO connections points as well as the corresponding active power - $\varphi = \pm 90°$, so $\alpha = 0$ and $\beta = \pm 1$

The outcome of these two first steps provides a set of four PQ points in the flexibility area perimeter (maximum and minimum of $P_{DSO \to TSO}$ and $Q_{DSO \to TSO}$). Based on them, it is already possible to have an approximated idea of which will be the upper and lower limits[4] of the flexibility area. The accomplishment of this first stage can be seen as the trigger to start exploring the space between each couple of consecutive PQ points. This second phase aims therefore to find possible non-convexities on the PQ Maps. However, the procedure previously exposed it would be insufficient to capture them since the simple changing of the objective function slope it would always lead to some extreme point of the map. This drawback can be overcome by carrying the following steps:

3. Compute $P_{central} = \frac{P_{max}+P_{min}}{2}$ and $Q_{central} = \frac{Q_{max}+Q_{min}}{2}$ where $P_{max}, P_{min}, Q_{max}$ and Q_{min} are the flexibility area points obtained in steps 1. and 2.

4. For each two consecutive points of the upper and lower limits $(P_i, P_{i+1}, Q_i, Q_{i+1})$, if the convergence criteria is not met, the following constraint (3.47) should be added to the optimization problem:

$$P_{DSO \to TSO} = m * \ Q_{DSO \to TSO} + b \tag{3.47}$$

where $m = \frac{P_{central} - (\frac{P_i + P_{i+1}}{2})}{Q_{central} - (\frac{Q_i + Q_{i+1}}{2})}$ and $b = P_{central} - (m * Q_{central})$. Geometrically, this equality constraint represents a straight line that intersects $P_{central}/Q_{central}$ as well as the mid-point between i and $i+1$. In other words, this new constraint reduces the search space to the number of points intersected by the straight line. The last step is to define the search direction since more than one PQ point can satisfy the above mentioned constraint although the goal is to find the one between i and $i+1$. To do so, a comparison between the central point and the mid-point between i and $i+1$ needs to be carried:

$$if(Midpoint\ P > \ P_{central}) \to \ \boldsymbol{\alpha} = \ \mathbf{-1} \to Maximizing\ P_{DSO \to TSO}$$

$$if(Midpoint\ P < \ P_{central}) \to \ \boldsymbol{\alpha} = \ \mathbf{1} \to \ Minimizing\ P_{DSO \to TSO}$$

In case $Midpoint\ P = \ P_{central}$, a similar comparison in terms of Q can be performed and β updated.

[4] The lower and upper limits are defined with respect to active power

Step 4 thus illustrates a closed loop that only stops when the convergence criteria are reached - Euclidean distance between two consecutive points and their reactive power distance.

$$\frac{\sqrt{\left(\frac{P_i - P_{i+1}}{P_{max} - P_{min}}\right)^2 + \left(\frac{Q_i - Q_{i+1}}{Q_{max} - Q_{min}}\right)^2}}{\sqrt{2}} < \sigma \tag{3.48}$$

$$\sqrt{\left(\frac{Q_i - Q_{i+1}}{Q_{max} - Q_{min}}\right)^2} < \varepsilon \tag{3.49}$$

The definition of the σ and ε thresholds depends on the accuracy level that the user wants to obtain in the PQ Maps. It can vary between 0 and 1 since the expressions stated in (3.48) and (3.49) already illustrate the normalized distances.

The methodology here presented not only allows the estimation of non-convex flexibility areas as well as avoids an exhaustive search of PQ points in their perimeter. Figure 22 sums up the main steps of the PQ Maps algorithm that were previously described.

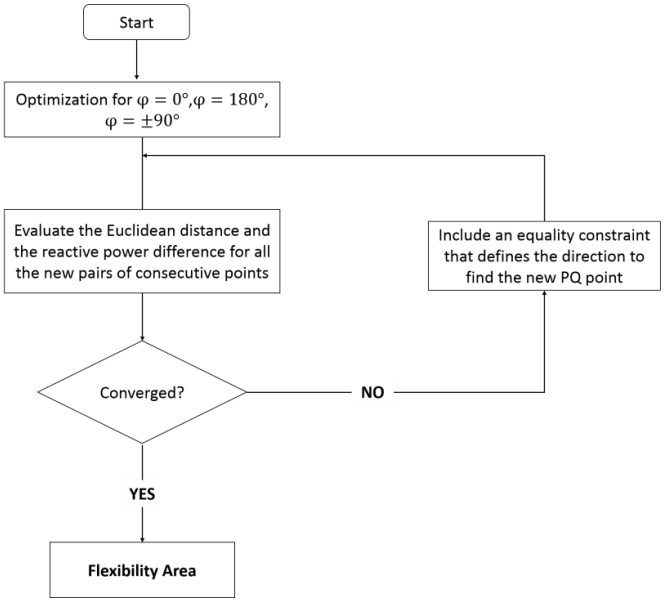

FIGURE 22 – FLEXIBILITY AREA IDENTIFICATION PROCESS

As detailed in last sections, the development of PQ Maps demands for the execution of OPF algorithms. A non-commercial solver fully developed by INESC TEC was used to fulfil this need. It is based on the primal-dual interior point method and fully exploits the sparsity of the optimization problem. This interior point method version i.e. primal-dual does not ensure mathematical stability in the process of finding the global optimum and shows some sensitivity to the starting solution/initial point. However, the global optimum search is a common problem to every optimization method, whether they are classical or based on artificial intelligence techniques. Considering this common drawback, the primal-dual method was selected to address this optimization problem due to two main reasons. Although the prima-dual method only ensures the global optimum for convex problems, it has a vast application to non-convex problems and, in particular, to the OPF due to its robustness. The results available on the literature show a good trade-off between optimality and computational burden. On the other hand, from

the experience obtained during the several tests that were carried out, stability on the final solution was obtained considering different starting points. In [20], this numerically stability is highlighted. Despite this, the developed methodology is flexible enough to allow the application of other optimization algorithms without affecting its effectiveness.

INTERNAL DATA MODEL AND PROGRAMMING LANGUAGES:

The PQ Maps methodology is entirely developed in C++ and makes use of some third party libraries to carry parsing processes and to enhance the computational performance of the algorithm. All these external libraries are publicly available and free of charge. Among them, Eigen [21] as a linear algebra library is one of the most important since in addition to the typical manipulation of vectors and matrices also allows to exploit sparse matrix techniques. Thanks to it, the computational burden usually associated to complex optimization algorithms can be overcome.

Building up the internal data model (e.g., C++ classes, sparse matrices) also requires parsing the input data. The development of the flexibility areas is mainly dependent of three different inputs that usually are provided by different operational systems: current network topology (e.g., grid electrical characteristics, physical connections, switching devices status), load and RES forecasts and flexibility availability. In which concerns the grid topology, the tool benefits from embedded support for data exchange in formats compatible with the latest standards - ENTSO-E CIM derived model CGMES. For the remaining input data, dedicated JSON structures were created and a JSON parser is employed in order to make use of this lightweight data-interchange format together with the internal C++ structures. The choice for JSON is mainly explained by two reasons: programming language independent and availability of collections of key/value pairs, which makes straightforward the description of timely dependent data.

The PQ Maps tool can be used as a standalone executable file (.exe) or as a pre-compiled static/dynamically linked library, which provides the necessary flexibility to integrate with other programming language rather than C++.

KEY ASSUMPTIONS AND BOUNDARIES OF THE METHOD

The PQ Maps methodology is a robust algorithm capable to provide contributes both for planning purposes and for real-time operation due to its interesting characteristics in terms of computational performance. The employment of the aforementioned Eigen library enables for fast linear algebra operations due to the exploitation of sparse matrix techniques. In addition, the PQ Maps is capable to deal with distribution grids with several non-interconnected parts. This means that it is capable to provide flexibility maps for more than one network island in a single execution of the algorithm. That being said, the main boundary of the optimization method is the quality of the input data (e.g., load and RES forecasts, flexibility modulation). Since the main goal of this methodology is to act as a decision-support process, the quality of the input data is of utmost importance in order to provide realistic estimations to the system operator.

The presented approach to develop PQ Maps is only accurate if considering an individual primary substation i.e. PQ flows keep unchanged in remaining substations. Therefore, the knowledge of the transmission network is necessary to overcome this drawback. One way of “knowing” the transmission network is the development of a network equivalent, as described in the following sections.

3.6.2 TRANSMISSION NETWORK EQUIVALENTS

The inclusion of transmission network equivalents allows estimating the total active and reactive power limits that can be exchanged in all the TSO-DSO interfaces while knowing how these fluxes redistribute themselves through each one of these connection points. That being said, the information about mutual dependencies is crucial to support the coordinated flexibility activation procedures between DSO and TSO (if this information would not be considered as a premise, then the PQ Maps estimation would be erroneous). The usage of a network equivalent rather than the full transmission network model is motivated by two main reasons. First of all, algorithm computational effort whereas all the data that would be required from detailed transmission and distribution networks. This would affect the processing time and therefore could be a problem for short-term analysis. Secondly, confidentiality issues concerning transmission network data accessible to the DSO and vice versa.

The innovation of this methodology is therefore the capability to provide more reliable information concerning the power flow that can be exchanged in the TSO-DSO grid connection points. In other words, the new PQ Maps algorithm illustrates the real PQ limits that the power flow at TSO-DSO interface can assume through feasible flexibility activations of DER.

OPTIMIZATION OBJECTIVES:

Contrary to what happens in the classical methods, the proposed approach to develop transmission network equivalent models is only based on the knowledge of AC quantities at the TSO-DSO interface nodes – $\mathrm{V}, \theta, \mathrm{P}, \mathrm{Q}$ – for a representative range of operation conditions. Departing from this target data, a metaheuristic – Evolutionary Particle Swarm Optimization (EPSO) [22], [23] – will be applied to fine-tune the parameters of a reduced network model ($\mathrm{V_g}, \mathrm{r}, \mathrm{x}, \mathrm{b}$ - Figure 23).

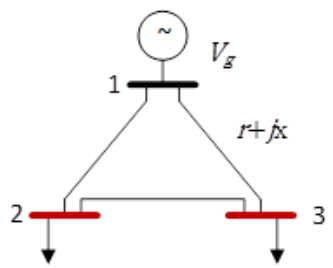

FIGURE 23 – EQUIVALENT NETWORK MODEL (TSO-DSO INTERFACE NODES IN RED).

The purpose of this procedure will be that the AC load flow results using the equivalent network are as close as possible to the ones observed in the target data.

$$Fitness\ f. = 1 \times 10^{10} \sum_{t=1}^{T} \left(\sum_{i=1}^{CN} \left(V_i^{Equiv} - V_{i,t}\right)^2 + \sum_{i=1}^{CN-1} \left(\left(\theta_i^{Equiv} - \theta_{i+1}^{Equiv}\right) - \left(\theta_{i,t} - \theta_{i+1,t}\right) \right)^2 \right) \quad (3.50)$$

where *T* denotes the number of operation scenarios and *CN* the number of connection nodes. Therefore, V_i^{Equiv} and θ_i^{Equiv} represent the voltage magnitude and angle at TSO-DSO interconnection i as a result of the AC load

flow run considering the transmission network equivalent. On the other hand, $V_{i,t}$ and $\theta_{i,t}$ have the same meaning, but concern to each t operation scenario of the target data. The voltage magnitude is measured in the p.u. unit system and the angles in radians.

As described by equation (3.50), the fitness function only aims to minimize the squared error, for the voltage magnitudes and angle at the interface nodes, between the two data sets. The fact that a single voltage set-point - V_g - can be defined at the slack bus generator prevents the possibility of replicate all the AC quantities. Therefore, in the AC load flow calculations to define the equivalent model, the active and reactive power flows at the interface nodes will be imposed. Other particularity of this fitness function regards to the voltage angle error that is being computed based on the angle difference between the TSO-DSO connection points. Although this means that θ_i^{Equiv} can be very different from $\theta_{i,t}$ at the end of the process, no particular issue arises from it. The accuracy on the development of the equivalent model is not affected since the coupling between the interface nodes remains unchanged. Following this approach, it is avoided the existence of large flows in the equivalent network – which could lead to models with less quality – so that the angle difference between the slack and the interface nodes could be created.

One of the common boundaries associated with the development of network equivalents is related with the existing dependency between them and the system operation conditions. In other words, a transmission network equivalent that is accurate in one operating scenario can lead to erroneous analysis in other scenarios. These situations are mainly associated with cases where the TSO-DSO interfaces are geographically distant, which usually can be translated into very different operating scenarios depending on the season and hour of the day (peak or valley). In such cases, it becomes a difficult task to develop a unique transmission network equivalent that encompasses all the scenarios of operation. To overcome this potential drawback, a clustering procedure based on different variables of the TSO typical operation is carried out. In addition to the already mentioned V, θ, P, Q in the TSO-DSO interface nodes, one-year of hourly historical data of Hydro and Wind Power active power injection as well as the total active and reactive power produced in the transmission side is used. Departing from this input data, the clustering process thus aims to define typical operation scenarios of the transmission network and consequently an optimal number of network equivalents to be developed. This clustering procedure can be divided in the following steps:

1. Pre-process the available historical data so that an efficient and meaningful analysis can be performed. Therefore, the first step of the clustering approach is the outliers' detection and removal. This helps to identify significant data trends and removes potential noise. The *rmoutliers* function available in Matlab® is used for this purpose.
2. Apply to the refined dataset a clustering technique named *k*-means aiming to partition *n* observations into *k* mutually exclusive clusters. This process assigns each dataset point to a cluster by minimizing the distance between it and the mean of its assigned cluster.

The number of *k* clusters is an input that needs to be provided to the *k*-means function. Sometimes, the data to be clustered contains natural divisions, which easily tell the user the appropriate number of clusters. However, in most cases, these divisions do not exist or are unknown. Thus, it is necessary to determine how well the date fits

into a specific number of clusters. To do so, a Matlab® function - *evalclusters* – capable to determine the optimal number of clusters is employed. This function can use different methods to perform this assessment e.g., Davies-Bouldin, Gap, Silhouette. In this specific case, the Silhouette approach proved to be effective in measuring how similar a data point is to its own cluster when comparing to the remaining ones.

In addition to the merits already described, the employment of the above mentioned steps allows to reduce the initial *T* operation scenarios (3.50) into 1 scenario per cluster. This scenario corresponds to the centroid of the clusters. As it will be shown in this deliverable, the usage of the centroid as target data is enough to achieve a proper transmission network equivalent. Thanks to this, the parameter tuning of the reduced network model performed by EPSO becomes much faster. Apart from the designing of the network equivalents is then necessary to understand which one of them is the most adequate to be used depending on the real-time/forecasted operating scenario. Therefore, a binary decision tree for classification is employed using *fitctree* Matlab® function. Ideally, the data used for training this decision tree would be composed by the set of eight variables that define the transmission network typical operation. However, from this set, only the Hydro and Wind power active power injection as well as the total active and reactive power produced in the transmission side are usually public available in near real-time/forecasting. Considering this, it does not make sense to train the decision tree with all the variables that compose the historical data. The constructed decision tree is then used to predict the cluster to which a specific operation scenario belongs. Figure 24 sums up the aforementioned clustering process.

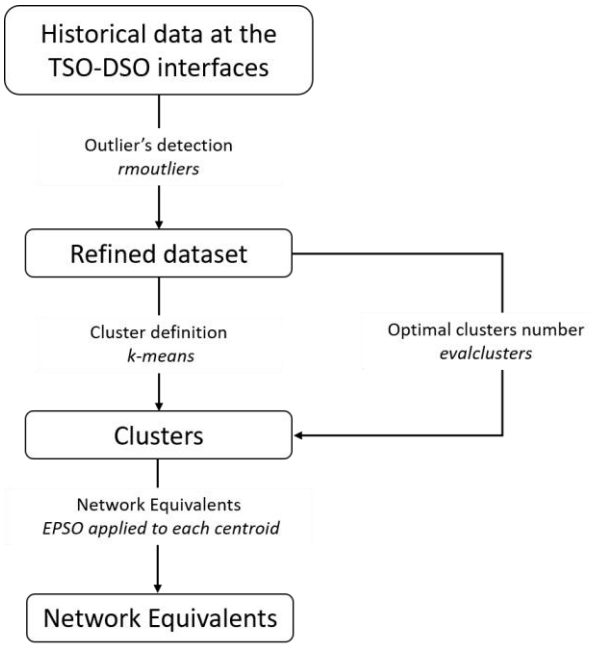

FIGURE 24 – DEFINITION OF THE NECESSARY NUMBER OF TRANSMISSION NETWORK EQUIVALENTS

BOUNDARIES AND CONSTRAINTS:

Going into detail regarding the boundaries and constraints of this algorithm only makes sense after a brief introduction about the chosen metaheuristic. As well as other approaches (e.g., Particle Swarm Optimization (PSO), Evolution Strategies (ES)), EPSO relies on the Darwin's natural selection paradigm to promote search towards the optimum. Concepts as reproduction (mutation and recombination) and selection are applied to a given population of particles. This entire process is also influenced by factors such as inertia, memory, and cooperation that try to emulate the existing social interaction between groups of animals. EPSO exploits the recognized novelties of previous methods (e.g., natural selection and self-adaption techniques typical of ES, PSO capabilities to speed-up the search without an excessive parameter tuning) while introduces new ideas. One of them is the Stochastic Star Communication Topology [23] that aims to constrain the information exchanged concerning the global best position found so far. This promotes the existence of pure cognitive movements, which proven to be very interesting to guide the search.

In the EPSO formulation, a new particle position ($\mathbf{X}_t$) is obtained from its ancestor ($\mathbf{X}_{t-1}$), from its best ancestor ($\mathbf{X}_b$), from the best position found so far ($\mathbf{X}_{gb}$) and from its current velocity ($\mathbf{V}_t$), as described below:

$$\mathbf{V}_t = w_i^* \mathbf{V}_{t-1} + w_m^* (\mathbf{X}_b - \mathbf{X}_{t-1}) + w_c^* \mathbf{C}\left(\mathbf{X}_{gb}^* - \mathbf{X}_{t-1}\right) \tag{3.51}$$

$$\mathbf{X}_t = \mathbf{X}_{t-1} + \mathbf{V}_t \tag{3.52}$$

where t illustrates the current particle generation and C is a diagonal matrix of Bernoulli variables with success communication probability P. A new matrix C is sampled in every t generation. Concerning the superscript *, it indicates the existence of a mutation process on the top of the corresponding parameter. A simple additive expression rules the mutation of a generic weight w:

$$w^* = w + \tau N(0,1) \tag{3.53}$$

where $N(0,1)$ is a number sampled from the standard Gaussian distribution and τ represents the mutation rate. All the weights shown in (3.51) must be within 0 and 1 and are also included in the selection process i.e. individuals that are part of next generations must keep their weights. A similar procedure is followed for the mutation of the global best position.

The description above provided only gives a high level view of the EPSO algorithm, but already allows to understand that the characterization of each particles position, $\mathbf{X}_t$, depends on the type of optimization problem. In the specific case exposed in this deliverable, V_g, r, x, b (Figure 23) are the decision variables that characterize the current position of each particle. Therefore, these parameters evolve and mutate throughout the entire process so that the fitness function can be minimized. However, this set of variable does not directly provide the V_i^{Equiv} and θ_i^{Equiv} that can be seen in the fitness function (3.50). This is why on the top of each particle (or each set of V_g, r, x, b) a Power Flow study is carried. Considering this, obviously the EPSO algorithm itself does not have any constraint, but the Power Flow analysis that must be carried needs to ensure the fulfilment of the active and reactive power balance equations.

OPTIMIZATION SOLVER AND ALGORITHMS:

Now that the basic concepts of the EPSO algorithm were explained and its materialization into a practical problem was carried out, some more details of how the population of individuals evolves throughout the generations need to be provided. The following steps help to understand this process:

1. A population of ***m*** particles is **initialized** as well as several optimization parameters (number of replicas per particle ***r,*** communication probability ***P***, mutation rate ***τ***, maximum number of iterations ***T***)
2. This initial population is **evaluated**, which can be translated into the definition of the personal and global best positions. The memory is also updated in this step.
3. The algorithm enters in a **while** loop, for which the conditional test is the number of iterations. These might be equal or lower than the maximum number of iterations defined by the user **(*t* ≤*T*)**. During this loop:
    a. Each particle ***m*** is **replicated *r*** times
    b. The strategic parameters of each ***r*** replicas are **mutated**
    c. Each particle ***m*** and its ***r*** replicas are **moved** accordingly equations (3.51) and (3.52). Figure 25 also illustrates very well these movement rules
    d. Compare each particle ***m*** with its ***r*** replicas, **select** the one with the best fitness (3.50) and include it in the new position
    e. Update the global best position

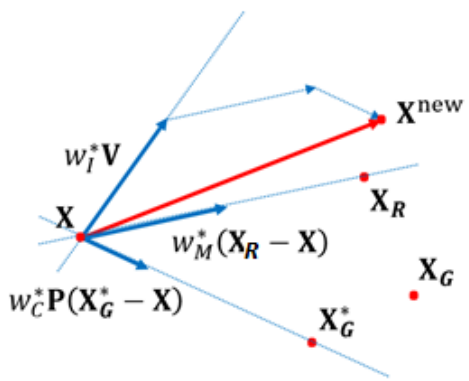

FIGURE 25 – ILLUSTRATION OF EPSO MOVEMENT EQUATION

The Power Flow studies mentioned above were carried out using the default solver of Matpower [24] (package of Matlab® M-files for solving power flow and optimal power flow problems), which is based on a standard Newton's method [25] using a polar form and a full Jacobian updated at each iteration. Concerning the EPSO, the algorithm is non-commercial and entirely developed by INESC TEC.

INTERNAL DATA MODEL AND PROGRAMMING LANGUAGES:

The proposed approach is fully developed in Matlab® and, as already mentioned, uses an external package – Matpower – in order to carry out Power Flow studies. One of the main reasons for using this package concerns to

the fact that it exploits the problem sparsity, which is always of utmost importance when dealing with complex problems.

As well as for the PQ Maps algorithm, the internal data model needs to be fed with input data that should follow particular formats. Particularly, the AC quantities of historical data representing the transmission network operating scenarios should be provided in .csv files.

KEY ASSUMPTIONS AND BOUNDARIES OF THE METHOD

As previously mentioned, it is evident that a single transmission network equivalent cannot illustrate all the different operating conditions of a transmission grid. This usually represents the main boundary associated with this type of approaches. The employment of the described clustering procedure allowed overcoming this issue by defining the optimal number of network equivalents to be designed. Based on them, a vast range of different operation conditions can be properly illustrated. Other boundary associated with the network equivalent methods concerns to the difficulty in catching potential constraints arising in the transmission network operation (e.g., Voltage or overloading problems). These methodologies are usually suited to illustrate how the fluxes in the transmission network redistribute themselves, but not to embed this type of information. Nevertheless, when there is no knowledge of the transmission grid, the usage of network equivalents is still a better option when comparing of only considering the distribution side.

3.6.3 PQ MAPS TEST CASES USING TRANSMISSION NETWORK EQUIVALENTS

The test cases carried to evaluate the effectiveness of the PQ Maps and transmission network equivalent algorithms used a modified version of the single-area variant of the IEEE Reliability Test System (RTS) [26]. Figure 26 shows the one-line diagram of the original single-area variant of the RTS-96. For the test case purposes, buses 1 to 10 illustrate the distribution grid while the remaining ones compose the transmission network. The modifications employed in this test network included the removal of the transformer connecting buses 3-24 so that only two TSO-DSO interfaces nodes remained. Therefore, the transmission network equivalent focus on the interdependencies between the primary substations connected to buses 11 and 12. In addition, the transformers connecting buses 11-10 and 12-9 changed their configuration and now connect buses 11-9 and 12-10. Therefore, the connections between buses 11-9 and 12-10 are composed by two parallel transformers. This being said, this modified version can be characterized as follows:

- 24 grid nodes divided in equal parts for the distribution and transmission sides
- 33 transmission lines, therefore 12 belonging to the distribution network
- 4 transformers 230/130 kV representing the TSO-DSO connections
- 7 different types of generation technologies within a total of 54 generators throughout the distribution and transmission grids – hydro, wind, PV, nuclear, steam coal and oil and a synchronous compensator.

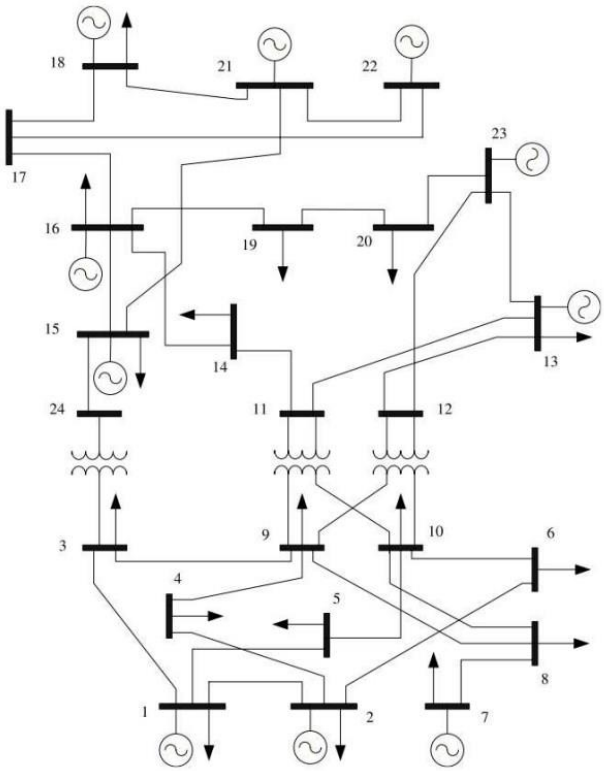

FIGURE 26 – 24-BUS POWER SYSTEM OF THE SINGLE AREA RTS-96

Since this 24-bus network is a test system, no historical data was available to describe the typical operation of the transmission network. Therefore, load and generation time series provided by the National Renewable Energy Laboratory in GitHub [27] were used to characterize the different scenarios of operation that can be observed in a transmission grid during one year of time horizon. Departing from this input, 8784 OPF's i.e. hourly OPF's for the entire year were run so that historical data concerning the needed AC quantities at the TSO-DSO interface nodes – V, θ, P, Q – were available. In the possession of this information, the conditions to develop the transmission network equivalents and consequently the PQ Maps were achieved. The testing procedure is divided in five different steps:

1. Clustering of the historical data
2. Development of the network equivalents
3. Computation of the PQ Maps with the complete knowledge of the grid (Transmission + Distributions)
4. Computation of the PQ Maps with information concerning only to the distribution side
5. Computation of the PQ Maps with the network equivalents

By comparing the different PQ Maps will be possible to understand the need for the transmission network equivalents and how accurate they are.

3.6.4 PQ MAPS EXAMPLARY SIMULATIVE RESULTS USING TRANSMISSION NETWORK EQUIVALENTS

The first results to be shown concern the clustering procedure and allow the conclusion that an entire year of operation can be clustered into four different sets. Figure 27 shows the dispersion of the dataset points while comparing the voltage magnitudes in each one of the interface connections between the transmission and distribution grids. A set of 8 different variables were used to develop these clusters:

- V, θ, P, Q in the TSO-DSO interface nodes
- Hydro and wind active power injection in the transmission side
- Total active and reactive power produced in the transmission grid

It becomes evident that the voltage magnitudes in the interface nodes have a clear impact for the clustering process. In other words, Figure 27 shows that a very well-defined range of voltage magnitudes is associated to each cluster. An exception to this well-defined association can be observed in cluster number 2. In fact, the arising of this cluster is more associated with other variables of the aforementioned set. Therefore, the set of 8 different variables used as input for the clustering procedure provided four different clusters and the voltage magnitudes had a clear influence on the arising of three of them.

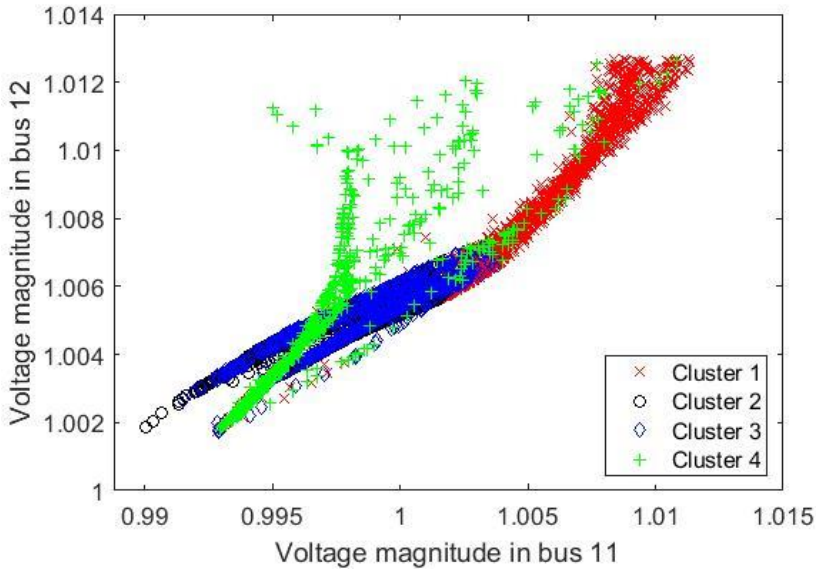

FIGURE 27 – CLUSTERS FOCUSING ON THE VOLTAGE MAGNITUDES ON THE TSO-DSO INTERFACES

Based on these clusters, four different centroids were defined as shown in Table 4. Using them, it is then possible to develop four different network equivalents that allow mapping the typical operating conditions of a transmission network.

TABLE 4 – CENTROIDS CORRESPONDING TO EACH ONE OF THE DEFINED CLUSTERS

V11 (p.u.)	V12 (p.u.)	$\theta 11 - \theta 12$ (Degrees)	P 9-11 (MW)	Q 9-11 (Mvar)	P 10-12 (MW)	Q 10-12 (Mvar)
0.9979	1.0049	2.6805	203.8809	26.2905	192.4091	-44.2483
1.0051	1.0083	2.6002	290.0649	42.1285	281.2053	-29.9945
0.9978	1.0057	3.3207	304.8866	35.0668	287.4517	-35.4316
0.9987	1.0051	3.0408	217.9157	28.0447	198.8326	-43.3914

P Hydro (MW)	P Wind (MW)	P Generation in TSO side (MW)	Q Generation in TSO side (Mvar)
116.5585	59.9882	963.4168	111.1147
145.0077	55.0283	1304.6749	270.5550
144.4088	394.2166	1366.8750	454.7786
96.2694	395.9512	990.0313	228.9158

The EPSO algorithm employed took 3m 20s to define the four reduced network models. For all of them, the fitness function achieved the minimum of zero since the target data is only composed by one observation that corresponds to the corresponding centroid. Table 5 shows the equivalent parameters after fine-tuned by the EPSO.

TABLE 5 – PARAMETERS OF THE TRANSMISSION NETWORK EQUIVALENTS

	Cluster 1	Cluster 2	Cluster 3	Cluster 4
Vg1 (p.u.)	1.0110	1.0008	1.0996	1.0094
R 1-2 (p.u.)	0.0018	0.0011	0.0324	0.006
X 1-2 (p.u.)	0.0021	0.0012	0.0061	0.0176
B 1-2 (p.u.)	0.2590	0.4660	0.4998	0.4601
R 1-3 (p.u.)	0.0028	0.0010	0.0369	0.0117
X 1-3 (p.u.)	0.0184	0.0289	0.0236	0.0448
B 1-3 (p.u.)	0.2636	0.1724	0.4579	0.2205
R 2-3 (p.u.)	0.4958	0.1896	0.2880	0.1714
X 2-3 (p.u.)	0.2177	0.0654	0.3089	0.2096
B 2-3 (p.u.)	0.0028	0.0271	0.0451	0.0665

With the knowledge of the transmission network equivalents it is possible to build reliable PQ Maps. The tests shown in this deliverable focus on a specific time instant of the historical data – 1st January at 12h. In this test case, the resources connected to buses 1 and 2 of the distribution network were able to provide active and reactive power flexibility both in the upward and downward directions. The amount of flexibility available corresponded to 20% of their current active and reactive power injections. Figure 28 compares the PQ map obtained with the full knowledge of the transmission network and the one achieved only considering the distribution network. These maps illustrate the total active and reactive power limits that can be exchanged through both primary substations.

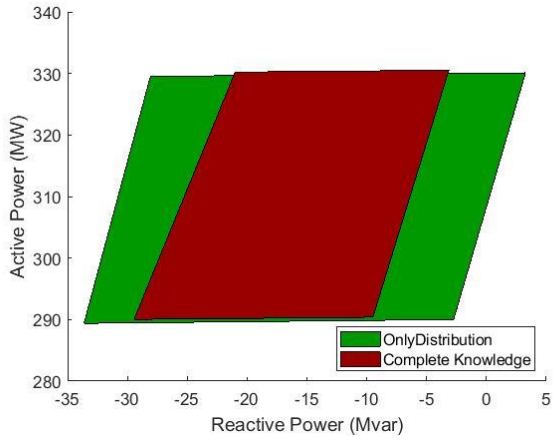

FIGURE 28 – PQ MAPS WITH DIFFERENT LEVELS OF KNOWLEDGE OF THE GRID TOPOLOGY

This result makes evident that there is a significant over-estimation in terms of reactive power limits that can be exchanged when only considering the distribution network. This highlights the need for knowledge of the transmission network e.g. in form of an equivalent. To overcome this drawback, the first test performed used a dummy network equivalent i.e. a network structure such as the one presented in Figure 23, but without any parameter tuning. Very small values of resistance, reactance and line susceptance were employed and a voltage magnitude of 1 p.u. was used in the slack bus. The results are shown in Figure 29.

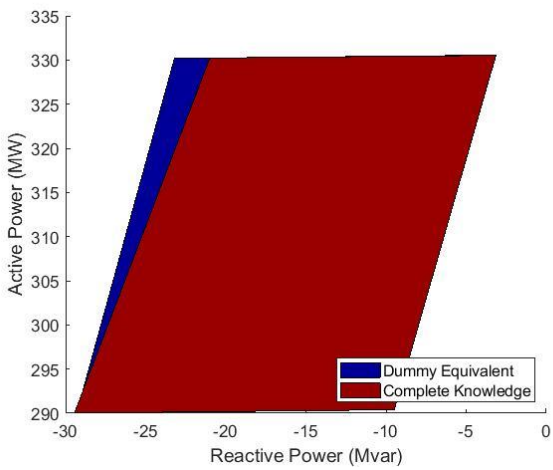

FIGURE 29 – THE IMPACT OF A DUMMY NETWORK EQUIVALENT IN THE PQ MAPS

From this result, it can be concluded that without any kind of parameter tuning it is possible to have a very good approximation of the real PQ map. The explanation behind this peculiar result is the following: when only considering the distribution network, the maximization/minimization of the power flow exchanged between the TSO and the DSO is being simultaneously performed in two different points i.e. the two primary substations. This was causing direct reactive power flows between them, which had nothing to do with the available flexibility. In other words, one primary substation was consuming more reactive power so that the other one could inject more. Of course, this would lead to an erroneous result. When only performing the maximization/minimization procedures using the slack bus of the network equivalent, these reactive power flows disappeared, and the PQ become much more realistic.

Despite this interesting result, it becomes clear that the true novelty of a proper network equivalent is the capability to illustrate how the active and reactive power flows are redistributed through the different primary substations. Figure 30 shows this redistribution per TSO-DSO interface when considering the full knowledge of the transmission grid and with the previous dummy equivalent. In other words, these PQ Maps illustrate how the maximization/minimization of the power flow exchanged between transmission and distribution grids impact on the flow of each primary substation.

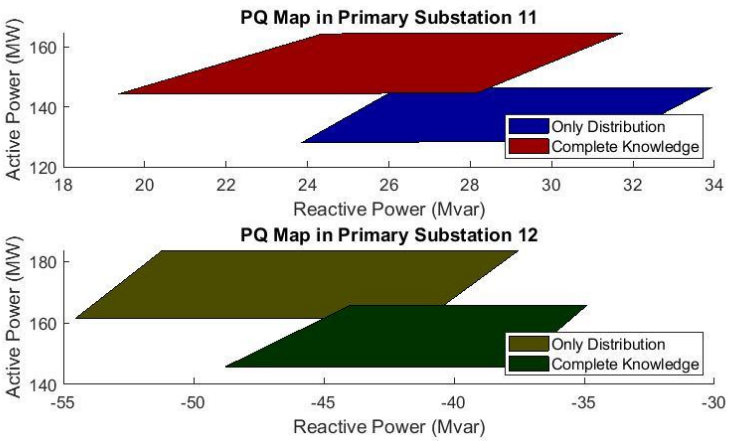

FIGURE 30 – FULL KNOWLEDGE OF THE TRANSMISSION NETWORK VS DISTRIBUTION NETWORK FOR COMPUTING PQ MAPS PER PRIMARY SUBSTATION

As expected, the usage of a dummy network equivalent would clearly lead to a bad estimation of the active and reactive power flows redistribution. The following test is to include the network equivalent computed using the EPSO algorithm. The time instant that is being analyzed in these test cases corresponds to cluster Nº4, thus the respective network equivalent must be used.

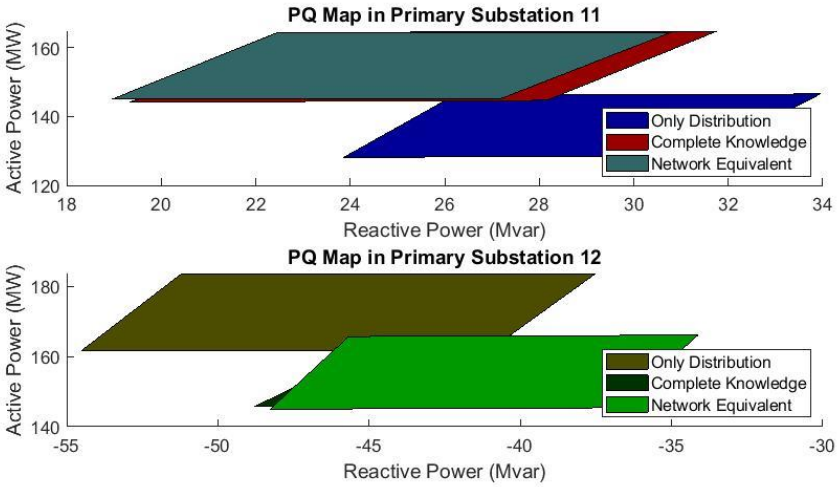

FIGURE 31 – THE IMPACT OF A ROBUST NETWORK EQUIVALENT IN THE PQ MAPS

Figure 31 shows the true novelty behind the presented approach. The accuracy of the developed transmission network equivalent allowed performing a very good estimation of the PQ Maps for more than one TSO-DSO interconnection. Therefore, it is not only possible to estimate the total PQ power that can flow though several primary substations as well as understand how these power flows are redistributed through each one of them. With this significant contribution for the current state of the art, one of the drawbacks associated with the PQ mMaps is now overcome. Although the presented test case only regards to a specific period, the methodology was validated using different time instants.

In order to understand the importance of the clustering process, a final test using a network equivalent from another cluster was carried out. To have a clear image, Figure 32 only shows the PQ Maps obtained with the correct network equivalent and with the one belonging to the other cluster. As can be observed in Figure 32, the usage of an inappropriate network equivalent leads to an erroneous estimation of the PQ Maps.

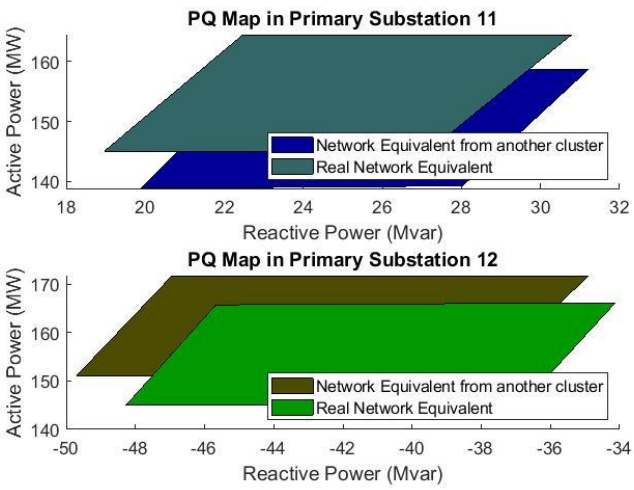

FIGURE 32 – THE IMPACT OF USING AN INAPROPRIATE NETWORK EQUIVALENT

3.7 CONCLUSION AND OUTLOOK

The fulfillment of the main objectives associated with the German demonstrator is ensured with the two tools that were developed by the two involved partners, Fraunhofer IEE and INESC TEC, in collaboration with the DSO MITNETZ:

The optimization tool of partner Fraunhofer IEE uses an interior point algorithm performing non-linear optimizations of extended load flow problems. Within the scope of this demonstrator, the algorithm was modified in order to calculate set-points for several generating units in the DSO grid taking into account various boundary conditions like voltage magnitudes, current limits as well as avoiding (n-1) problems. The algorithm is operating in real-time even for networks with a large number of nodes and can be adapted to several different needs of system operators (TSOs as well as DSOs). These features make it suitable for the analysis of transmission and distribution networks with a certain amount of flexible resources guaranteeing optimal operational set-points for these units. In order to achieve these goals and fulfil the constraints, new functionalities have been added to the core algorithm for exploiting this tool in the context of the German demonstrator within the EU-SysFlex project: consideration of several different reactive power capabilities based on active power infeed or voltage magnitudes as well as the introduction of a “load angle” constraint (ratio between active and reactive power), which allows limiting the reactive power flow within lines in relation to the active power values. Additionally, several hard constraints are moved to the objective function to ensure solvability of the given problem at any time. Nevertheless, this will only occur in case of an already unsecure grid layout which should be optimized (the grid which is being given to the optimization tool is not (n-0)/(n-1) secure and this problem cannot be solved modifying the generation only). Of course, it is being reported if an optimal solution could not be found due to such an event. Apart from that, the calculated flexibility can be requested without any problem relating any violated network constraints. The resulting optimization tool is capable to carry out the functionalities described in the SUCs presented in D6.1 [31], adequately fitting in the business process defined for the German demonstrator. Simulations of network scenarios with different shares of controllable resources allowed testing the capabilities of the optimization tool. They lead to accurate and realistic results and returned valuable knowledge for the field tests of Task 6.4. At the moment, the optimization tool takes only a single set-point into account like controlling the active power magnitude at a single grid connection point. In case of corresponding demands of the system operator, the objective function of the optimization can be modified to take into account multiple demands.

Additionally, the innovative approach of the PQ Maps, developed by partner INESC TEC, provides the degrees of PQ-flexibility available for the EHV grids of a TSO by exploiting the flexible resources available in the HV networks belonging to the DSO. The proof of concept concerning the need and the impact of using robust transmission network equivalents for achieving reliable PQ Maps was carried in this deliverable. The performed test cases allowed understanding how important a prior clustering process is for a proper definition of the network equivalents. This improved version of the PQ Maps algorithm provides a step towards a reinforced cooperation between the distribution and transmission system operators. That should lead to improved system security, in a context of increasing penetration of DRES/DER. Services such as the technical validation of flexibility and cross-actor exchange of information are now empowered with a methodology capable to support their inherent tasks.

Both tools developed in the scope of the German demonstrator have a direct contribution to the fulfillment of its inherent objectives:

- The NETOPT tool is capable to calculate active as well as reactive power flexibilities taking into account several presently existing conditions like actual feed-in and the operation modes of the flexible units.
- Using NETOPT, various constraints like (n-1) security, voltage limits, load angle restrictions are taken into account. Additional limitations could be defined easily.
- Different set-points relating the TSO-DSO connection point/points have been computed, leading to optimized, individual set-points for the controllable flexible units in the DSO grid.
- Even in case a desired request (set-point) relating the TSO-DSO connection point/points cannot be realized, the optimization algorithm of NETOPT ensures optimal system operation.
- The PQ Maps tool is capable to enhance the exchange of information between TSO and DSO. The key behind this enhancement is the ability to show how flexibility exploitation can impact on the TSO-DSO interfaces without disclosing confidential information e.g., topology data.
- The German demonstrator set-up is applied in a part of the German 110kV high voltage distribution network that has more than one CGP to the extra-high voltage side. The new version of the PQ Maps is suitable for this type of networks since has the capability to compute transmission network equivalents. Therefore, is possible to empower both TSO and DSO with the knowledge of how the active and reactive power flows are redistributed throughout their several interfaces. Once again, this information is provided without disclosing confidential information.
- The entire process carried within the PQ Maps algorithm examines the potential of the available flexibility resources while complying with congestion and voltage constraints.

4. OPTIMIZATION IN THE ITALIAN DEMONSTRATOR

The Italian demonstrator is built up in a portion of a MV distribution network, heading to a single HV/MV primary substation (TSO-DSO interface), characterized by high PV penetration and low load consumptions. Due to frequent back-feeding phenomenon, this network has been selected for testing smart grid solutions: the network control system integrates a new generation of Intelligent Electronic Devices (IEDs) - allowing the remote control of some flexible generators – and an advanced network calculation platform, which allows to run techno-economic optimization procedures aimed to efficiently manage flexible resources. In addition to private RES, the Italian demonstrator includes also some DSO-owned flexible resources: one 1 MVA/1 MWh Battery Energy Storage System (BESS) directly connected to a node along the feeder and two 1.2 MVAr Static Synchronous Compensators (STATCOMs) modules directly connected to the MV busbars in the Primary Substation. The activities of the Italian demonstrator will investigate the potential of these assets in supporting the ancillary services provision from distributed resources.

The purpose of the Italian demonstrator, within the project framework, is to analyze how the DSO (and/or a local Market Operator) can manage the full portfolio of flexibilities in order to support ancillary service provision to the TSO network. This process was modelled in Task 3.3 and is presented in Deliverable 3.3 through two Business Use Cases: the first one (IT-AP) describes a business process focused on provision of active power flexibilities from distribution grid for mFRR/RR and congestion management services; the second one (IT-RP) describes a business process focused on the management of the reactive power exchange at primary substation interface, for supporting voltage control and congestion management services. These goals must be necessarily achieved guaranteeing secure operations of the distribution grid; therefore, these business processes need, specifically, the support of functions for network techno-economical optimization.

These functions were modelled in Task 6.2 and are presented in Deliverable 6.1 in two System Use Cases. They describe, respectively: the optimization of the distribution network in presence of active power flexibility bids and their aggregation in a power/cost parametric curve (IT - AP OP); the optimization of the distribution network in presence of a reactive power constraint at primary substation (IT – RP OP). The optimization tool presented in the next sections has been developed to carry out the functionalities that support the above-mentioned system functions; a schematic overview of the links between Use Cases (Business and System), functionalities and developed tools, is presented in Figure 33.

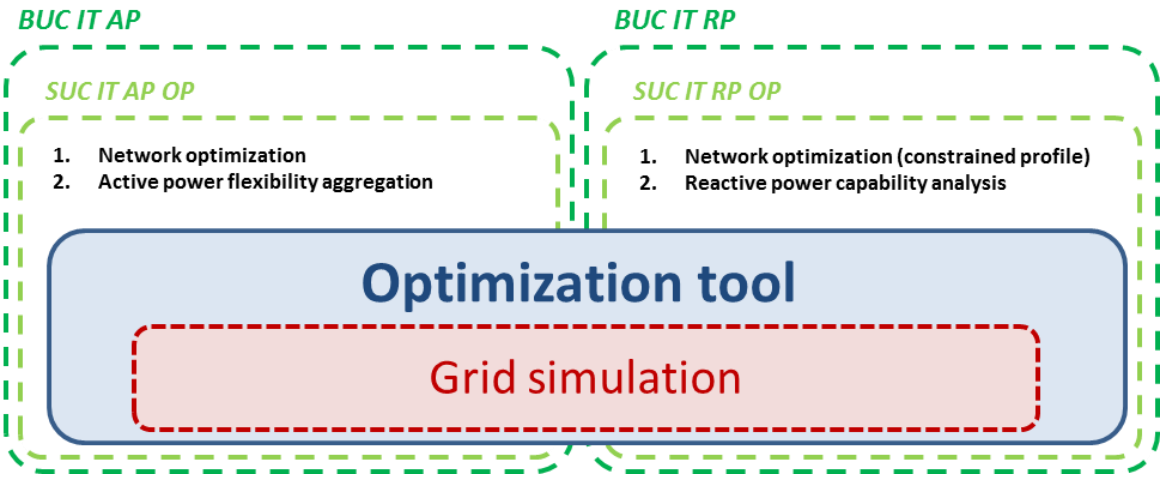

FIGURE 33 – USE CASES, FUNCTIONALITIES AND TOOLS RELATIONSHIPS SCHEME

4.1 NEED FOR THE OPTIMIZATION TOOL

In the Italian demonstrator, the optimization functionality is carried out by a dedicated software tool, embedded in the NCAS (Network Calculation Algorithm System) module of the SCADA; the core algorithm of the tool solves a multi-period Mixed Integer Non-Linear Programming (MINLP) model, considering intertemporal energy balance constraints. To reduce computational efforts (directly proportional to the network node number), the optimization process exploits non-linearity and integrality decoupling. These features result in reasonably fast OPF calculations even for large distribution networks and in presence of storage units.

Through this optimization tool, the system operator can manage its own assets and other controllable resources, minimizing the dispatching costs, avoiding network violations and RES curtailment (hosting capacity of the network is also positively affected). From this perspective, the algorithm presented here fulfils one of the objectives of the WP6 activities: guaranteeing an optimal state of distribution network.

Different types of constraints can be included in the optimization problem, including power exchange constraints at DSO-TSO interface, in the HV/MV primary substation node (slack node): this feature allows to modelling the constrained profile of active and reactive power flows resulting from a specific request from the TSO.

New features have been specifically developed for the Italian demonstrator activities, as the flexibility aggregation/disaggregation, the reactive power capability calculation and the cost-active power parametric curve.

The flexibility aggregation/disaggregation feature is essential to calculate the correct set-points for assets and flexible resources based on a suitable allocation of flexibility range, respecting both the constraints of the distribution network and the constraints shared between the DSO and the TSO at connection node. The allocation of flexibility is carried out within the optimization process, exploiting the capability calculation and the parametric curve calculation features, respectively for reactive and active power.

The integration of these functionalities in a single algorithm allows a more efficient calculation process, guaranteeing also that the consequent flexibility activations respect the network constraints, avoiding the need to run another optimization process after the flexibility selection from the TSO.

The optimization tool developed for the Italian demonstrator, in line with BUCs and SUCs presented in D6.1, is an essential tool to support the operations of a DSO or a Market Operator at distribution level in fulfilling the other two objectives of WP6, i.e. improvement of DSO-TSO coordination and meeting specific requests from the TSOs.

4.2 OVERVIEW OF THE OPTIMIZATION FUNCTIONALITIES

The optimization algorithm can be used for any kind of electrical AC network. Some of the functionalities have been optimized for distribution networks also to better model the interface between DSO and TSO.

TABLE 6 – BRIEF OVERVIEW OF THE OPTIMIZATION FUNCTIONALITIES

Optimization	Italian Demonstrator
Voltage Level	15 kV
Interconnection between:	DSO and TSO (15 kV and 132 kV)
Objective	Active and reactive power management at primary substation.
Boundaries	Primary substation or the HV/MV transformers
Constraints	Grid Constraints: Bus Voltage ±5 % (adjustable) Line Loading 100% Storage charge constraints DER capability (active and reactive power)
Solver / Methods	Interior point with logarithmic barriers
Algorithms	-
Programming Language	Matlab, Fortran
Data Model	-
Aimed Accuracy	10^-4
Risks	The effectiveness of set-points relies on the accuracy of state estimation and of the parameters of network and generators.

4.3 TECHNICAL DESCRIPTION OF THE OPTIMIZATION TOOL

The optimization algorithm is an Optimal Power Flow (OPF) that allows a techno-economic optimization of a distribution networks and it is already described in previous works [20]. The main characteristics of the algorithm are the same of a generic OPF, but the efficient design of the solver and some specific characteristics make it fast and able to fulfil the new functionalities requested by the project.

The objective of the optimization process is to minimize the active and reactive power modulation of the available generators with respect to the initial starting point (4.1):

$$\min \sum_{g \in \mathcal{G}} \left(c_g^{\Delta P^+} \Delta P_g^+ + c_g^{\Delta P^-} \Delta P_g^- + c_g^{\Delta Q^+} \Delta Q_g^+ + c_g^{\Delta Q^-} \Delta Q_g^- \right) \tag{4.1}$$

Where ΔP_g^+ and ΔP_g^- are the increase and decrease of active power of generators g and the parameters $c_g^{\Delta P^+}$ and $c_g^{\Delta P^-}$ the related costs. Instead, ΔQ_g^+ and ΔQ_g^- are the increase and decrease of active power of generators g and the parameters $c_g^{\Delta Q^+}$ and $c_g^{\Delta Q^-}$ the related costs. The parameter $\mathcal{G}$ represents the set of the controllable generators, which are one of the set of variables of the optimization process. In addition to the controllable generators, one generator is always added to the node of the transmission network. This generator behaves like a slack, it represents the transmission network and it is used to model the interaction between distribution and transmission.

The second main set of the equations that build the core of the algorithms are the constraints related to the power flow equations of branch and transformers:

$$TA_{i,j} = \left(\frac{\sin \delta_{i,j}}{Z_{i,j}\, TC_{i,j}^2} + \frac{X_{i,j}}{TC_{i,j}^2} \right) V_i^2 + \frac{\sin(\theta_i - \theta_j - \delta_{i,j})}{Z_{i,j}\, TC_{i,j}\; Vn_{j,i}} V_i\, V_j \tag{4.2}$$

$$TR_{i,j} = \left(\frac{\cos \delta_{i,j}}{Z_{i,j}\, TC_{i,j}^2} - \frac{Y_{i,j}}{2\, TC_{i,j}^2} \right) V_i^2 - \frac{\cos(\theta_i - \theta_j - \delta_{i,j})}{Z_{i,j}\; TC_{i,j}\; Vn_{j,i}}\; V_i V_j \tag{4.3}$$

Where $TA_{i,j}$ and $TR_{i,j}$ are the active end reactive power flow between nodes i and j, $\delta_{i,j}$ is the loss angle of series impedance, $Z_{i,j}$ the series impedance, $TC_{i,j}$ the voltage due to the transform ratio, $X_{i,j}$ transversal conductance of node i, $Y_{i,j}$ transversal susceptance of node i, V_i voltage of node i, θ_i phase angle of node i, $Vn_{i,j}$ the rated voltage at node i. The formulation used to express the power flow equations allows also integrating the transform ratio of transformers as a variable of the optimization process. All the variables presented in the previous equations (i.e. voltages, phase angles and transform ratio voltage) have their own minimum and maximum boundaries. Besides this, also maximum current limits of branches can be set as a constraint. Additional constraints are the capabilities of generators, which are rectangular, according to the Italian regulation (Figure 34, [29]). Depending on the generator characteristics they might not provide reactive power when the active power production is too low (e.g. the PV plants do not exchange reactive power in the night).

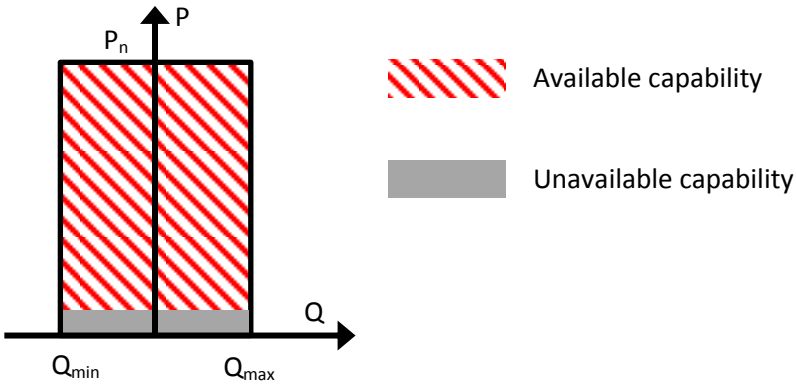

FIGURE 34 – GENERATOR CAPABILITIES CONSIDERED IN THE ALGORITHM

These boundaries represent the main electrical variables that have to be controlled in a distribution network.

The last set of equations is the one expressing the power exchange at each node:

$$\sum_{g \in \mathcal{G}_i} P_g = C_i + G_i V_i^2 + \sum_{(i,j) \in \mathcal{L}} TA_{i,j} \tag{4.4}$$

$$\sum_{g \in \mathcal{G}_i} Q_g = D_i + B_i V_i^2 + \sum_{(i,j) \in \mathcal{L}} TR_{i,j} \tag{4.5}$$

Where P_g and Q_g are the total active and reactive power injection of generator g connected to the node i, $C_i$and D_i are the total active and reactive power of loads, G_i and D_i the shunt conductance and susceptance. The described equations, the objective function and the constraints on voltages, on currents and on the capabilities of generators are the main element of the algorithms.

The algorithm can also consider the presence of electrical storage units, that are optimized in the optimization process taking into account also the charging constraints (i.e. maximum and minimum state of charge) in order to fulfil network constraints and to optimize the objective function. In this way the algorithm can make a multi-period optimization, where the set-points of the resources are computed taking into account not only the present state of the network, but also the forecasts of loads and generators. This functionality, which where one of the main objective of previous projects, is not deeply investigated in these simulations.

The optimization algorithm is developed in the Matlab® environment allowing an easy interface with the SCADA system. The functions developed in Matlab® formulate the optimization problem in the correct format, but the optimization itself is made by external functions written in Fortran. The solver was developed internally and it is based on a modified interior-point method with logarithmic barriers. This approach allows to achieve higher computational performances with respect to other languages and methods and thus to solve higher dimensional problems in a time compatible with the network operations. The data model used in this tools has also been developed internally and it does not follow a specific standard.

4.4 TEST CASES FOR THE OPTIMIZATION

As explained in the introduction paragraph, the optimization tool has been developed to carry out the functionalities supporting the System Use Cases IT-AP OP and IT-RP OP, presented in D6.1.

These two System Use Cases describe, respectively, the optimization of the distribution network in presence of active power flexibility bids and their aggregation in a power/cost parametric curve and the optimization of the distribution network in presence of a reactive power constraint in primary substation. Therefore, the optimization problem can be formulated in two different ways in order to perform active power provision and reactive power provision from distributed flexible resources. In addition, also the optimization of the network in normal operation (i.e. without flexibility provision to the transmission network) is investigated; the corresponding results can be used as a baseline for comparison. In this case, the DSO takes advantage of the coordination between local resources and its own asset (OLTCs, STATCOMs, Storage, etc.) to maintain the network within its operational limits and to reach other objectives, as the reduction of active power losses or the containment of reactive power exchange at primary substation. The algorithm, thus, is used as a normal OPF: it optimizes the use of resources based on the state of the network received from the SCADA.

ACTIVE POWER FLEXIBILITY PROVISION

Provision of active power modulation from distributed resources is supported by the optimization tool, besides maintaining the distribution network in an optimal state, through the aggregation of active power flexibilities from distributed resources in a cumulative parametric curve (energy/cost). The build-up process of this curve is depicted in the schematic of Figure 35:

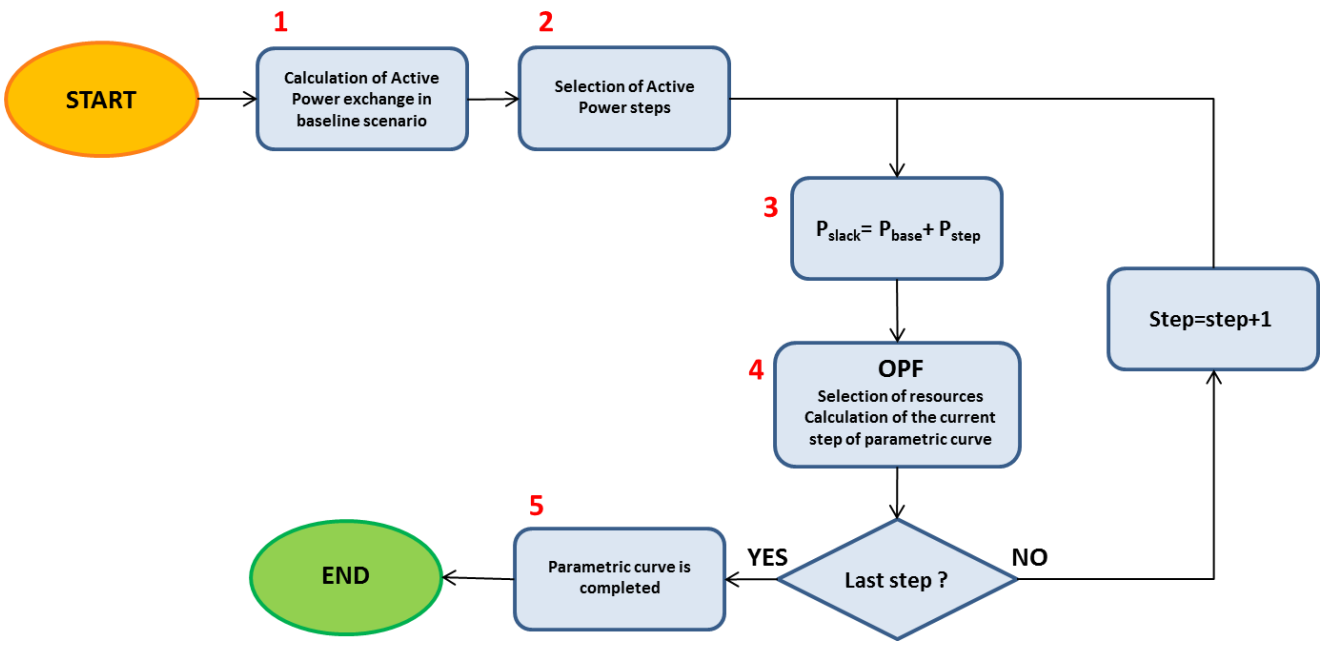

FIGURE 35 – PARAMETRIC BIDDING CURVE CALCULATION FLOW CHART

The steps of the iterative process are described in the following:

1. Evaluation of the active power exchange in HV/MV primary substation, in the baseline scenario;
2. Selection of active power steps, based on the total available power modulation and the requested precision of the parametric curve. This set of values represents the power variation in respect to the baseline;
3. The active power set-point of the slack node is fixed equal to the sum of the baseline active power value and one of the values from the active power variation set (from the first onwards);
4. The resources which can support the active power exchange set-point calculated in step 3, at minimum cost, are identified carrying out an OPF. Based on the resources activated and their costs, the total and marginal costs for each step of the parametric curve can be calculated. Besides, this allows the system operator (or market operator) at distribution network level to simply assign the activated resources to each bid of the parametric curve. The process is repeated cyclically until the last power step (no more resources can be activated, e.g. all the resources are used).
5. The parametric curve is completed and can be communicated to the transmission network level.

This process is repeated both for upward and downward regulation and for all the desired time intervals. After that the parametric curve can be communicated to the transmission network level where the business actor in charge for ancillary services acquisition can select the bids to be activated. The corresponding activation signal is then sent back to the system operator (or market operator) at distribution level who, based on the correspondence between the bids and the resources, send the activation signal to the selected resources. In this way the desired active power variation can be achieved. The effectiveness of this procedure strictly depends on the availability of good forecast of available resources, otherwise the activated variation will be affected by the forecast error.

REACTIVE POWER FLEXIBILITY PROVISION

Provision of reactive power modulation from distributed resources is supported by the optimization tool in two different phases:

A. A first optimization (OPF 1) is run for determining the total reactive power capability that can be provided by distributed resources. This process is based on the methodology developed in [30]: a quite high (several times more than the value observed in baseline scenario) reactive power set-point is imposed at the interface with the transmission network (HV/MV primary substation); then, the cost values for the reactive power variation ($c_g^{\Delta Q^-}$ and $c_g^{\Delta Q^+}$) of the available generators are selected much lower than the cost value of the reactive power variation corresponding to slack node generator, i.e. HV/MV primary substation node. In such a way, the optimization tool minimizes the use of the slack generator as much as possible, fully exploiting the available distributed resources in order to maximize the reactive power exchange at HV/MV primary substation. This process is repeated two times, for computing the maximum power absorption and for the maximum power injection of the distribution network. All the network constraints are considered, so that the resulting capability area corresponds to the actual flexibility range that can be exploited safely for the distribution network;

B. A second optimization (OPF 2) is run for calculating the optimal set-points for the distributed resources, in order to fulfill the requested reactive power exchange in the HV/MV primary substation (TSO/DSO interface). Once the TSO returns the desired set-point(s) for reactive power exchange at HV/MV primary substation, they are in introduced in the optimization problem as set-point(s) for the slack node generator; similarly to the previous case, the cost value for reactive power variation for slack generator is selected as high as possible in order to allow the algorithm to exploit all the available distributed resources, within the network constraints, achieving the requested power exchange at TSO/DSO interface.

The calculation processes behind the reactive power flexibility provision, carried out by the optimization tool (Steps 1 and 5), and the linked Business level interactions (Steps 2, 3, 4) are presented in Figure 36:

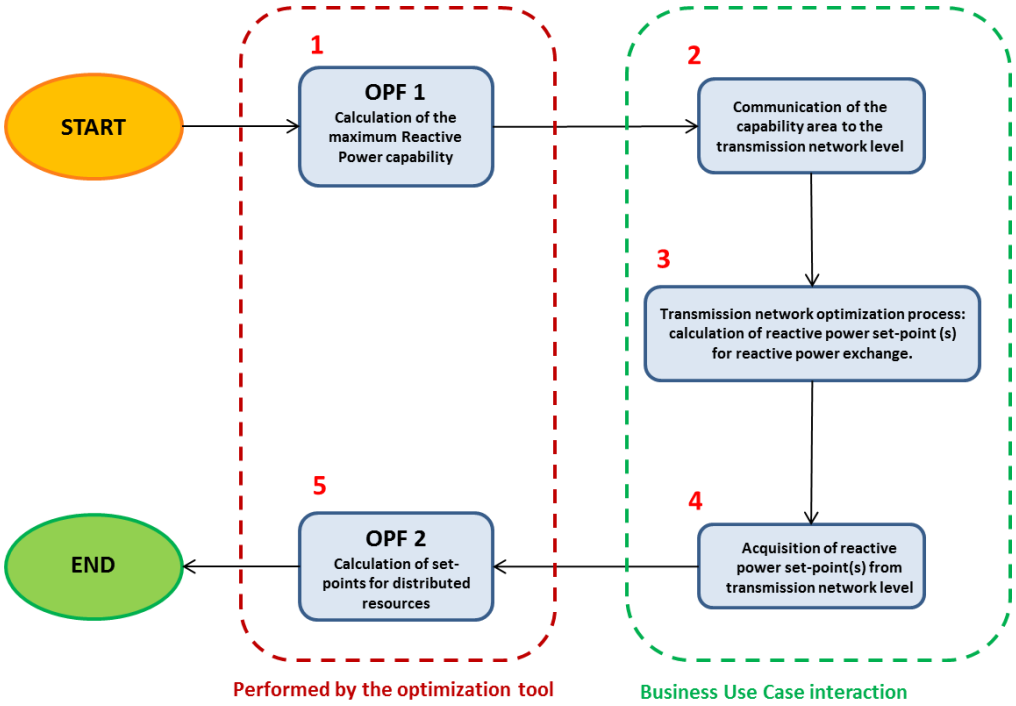

FIGURE 36 – REACTIVE POWER CAPABILITY AND RESOURCES SET-POINT CALCULATION FLOW CHART

The process steps are described in the following:

1. Calculation of maximum reactive power absorption and injection and build-up of the available capability area, within network constraints (OPF1);
2. Communication of the capability area from distribution network level (MV) to transmission network level (HV);
3. Inclusion of the capability area in the optimization process of transmission network: calculation of reactive power set-point(s) at HV/MV primary substation (TSO/DSO interface);
4. Communication of reactive power set-point(s) from transmission network level to distribution network level;

5. Calculation of reactive power set-points for distributed resources, considering the set-point(s) for reactive power exchange at primary substation interface (OPF2).

Both the test cases explained above have been tested considering the assumptions and the case scenarios described in D6.3 [31]; scenario details and a schematic picture of the demonstrator network are reported, respectively, in Table 7 and in Figure 37.

TABLE 7 – FLEXIBLE RESOURCES SET-UPS FOR THE SIMULATED CASES

	Case 1	Case 2	Case 3	Case 4	Case 5
Resources	4 PV generators (G8, G19, G20, G25)	Case 1 + BESS	Case 2 + STATCOMs	All PV gens + BESS + STATCOMs	All gens + BESS + STATCOMs

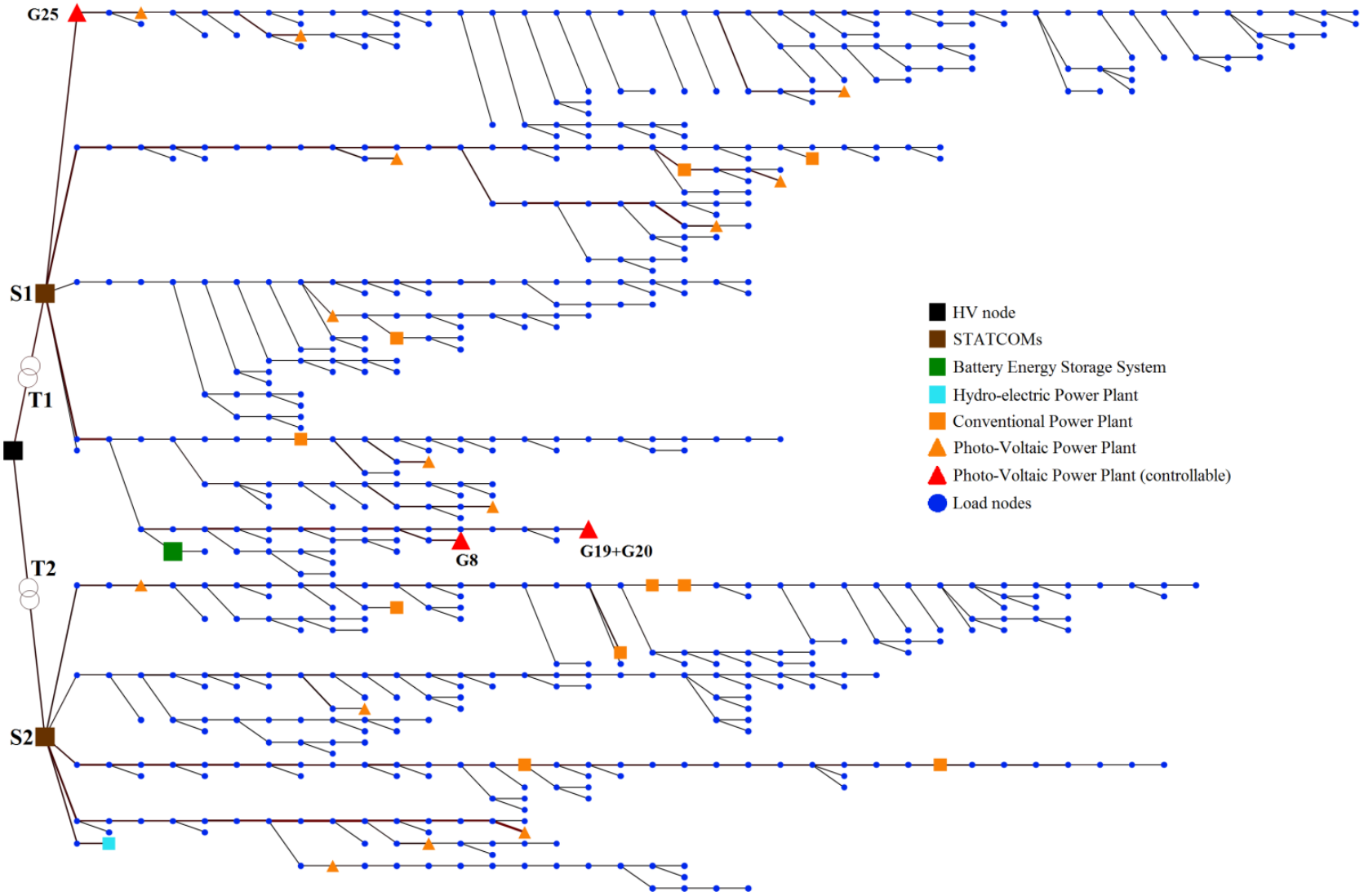

FIGURE 37 – SCHEMATIC PICTURE OF THE ITALIAN DEMONSTRATOR NETWORK

This project has received funding from the European Union's Horizon 2020 research and innovation programme under grant agreement No 773505.

4.5 EXEMPLARY SIMULATIVE RESULTS FROM THE ITALIAN DEMONSTRATOR

In this section a sample of the results achievable through the optimization tool is presented and discussed; it is based on the simulations focused on the evaluation of the reactive power capability presented in deliverable D6.3 *"Grid simulations and simulation tools. Preliminary results"*. The first example presented here shows how the optimization tool manages the share of reactive capability between the flexible resources, taking into account potential OLTC shifting constraints.

In addition, a realistic external set-point for reactive power exchange at primary substation is introduced in the second example, simulating a reactive power profile request from the TSO.

4.5.1 REACTIVE CAPABILITY SHARE VERSUS TAP SHIFTING RANGE

In deliverable D6.3, the management of the OLTCs has been simulated in the baseline scenario, for losses minimization, in order to estimate how many tap shifts they perform on average in the considered normalized periods. The results showed that tap shifts are 6-7 per day in the worst cases, and always within the maximum operational limits, fixed at 10-12 shifts per day by the system operator (*e-distribuzione*).

Furthermore, the maximum theoretical reactive power capability has been calculated as well as how much it has to be reduced in order to avoid constraints violations, without rely on the network optimization.

Starting from these background analysis, the aim of this example is to show how the optimization tool can manage the maximum potential reactive power provision to the transmission network, sharing the capability between the resources, for several tap shifting ranges (i.e. with limited OLTCs operations).

For this analysis, the optimization tool is run starting from zero tap and then increasing, one step at a time, the number of tap shifts the OLTCs are allowed to do above or below the zero tap. Case 3 and case 5 scenarios (see Table 7) are simulated for Sunday of the second quarter of year (Apr-Jun). Figure 38, Figure 39 and Figure 40 show the results for case 3 scenario, for negative tap positions (voltage downward regulation).

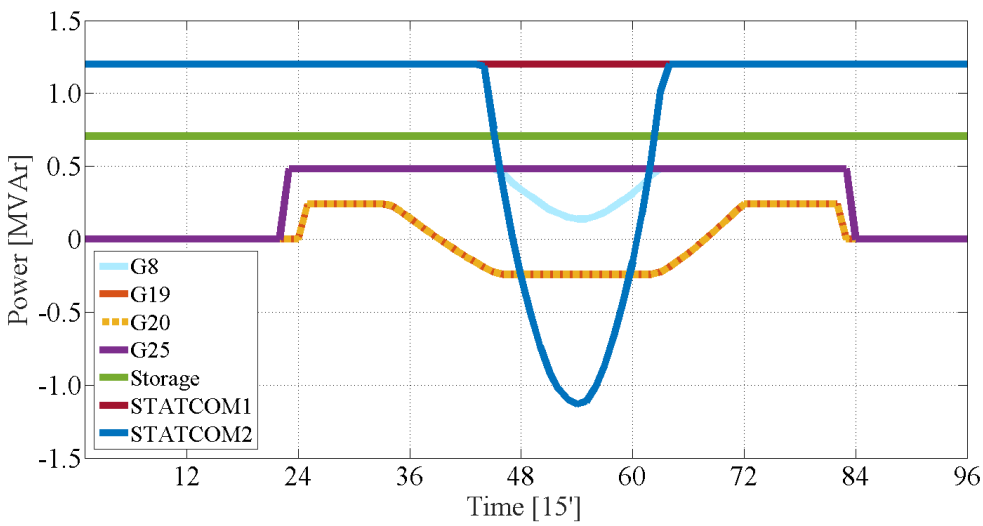

FIGURE 38 – REACTIVE POWER PROFILES, ZERO TAP; CASE SCENARIO 3

This project has received funding from the European Union's Horizon 2020 research and innovation programme under grant agreement No 773505.

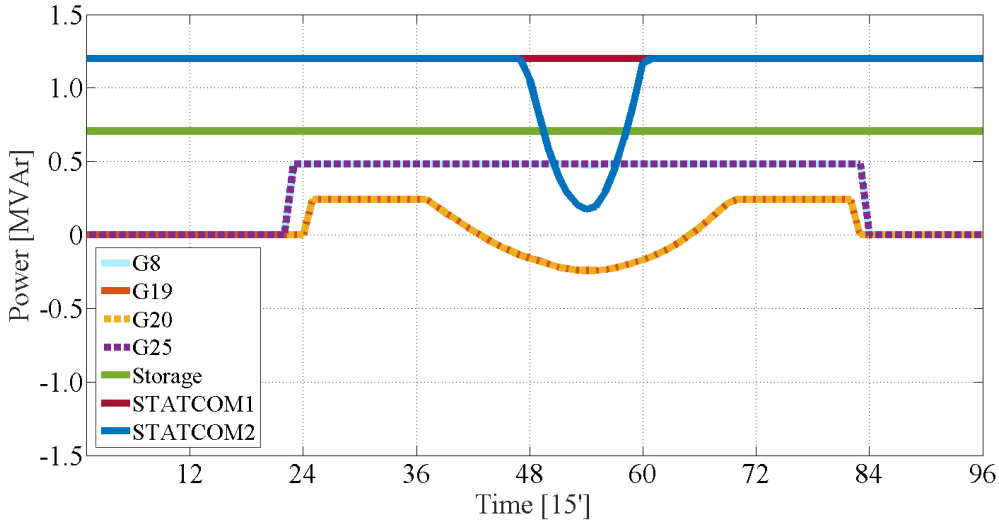

FIGURE 39 – REACTIVE POWER PROFILES, - 1 TAP, CASE SCENARIO 3

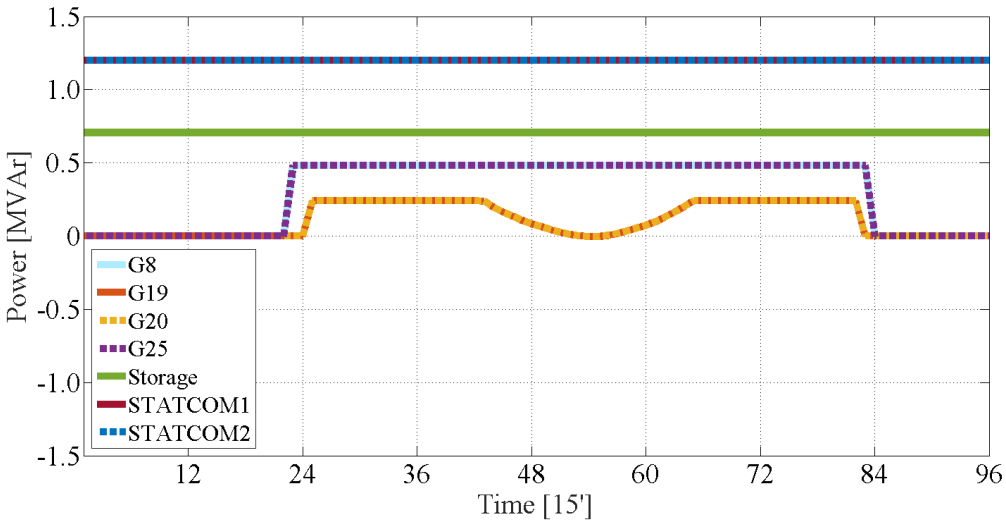

FIGURE 40 – REACTIVE POWER PROFILES, - 2 TAP, CASE SCENARIO 3

Figure 38 shows the share of reactive power capability between the flexible resources corresponding to case 3 scenario (four PV generator, STATCOMs and BESS) for a zero tap position (both the OLTCs), in presence of a provision of reactive power to the transmission network. As can be seen, the only resources whose capability can fully exploited during the whole time period are STATCOM 1, PV generator G25 and the battery storage. Indeed, in the central part of the day, when the PV production reaches its maximum, the optimization tool decreases the reactive power production of PV generators G8, G19, G20 and STATCOM 2 in order to reduce voltage level in their nodes and avoid constraints violations, without affecting active power delivery. Furthermore, for all these resources except G8, the optimization tool requests the absorption of reactive power instead of injecting. From Figure 37 it can be noticed that G19 and G20 are connected at the end of the feeder so their production can sensibly affects voltage; G8 can also influence voltage, even if in a lesser extent since it is closer to primary substation. If optimization tool cannot rely on transformer secondary voltage reduction as in this case, it has to exploit such generators mainly for local voltage control than for reactive power provision and this explains why G19-G20 absorb reactive power instead of injecting it. On the other side, STATCOM 2 is connected to a portion of

the demonstrator network whose generators cannot be controlled for case 3 scenario: as a result, the optimization tool uses it in place of OLTC 2 to compensate the voltage increase due to PV production.

Figure 39 shows the capability share resulting from increasing the tap shifting range to +/-1 taps and thus allowing the optimization tool to have more "freedom" in controlling node voltage. In this case, reducing the busbar voltage, the optimization tool is able to better maintain the nodes voltage levels within the limits, relying on local reactive power modulation to a lesser extent; as a result, the reactive power capability of G8 can be fully exploited and STATCOM 2 can be used for reactive power injection instead of absorption (with only a small injection reduction in the central hours of the day). Generators G19 and G20 have still to absorb reactive power, even if they barely reach the lower limit of their capability compared to the previous case. Enlarging the tap shifting range to +/-2 tap allows the optimization tool to further reduce the busbar voltage (Figure 40): as a result, STATCOM 2 capability is now fully exploitable for reactive power provision and G19 and G20 can be exploited for power injection instead of absorption, even if limited during the central part of the day.

From these results it can be concluded that, for limited tap shifting ranges, the optimization tool has to exploit reactive power flexibility from distributed resources for nodes voltage control, subtracting flexibility shares from the total network capability and thus hampering the reactive power flexibility provision to the transmission network.

Same analysis is carried out also for case 5 scenario, with a higher share of flexible resources than the case 3 (see Table 7); the corresponding results are pictured in Figure 41 and Figure 42. For comparison purposes, the capabilities of the PV plants of case 3 scenario are represented separately by those of the other PVs and conventional plants (which are combined in two groups named, respectively, as "PV" and "Other").

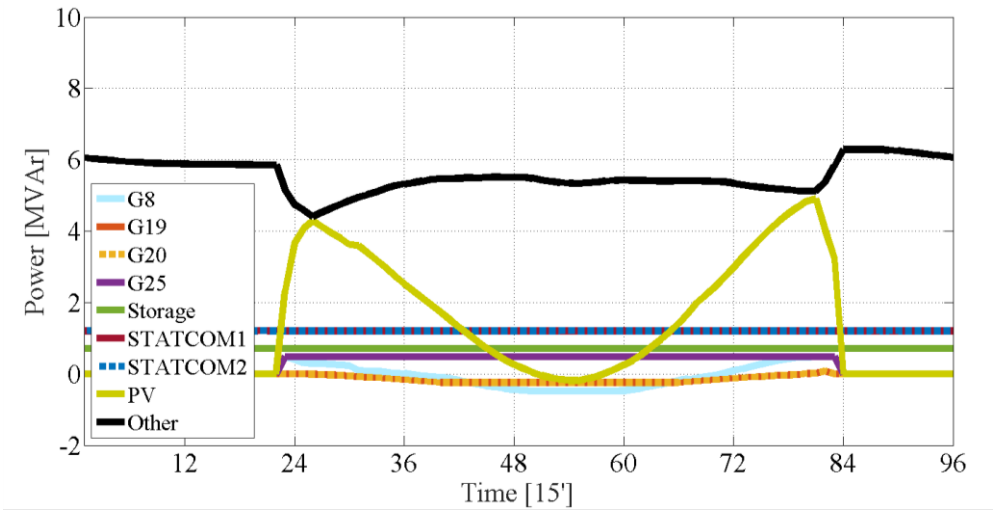

FIGURE 41 – REACTIVE POWER PROFILES, ZERO TAP; CASE SCENARIO 5

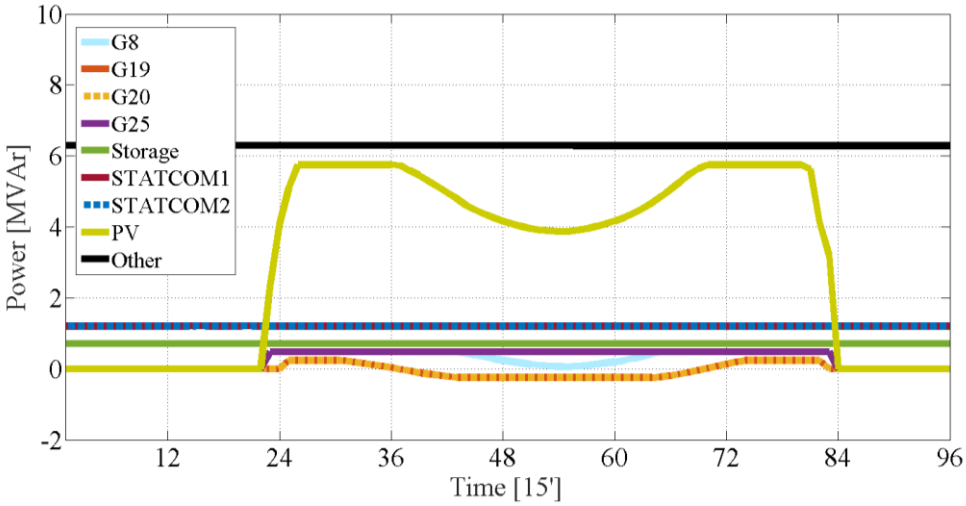

FIGURE 42 – REACTIVE POWER PROFILES, - 3 TAP, CASE SCENARIO 5

Figure 41 shows the share of reactive power capability between the flexible resources corresponding to case 5 scenario for a zero tap position, in presence of a provision of reactive power to the transmission network. As can be seen, all the capability profiles, except those of battery storage, G25 and STATCOMs, are reduced in the central part of the day. Even in this scenario, the optimization tool has to exploit reactive power absorption from PV generators G19-G20 and G8 during the high-peak of PV production for avoiding local over-voltages; same operations are also applied to other PV plants as the total PV capability profiles assume negative values in the central hours of the day.

The optimization process leads to a reduction also of the reactive power capability of conventional power plants, more consistently in correspondence of the maximum shares of PV capability (i.e. during early morning and late afternoon). Indeed, when the PV production is low or zero, the reactive power injection from conventional generators may cause over-voltages in some areas of the network; conversely, when the PV production is higher, its impact on node voltages may be stronger compared to conventional generators. This behavior can be clearly seen in Figure 41, where the capability profile of conventional plants is reduced in the early morning, then it is increased when the PV plants capability is reduced during high-peak production, and it is reduced again in the late afternoon when the PV plants active output decreases.

As done for case 3 scenario, increasing tap shifting ranges have been tested with case 5 scenario network data. Figure 42 shows the capability shares for a shifting range of +/-3 taps: as for the previous tests, the capability of further lowering the busbar voltage allows the optimization tool to achieve better nodes voltage control without completely relying on modulation of reactive power from resources, since G8 and the other PV plants experience only a reduction of the reactive power injection and the capability from conventional power plants is unaffected compared to the previous case, presented in Figure 41. Further enlarging of tap shifting range leads to higher capability shares: specifically, for -5 tap setting only G19 and G20 reactive power capabilities are still exploited by the optimization tool for local voltage control during the high PV production period, while for lower tap settings the full capability of the network can be made available for reactive power provision at HV/MV primary substation.

These results confirm what has been observed for case 3 scenario: limited tap shifting ranges lead the optimization process to exploit reactive power flexibility from distributed resources for nodes voltage control, subtracting flexibility shares from the total network capability. The studies carried out for case 5 scenario show that, for higher shares of reactive power, the optimization tool needs wider tap shifting ranges for being able to keep nodes voltages within the limits and, as the same time, make available the full reactive power capabilities from distributed resources for reactive power provision. Furthermore, significant busbar voltage reduction is often necessary for allowing dispersed resources to provide their reactive power share for increase global aggregated capability instead of exploit it for avoiding local voltage violations.

Further analysis is carried out, considering case 5 scenario, for assessing how the total network capability is affected by OLTC operations. The scope of this analysis is two-fold: calculate optimum tap position profiles and determine how each tap position influences the aggregated capability area. Figure 43 pictures the tap position profiles of both the OLTCs calculated by optimization tool.

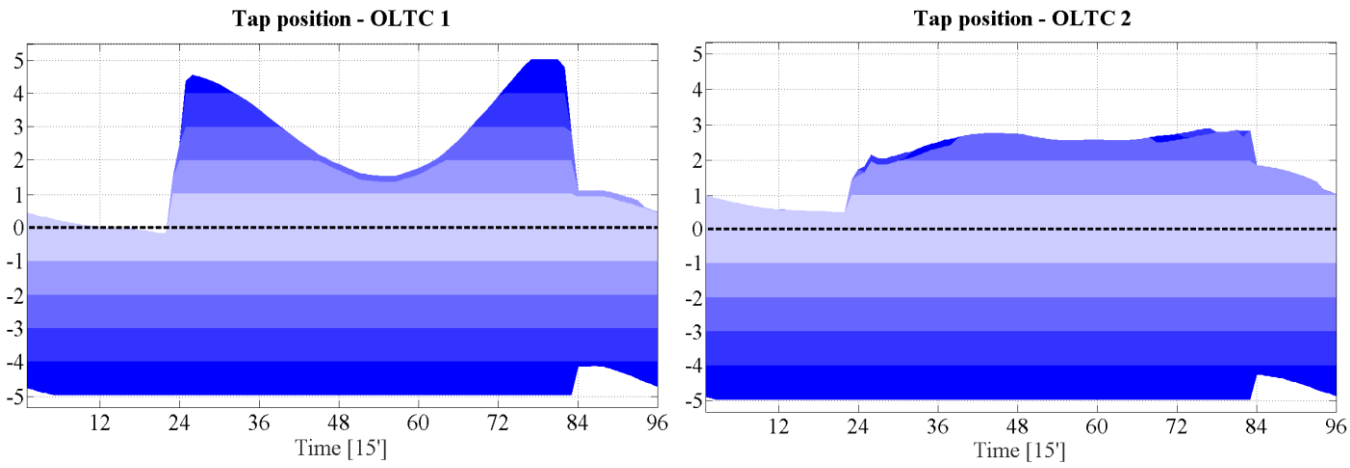

FIGURE 43 – OLTC TAP SHIFTING RANGES, CONTINUOUS, CASE SCENARIO 5

Based on the tap shifting range selected, the corresponding tap position profiles are calculated for upward regulation (positive tap settings, voltage increasing) and for downward regulation (negative tap settings, voltage decreasing). For each range, the optimization tool carried out a network optimization calculating the optimum tap profile for each of the OLTC, considering two main operating conditions: maximum reactive power injection and maximum reactive power absorption, versus the transmission network. The analysis is limited to +/-5 shifting range for ease of calculation.

From Figure 43, the upper profiles, corresponding to +5 tap position, represent the limit profiles for upward regulation, i.e. the highest voltage levels which are sufficient for avoiding under-voltages for maximum reactive power absorption. As can be seen, for OLTC1 0 to +5 tap range is suitable for regulating network voltage for most of the day (except for the late afternoon), while for OLTC2 0 to +3 tap range is sufficient. This depends on the specific characteristics of the part of the network belonging to each transformer/OLTC set-up. On the other side, the flat tap profiles for -5 tap position mean that the downward regulation limit is not reached and thus a wider regulation range would be necessary for allowing full exploitation of upward reactive power capability.

Figure 44 shows the variation of reactive capability area depending on the allowed tap shifting range; each shade of color corresponds to the same shade pictured in Figure 43 for the tap position profiles.

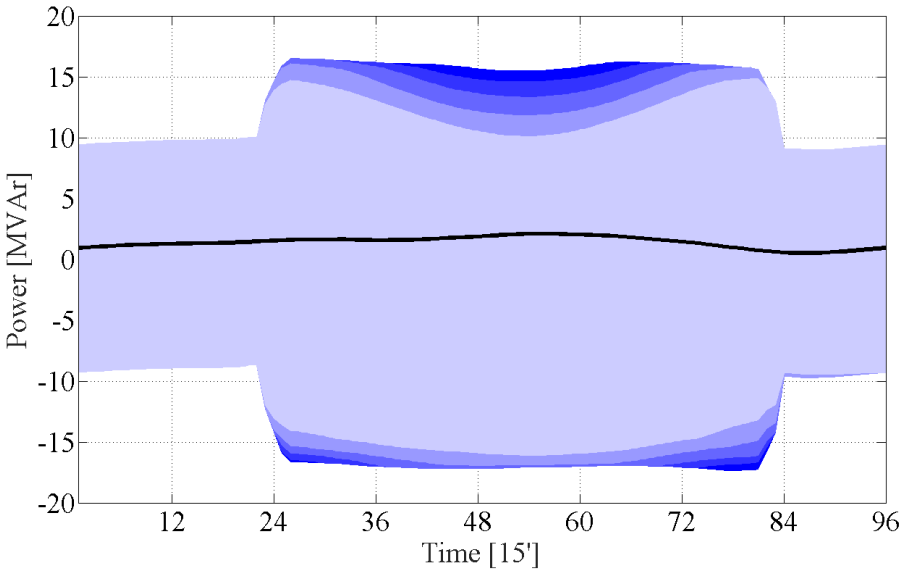

FIGURE 44 – REACTIVE POWER CAPABILITY AREA VERSUS OLTC TAP SHIFTING RANGE, CASE SCENARIO 5

It can be noticed that the +/-1 tap shifting range is suitable for exploiting the most of the capability area, while wider ranges are needed only for maintaining the full capability area in specific periods of the day:

- extending the downward tap range is necessary for the central part of the day, when the PV production is at its peak and the network voltage should be reduced for avoiding over-voltages;
- extending the upward tap range is necessary, mostly, in early morning and late afternoon, when PV production is low but the load is high and the network voltage should be increased for avoiding under-voltages;

Concluding, since for nodes voltage control the optimization tool can rely on busbar voltage modulation or local reactive power flexibility management, if it is necessary to exploit the full reactive capability of the demonstrator network, suitable OLTCs tap shifting ranges should be allowed. In such a way, the optimization tool is “free” to control the nodes voltages by the means of slack node voltage regulation instead of rely on local reactive power modulation, making flexibilities from local resources available for the reactive power flexibility provision to the transmission network. Anyway, if the amount of available reactive power share from distributed resources is substantial (like in the considered case 5 scenario) the available capability area is already large and it may not be necessary to achieve a full exploitation of the aggregated capability. In such conditions, more suitable optimization strategies can be adopted to better use the resources, for example the reactive power contribution from each resource can be tailored based on the voltage sensitivity of the corresponding node, reducing the occurrence of constraints violation and thus naturally limiting the usage of OLTCs for reactive flexibility provision purposes.

4.5.2 REACTIVE POWER MODULATION IN PRESENCE OF AN EXTERNAL SET-POINT

In this exemplary analysis, a defined set-point profile for reactive power exchange at primary substation is introduced as a constraint in the optimization problem. The scope of this exercise is to simulate the actual sending of reactive power set-points, during the whole day from the TSO, realizing the system process described in SUC IT RP OP (*"Perform distribution network management and optimization for the Italian Demo")* which supports the business process described in BUC IT RP ("*Manage reactive power flexibility to support voltage control and congestion management in the Italian demo"*). A schematic picture of the set-point profile is presented in Figure 45:

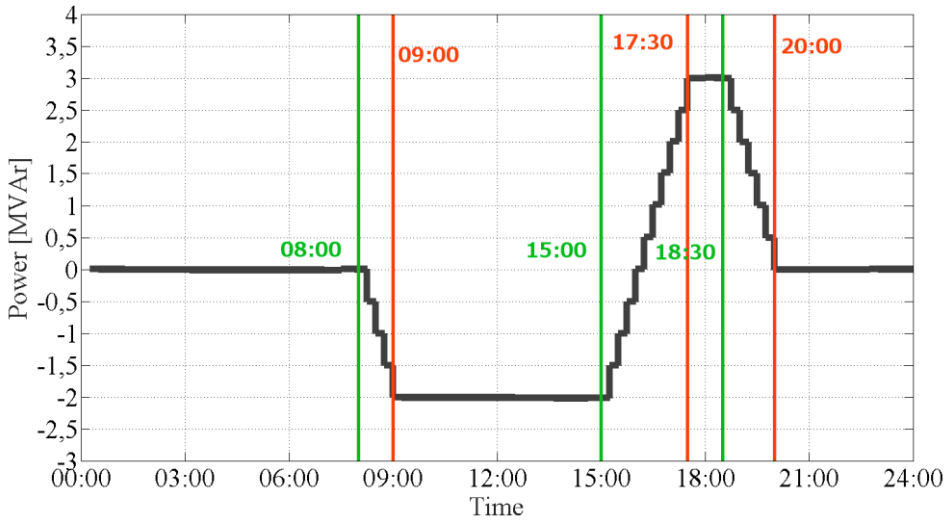

FIGURE 45 – SET-POINT PROFILE FOR REACTIVE POWER EXCHANGE AT HV/MV PRIMARY SUBSTATION

The hypothesis behind the selected set-point profile is the mitigation, through a suitable reactive power modulation, of the effects of active power injection/absorption from the demonstrator network on the voltage levels in the transmission network. Based on this, the profile has been built considering the following characteristics:

- reactive power exchange must be zero during the night, for not influencing the transmission system; this translates in to zero value set-points for 12 hours, from 20:00 to 08:00;
- reactive power must be absorbed during the central hours of day, for compensating the peak production of generators (specifically PV plants) and the corresponding voltage levels increase; this translates into negative set-points (maximum value -2 MVAr) for 8 hours, from 08:00 to 16:00;
- reactive power must be injected in the late afternoon, for compensating the peak load and the corresponding voltage levels decrease; this translates into positive set-points (maximum value 3 MVAr) for 4 hours, from 16:00 to 20:00.

The three transients to which the profile is exposed are shown in Figure 45, with the corresponding start (green line) and stop (red line) timestamps. The increase ratio is fixed to 0,5MVAr/15' as it is considered not too demanding for the controlled resources, and the peak values for reactive power exchange are selected empirically

based on the analysis of the demonstrator network operations. These values should be intended only for exemplary purposes and they can be modified based on actual needs of the system operators.

The set-point profiles described above are applied to case 3 and case 5 scenario, in the same time-period considered for the previous example, i.e. Sunday of the second quarter of year (Apr-Jun). Figure 46 shows the optimized reactive power profiles of the involved flexible resources for case 3 scenario.

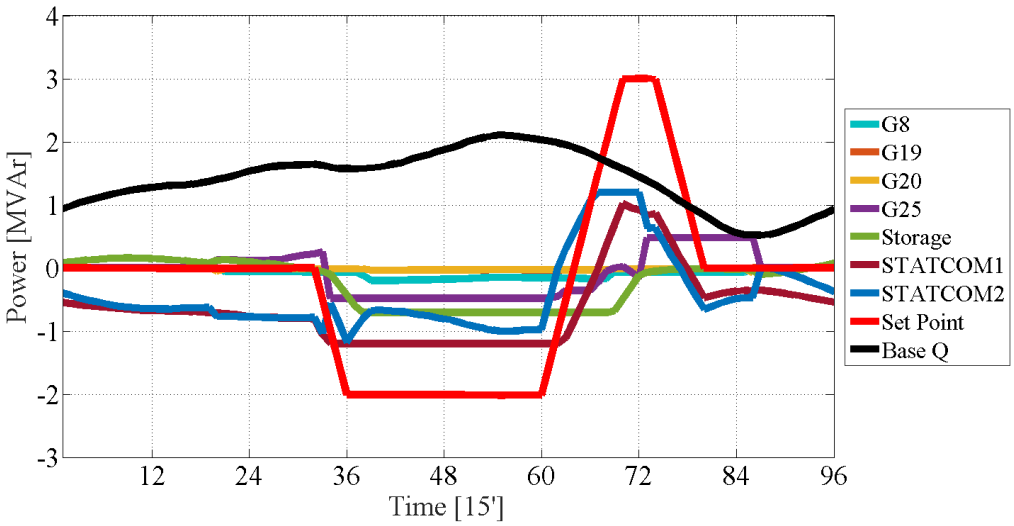

FIGURE 46 - REACTIVE POWER PROFILES, EXTERNAL Q SET-POINT, CASE 3 SCENARIO.

In addition to the resources profiles, also the set-point profile and the base reactive power profile are pictured for clarity. This later profile is build up by the reactive power absorption of the loads and the reactive power injection due to the capacitive reactance of the network. As reported in previous chapters, the demonstrator network is quite large and this entails a strong power injection due network capacitive reactance (3 MVAr on average): this aspect, in conjunction with the low load consumption, turns the base reactive power profile into a substantial reactive power injection versus the transmission network. From Figure 46 is evident that the optimization tool exploits the STATCOMs to compensate the base Q profile and to follow the set-point profile in the early hours of the day (00:00 to 08:00): in this case scenario their contribution during the night hours is essential since they are the only flexible assets available for reactive power modulation.

From the 08:00 onwards, the optimization tool exploits also the battery storage, generator G25 and, to a small extent, generator G8, in addition to STATCOMs for absorbing the necessary amount of reactive power for following the set-point profile. It must be noted that both G25 and STATCOM 1 are operated at their operational limits during the central hours of the day, as can be observed from their steady flat power profiles. This may happens since they are both connected close to the primary substation and the optimization tool can exploit their full reactive capabilities without or slightly affecting node voltages, opposite to G8, G19-G20, for instance, who are close to the end of their feeder (refer to Figure 37). Generator position can negatively affect node voltages and network losses: indeed, reactive power capabilities of generators G19-G20 are not exploited at all.
It is important to highlight that the part of the network belonging to Transformer/OLTC1 is larger than the other part and experiences the higher PV production; hence, the optimization tool exploits the reactive power downward capability of flexible assets connected to it also for reducing over-voltages risk as well as losses.

During late afternoon (after 17:00), the optimization process relies mainly on STATCOMs and generator G25 to follow the set-point profile. It should be noted that generator G25 is operated at its upward capability limit, continuing injecting reactive power long after 20:00 (i.e. when the set-point profile reaches again the zero value). This may happen since, in case 3 scenario, G25 is the only controllable resource of its feeder and so, being connected in the first node, the optimization algorithm exploits its reactive power injection to contain the voltage drop following the load increase. Figure 47 shows the OLTC tap profiles corresponding to the example presented above.

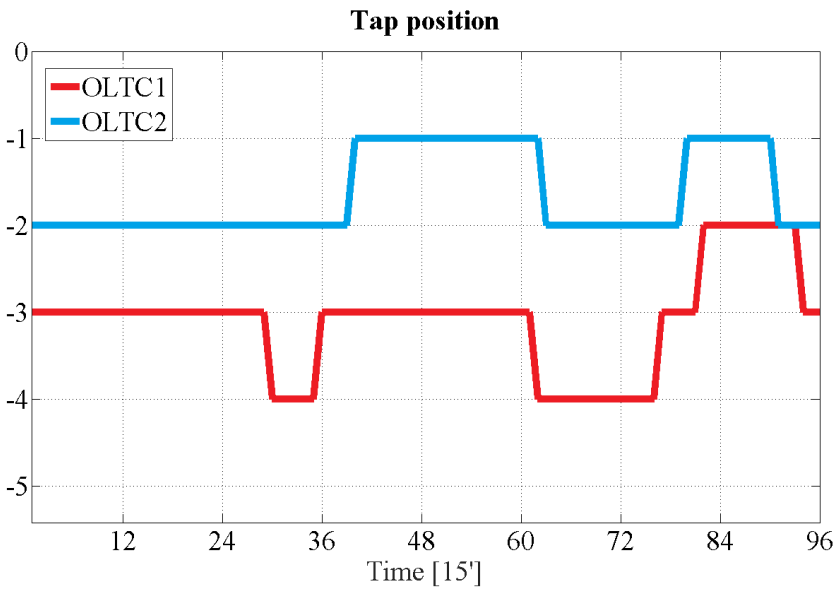

FIGURE 47 – TAP PROFILES, EXTERNAL Q SET-POINT, CASE SCENARIO 3

It can be seen that both the OLTCs perform a limited number of shifts (6 for OLTC1 and 4 for OLTC2), comparable with the figures observed for the baseline scenario analyzed in deliverable D6.3 and far below the operational limits (10-12 shifts per day).

Initial taps are calculated by the optimization tool so that the resulting voltage levels could be as low as possible in order to maximize loss reduction, compatibly with the specific network operating conditions. Then, taps are shifted downward or upward, according to the results of the optimization processes carried out during the day. Around 7:30, OLTC1 is shifted down one tap more for compensating the voltage increase due to PV production starting. This does not happen for OLTC2, since the share of PV plants in its part of the network is smaller than that one of OLTC1. Both OLTCs are shifted up of one tap in correspondence with the reactive set-point shifting versus power absorption (around 9:00-9:30), for compensating the corresponding voltage decrease. These taps are maintained until the set-point profile starts to rise from absorption to injection (around 15:00-15:30), then the OLTCs are both shifted down of one tap again for compensating the voltage increase due to reactive power injection. Finally, around 20:00, they are shifted up of one tap again, since it is still necessary to compensate voltage drop due to peak load just after the set-point profile shifts from power injection to zero; then, around 23:00, they are moved again to the initial tap. OLTC1 experiences two tap shifts more than OLTC2 since for its part of the network a wider regulation range is necessary: indeed, being it larger than the one connected to OLTC2, the optimization process has to deal with wider voltage variations.

From the results presented above, it can be concluded that with the limited number of flexible resources available in case 3 scenario, the only resources the optimization tool can exploit mainly to provide the necessary power flow to follow the external set-point are those connected closer to the slack node (i.e. primary substation), specifically the STATCOMs, since their operations do not affect (or lightly affect) node voltages and line loading. Conversely, the reactive flexibility from resources connected far from slack node can be lesser exploited for following the set-point due to the higher voltage sensitivity of the connection nodes and consequently it may be often exploited by the optimization tool for local voltage control. Besides these aspects, even with the case 3 scenario network, the optimization tool is able to follow the external set-point for the whole duration of the day. It is essential to point out that, without any OLTC shifting constraint, the optimization tool is able to maintain a suitable voltage level for efficient local voltage control and losses reduction right from the beginning of the day, relying on tap shifting only when changing slack node voltage is essential for following the external reactive power set-point; as a result, a suitable tap shifting range allows to perform a limited number of shifts per day, even in presence of external power constraints.

The set-point profile presented above (see Figure 45) is applied also to case 5 scenario. For better visualization and understanding, the flexible resources are divided in two groups, related to sub-network 1, connected to Transformer/OLTC1, and sub-network 2, connected to Transformer/OLTC2 (see Figure 37 for further details). The corresponding reactive power profiles are presented, respectively, in Figure 48 (sub-network 1) and Figure 49 (sub-network 2). The base reactive profile, i.e. the algebraic sum of reactive power absorption from the loads and reactive power injection due to network capacitive reactances, is also split in two profiles for the sake of clarity.

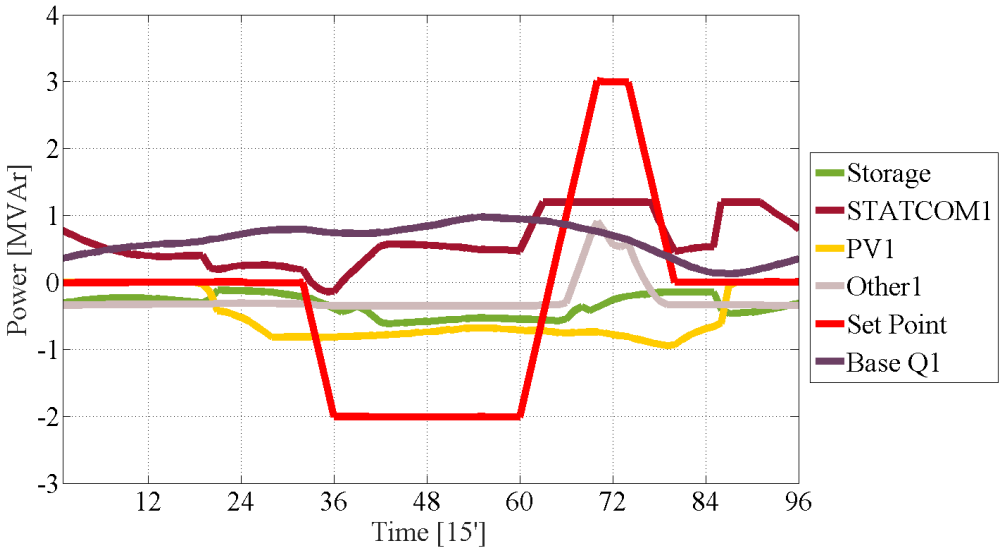

FIGURE 48 – REACTIVE POWER PROFILES, EXTERNAL Q SET-POINT, CASE SCENARIO 5, SUB-NETWORK 1

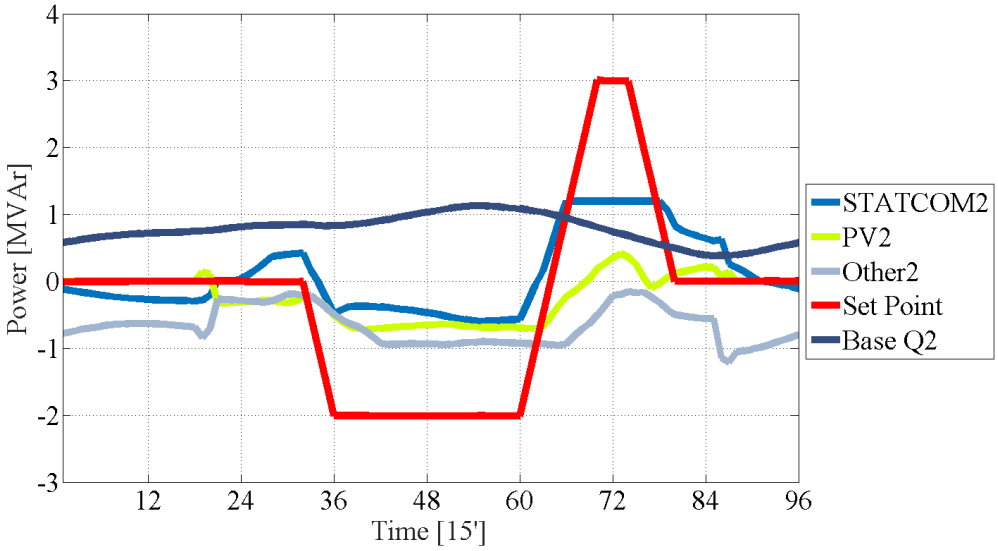

FIGURE 49 – REACTIVE POWER PROFILES, EXTERNAL Q SET-POINT, CASE SCENARIO 5, SUB-NETWORK 2

From Figure 48, it can be noted that PV generators and battery storage are operated only in reactive power absorption mode for the whole duration of the day; similarly, the reactive power absorption from conventional generators is exploited to its maximum, except between 17:00 and 19:00, when the optimization tool operates the conventional generators for reactive power injection, exploiting them for following the reactive power injection requested by the set-point profile. On the other side, the optimization tool operates STATCOM 1 for reactive power injection for almost the whole day, and up to its operational limit during the late afternoon and shortly after nightfall. Furthermore, during the maximum request for reactive power absorption (from 09:00 to 15:00), STATCOM 1 reactive power injection is quite high.

These conditions may be driven by the losses reduction carried out by the optimization tool. Reactive power absorption by dispersed resources allows to keep node voltages as low as possible and to compensate the reactive power injection from capacitive reactances of the lines; then it is necessary to exploit the STATCOM 1 to balance this absorption for reducing the power losses of transformer 1. Moreover, it seems that, as a result of the optimization problem, the dispersed resources are mainly exploited for following the negative set-points (request of power absorption), while the STATCOM is mainly exploited for following the positive set-points (request of power injection). This underlines the importance of the STATCOMs as modulation assets, suitable to potentially “de-couple” the local operating needs of the distribution networks from the global needs of the transmission systems.

Anyway, this “role-separation” cannot be considered general, since the results of the optimization problem can be different from case to case. For instance, it is not so evident for sub-network 2: indeed, observing Figure 49, it can be seen that, even if the dispersed resources are still exploited mainly for reactive power absorption, their profiles, as well as the one of STATCOM 2, seem to follow the reactive power set-points profile closer than the previous case. There is one aspect which is clearly noticeable also from sub-network 2: even STATCOM 2 is exploited up to its operational limits between 17:00 and 19:00, when transmission network requests reactive power injection.

A similar behavior is observed also for case 3 scenario, in which the optimization tool relies mainly on STATCOMs when consistent reactive power injection is requested from the demonstrator network.

This means that, even if all the flexible resources connected to the demonstrator network can be potentially exploited for reactive power injection, the corresponding increase in node voltages could be more harmful in terms of over-voltage risk and network losses increase. Therefore, if the optimization strategy described in the previous sections is adopted, the use of assets capable of modulating the injection of reactive power in place of the dispersed flexible resources should be recommended. STATCOMs allow, in such conditions, to address the needs of the transmission network without impacting the efficient and secure management of the distribution network, as envisioned by the WP6 and EU-Sysflex project objectives.

As done for the case 3 scenario, also in this case the OLTCs tap profiles are analyzed. Figure 50 shows the OLTC tap profiles for case 5 scenario.

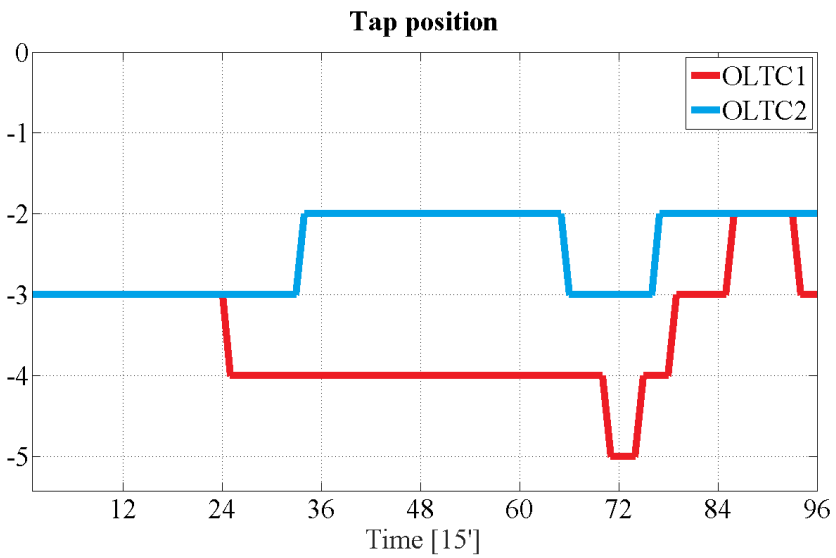

FIGURE 50 – TAP PROFILES, EXTERNAL Q SET-POINT, CASE SCENARIO 5

Compared to the previous case, the OLTCs are subjected basically to the same number of shifts, 6 for OLTC 1 and 3 for OLTC 2, demonstrating that the application of reactive power set-point profile to case 5 scenario does not result in heavier operating conditions for the OLTCs.

OLTC 2 tap profile is quite similar to the previous case, showing two one-tap upward shifts, one corresponding to the reactive set-point shifting versus power absorption (around 9:00-9:30) and the other corresponding to the start of voltage drop due to peak load (around 19:00). The main difference is that the whole profile is translated one tap lower than before; this may be caused by a local voltage increase in sub-network 2 due to exchange of reactive power from the resources which lead the optimization tool to select a different set-point for the OLTC 2.

On the other hand, OLTC 1 tap profile reflects the operations of STATCOM 1: indeed, within the 09:00 to 15:00 time interval, STATCOM 1 injects reactive power, instead of absorb it like in case 3 scenario, causing a voltage increase. Therefore, OLTC1 is not shifted up when reactive power absorption is requested by the transmission

network. Its tap is shifted down again just before the peak of reactive power injection (around 18:00), and then is shifted up three times from late afternoon to the nightfall to compensate voltage drop caused by load increase.

The application of a realistic reactive power set-point profile to the demonstrator network optimization process, by simulating a reactive power exchange request from the transmission network, allows to analyze in details: how the optimization tool shares the power request between the flexible resources; to which extent each resource (or each type of resource) is exploited; how the exploitation of specific resources affects the exploitation or the operating conditions of the others. From the analysis presented above, it can be seen that STATCOMs can play an important role in reactive power modulation for fulfilling external request. If only a small amount of flexible generators is available (i.e. case 3 scenario), they can practically sustain the most of the power exchange on their own. For higher number of flexible resources (i.e. case 5 scenario), they can be successfully employed for modulating reactive power, in order to allow dispersed resources to provide their reactive power capabilities in the most efficient way for the distribution network operations. Furthermore, it can be observed that, in presence of a realistic reactive power request, OLTC operations may not be so severe to reach their reliability limits.

Concluding, the availability of a wide reactive power capability build up by different types of flexible resources allows, with suitable optimization strategies, to fulfil power exchange requests with an efficient exploitation of each resource.

4.6 CONCLUSION AND OUTLOOK

The analysis and tests carried out showed that the optimization tool developed for Italian demonstrator is suitable to fulfil the tasks described at the beginning of chapter 4 and in section 4.1. New features like flexibility aggregation/disaggregation, reactive power capability calculation, as well as the addition of power exchange constraints in the primary substation node (slack node), has been successfully implemented and tested. This optimization tool is capable to efficiently manage the distribution network allowing, at the same time, the exploitation of flexible resources for supporting the needs of the transmission network; it realizes the functionalities described in the SUCs described in D6.1, adequately fitting in the business process defined for the Italian demonstrator.

Further investigations have been carried out for assessing the impact of OLTC management on aggregated capability exploitation, as presented in section 4.5.1. In section 4.5.2, the operational conditions envisioned in accordance with business processes described in Italian BUCs, have been modelled by defining a realistic set-point profile for reactive power exchange versus transmission network.

From this analysis and the corresponding simulative tests, the following conclusions can be drawn:

1. The full exploitation of theoretical reactive capability requires a specific management of the OLTCs, which may be quite demanding in terms of tap shifting, compared to a limited gain in capability area;
2. The reactive power request modelled through the realistic set-point profile does not require to reach the limits of the available capability, even with a small amount of flexible resources (case 3 scenario);
3. Higher shares of flexible resources (i.e. case 5 scenario) allow to address better both the needs of DSOs (efficient management of distribution network) and the needs of TSOs (support of transmission network management);
4. Flexible resources close to primary substation are better suited for flexibility provision versus the transmission network, since dispersed resources cannot be exploited fully due to network constraints and their better capability to support local voltage control;
5. Assets like STATCOMs can provide an essential contribution, in presence of flexibility provision versus the transmission network, since they can virtually separate distribution and transmission networks in terms of reactive power fluxes, leading to an efficient management of distribution network and a better fulfilment of TSO requests;
6. Suitable management of the STATCOMs may relieve the OLTCs operation, allowing a better voltage and losses control by the means of reactive power modulation;

This tool will be exploited fully in field tests to be carried out within Task 6.4 activities. Such tests will be structured using the simulative tests carried out within Task 6.3 as a reference for defining relevant cases for evaluating the actual capabilities of the demonstrator set-up to address the project objectives.

5. OPTIMIZATION IN THE FINNISH DEMONSTRATOR

The focus of the Finnish demonstrator is on the use of distributed flexibility resources for the provision of frequency services for the TSO and of reactive power products for the DSO. That is achieved by the means of an aggregator role which can be the single contact for the system operators, but also has the possibility to combine its assets in order to lower the risks due to forecasting errors and operational uncertainties.

In the demonstrator the aggregator role is taken by Helen Ltd., an energy producer and retailer already active on TSO ancillary markets for reserves and balancing power in Finland. Its first objective in the demonstrator is to provide Frequency Containment Reserves (FCR-N for normal operation and FCR-D activated in cases of larger disturbances) to Fingrid, the Finnish TSO, by using the flexibility of various resources. Its second objective is to provide reactive power services to Helen Electricity Network Ltd., the DSO operating in the area of Helsinki, by using the extra capacity of the inverters connecting large batteries and PV production facilities.

The assets used in the demonstrator are the following:

- An industrial-scale Battery Energy Storage System (BESS) connected to the 10 kV medium voltage network. Its rated power output is 1.2 MW with an energy capacity of 0.6 MWh. It can be used fully for the purposes of the demonstrator and its converter is dimensioned in such a way that it can provide active and reactive power at the same time without limiting each other under the current FCR-N market rules. In the Finnish demonstration, active power is applied in the FCR-N market and reactive power for DSO's services through reactive power market (proof of concept).
- Eight consumer-sized batteries with a total power capacity of 24 kW. The primary objective of these batteries for the customers is to be able to store their excess PV energy production. They could however be used to provide flexibility services if they do not prevent the primary objective. Also, active power of these flexibilities is demonstrated to participate to the FCR-N market.
- Public charging stations for electric vehicles (EV) for an aggregated maximum capacity of 3 MW. Electric vehicles are a growing trend in Finland as in most European countries. When the charging is made using smart and connected charging stations, it is possible to modify the charging patterns in order to allow them to provide flexibility services. Flexibility of EV charging stations is targeted to be utilized in the FCR-N or FCR-D market in the Finnish demonstration.
- Residential heating loads with AMR for a total capacity of about 20 MW. Although the communication infrastructure using the current meters is not fast enough for balancing and reserves markets, the active power flexibility potential of these loads will be evaluated. It is expected that a new AMR roll-out will take place in Finland in about 10 years, most probably improving the communication capabilities of the system.
- The inverters (2x500 kW) of a 850 kW_p PV plant connected to the medium voltage network in Helsinki can provide reactive power to the DSO.

The products, and their relevant characteristics, considered for these assets are the following:

- FCR-N: Frequency Containment Reserves for Normal operation: The reserves are used to maintain the frequency within the desired range at times when the deviations are due to normal variations in production or consumption. They need to be fully activated within a maximum of 3 minutes. They should be symmetrical in providing up- and down-regulation. They are expected to follow a control curve such as displayed in Figure 51 with an extra accepted dead-band of ±0.05 Hz, reduced to ±0.01 Hz in the beginning of 2020. They should be dimensioned so that they can provide their maximum capacity for at least 30 minutes [32].

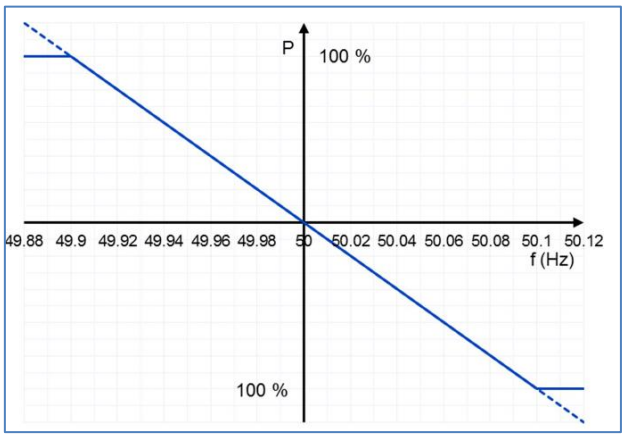

FIGURE 51 – LINEAR CONTROL CURVE FOR FCR-N IN FINLAND

- FCR-D: Frequency Containment Reserves for Disturbances: The reserves are used when the frequency changes due to a large disturbance such as a large production plant shutting down or an important transmission line being disconnected. They should be activated half within 5 seconds and fully in 30 seconds. They need to react only to drops in frequency (up-regulation). They should also be dimensioned so that they can provide their maximum capacity for 30 minutes.
- mFRR: Balancing energy market is market place for manual frequency restoration reserve (mFRR) which is used to balance the electricity generation and consumption in real time. The Balancing energy market organized by Fingrid is part of the Nordic Balancing energy market that is called also Regulating power market. Fingrid orders up- or down-regulation. Up-regulation considers increasing of production or reducing of consumption and down-regulation decreasing of production or increasing of consumption. The minimum bid size is 5 MW when electronically controlled. The market is closed 45 min before the delivery hour, and the decision of approved bid is received 15 min before the delivery hour. In the Finnish demonstration, the AMR heating loads were planned to be tested to participate to the mFRR market. However, during the project it has now been analyzed that the residential heating loads cannot be controlled fast enough for frequency control when using the current generation of AMR. The potential is however there for the future and the next generation of AMR. Simulated scenarios will be studied during the demonstration phase of the project, but no optimization process will be tested. It is thus left out of this deliverable.
- Reactive power: The reactive power reserves are used by the DSO to maintain its balance with the TSO within the required PQ-window. In the current state of design, the reserves should be able to follow an

hourly profile received day-ahead. Currently, the operation of DSO owned 110 kV reactor/capacitors is automatically controlled during the operating hour.

The PV plant is dimensioned so that it can provide reactive power compensation at any time also without active power production e.g. during night. This means that it can provide its services to the DSO whenever required as long as the price is above the additional operating costs. This leaves no room for optimization. The priority of the PV plant is to produce solar energy. Apparent power sets the limits for active and reactive power. Solar energy production is the priority and reactive power compensation would be limited in a case that the maximum apparent power is reached.

It has been analyzed during the project that the residential heating loads cannot be controlled fast enough for frequency control when using the current generation of AMR. The potential is however there for the future and the next generation of AMR. Simulated scenarios will be studied during the demonstration phase of the project, but no optimization process will be tested. It is thus left out of this deliverable.

For the EV stations and the BESS, very different optimizations are realized. For that reason, they are presented hereafter each as their own section.

The behavior of the consumers' batteries is ruled primarily by the consumers' behavior, which are to make sure that as much as possible of their excess solar production is used locally. In practice, this means that the batteries are available for providing frequency services only at the times between the sun rises and solar production starts to charge the batteries and after the evening consumption has brought the state of charge of the batteries low enough for the consumers to be satisfied that their production has been used for their own needs. During those times, the provision of FCR is possible while using the same optimization strategy as for the BESS.

5.1 OPTIMIZATION OF THE BESS AND CONSUMER-SIZED BATTERIES

The two types of batteries have similar characteristics. They can be controlled quickly, with a response time faster than required for any of the reserve markets existing in Finland (3 minutes for FCR-N and 5 seconds for FCR-D). They are however limited by their capacity. The capacity of the BESS can be fully used for the provision of services to the TSO supporting the frequency by active power provision as well as the DSO providing reactive power to assist in the PQ-window. The markets and pricing mechanisms are designed so that the most beneficial market for an asset that is sufficiently flexible is the one with the strongest constraints. In this case, the most beneficial market for batteries is the FCR-N market.

During preliminary testing, the BESS has been operated by providing an amount of FCR-N capacity such that it could provide it for 30 minutes (as required by the TSO). That quantity is determined by the following equation:

$$P_{\mathrm{Bid}} = \frac{0.5 * (0.95 * E_{\mathrm{BESS}} - 0.05 * E_{\mathrm{BESS}})}{0.5\ \mathrm{h}} = 540\ \mathrm{kW} \tag{5.1}$$

where P_{Bid} is the capacity that can be bid on the market, E_{BESS} is half of the total capacity of the BESS (600kW), here reduced by 5% of both ends to reduce the stress on the battery (The FCR-N product has to be bidirectional, see Figure 51, the starting point should be with a state of charge (SOC) of around 50% (0.5 is used for the dimensioning, but in practice, due to different efficiency impacts for charging and discharging, the starting point would be slightly different) and going either up or down) and 0.5 h is the time for which the capacity has to be provided.

5.1.1 NEED FOR THE OPTIMIZATION TOOL

As a result of tests in which the BESS was operated continuously with its maximum capacity, it has been noticed that the BESS is very often running itself completely full or completely empty. This is not efficient and hence optimization measures have to be applied here. The frequency deviations do not fluctuate up and down sufficiently for the SOC to remain around 50%. As a consequence, there are extended periods of time during which the BESS is not able to provide the service and is charged a penalty for it.

Therefore, there is an incentive to stop providing the FCR services at specific times and instead charge or discharge the battery in order to bring it back closer to a SOC of 50%. Here, a balance must be found between the benefits of allowing the BESS to provide its services during more time periods on one hand and the costs of running the battery as well as imbalance costs on the other. Finding this balance is where the optimization process can take place.

5.1.2 OVERVIEW OF THE OPTIMIZATION FUNCTIONALITIES

Table 8 gives an overview of the optimization that is run for the BESS and the consumer size batteries.

TABLE 8 – BRIEF OVERVIEW OF THE OPTIMIZATION FUNCTIONALITIES

Optimization	Finnish Demonstrator - BESS
Voltage Level	10 kV
Interconnection between:	Aggregator and TSO in most cases at 400kV/110kV interface
Objective	Maximize revenue
Boundaries	Power rating of the BESS: $P_{min} < P < P_{Max}$ where $P_{Max} = -P_{min} = 1.2\ MW$
Constraints	State of Charge: $SoC_{\min} \leq SoC_{\mathrm{m}} \leq SoC \leq SoC_{\mathrm{M}} \leq SoC_{\mathrm{Max}}$
Solver / Methods	Non linear solver
Algorithms	fmincon function
Programming Language	Matlab
Data Model	Custom
Aimed Accuracy	0,1%
Risks	Finding a local optimum instead of the absolute one. This could potentially lead to results far from what we would expect them to be.

5.1.3 TECHNICAL DESCRIPTION OF THE OPTIMIZATION TOOL

The objective of the optimization tool is to maximize the revenues obtained by the BESS by participating to the FCR-N market. The revenues can be expressed as:

$$R = \begin{cases} R_{\mathrm{cap}} + R_{\mathrm{E}} - C_{trf} - C_{\mathrm{pen}} - C_{\mathrm{deg}} & ,\text{if } \pi_{\mathrm{FCR}} \geq \pi_{\mathrm{bid}} \\ -C_{\mathrm{deg}} - C_{trf} & ,\text{if } \pi_{\mathrm{FCR}} < \pi_{\mathrm{bid}} \end{cases} \tag{5.2}$$

where R are the total revenues for the considered working period, R_{cap} are the revenues obtained from offering the capacity, R_E are the revenues obtained from the energy provided during the service provision, C_{trf} is the tariff cost for connecting the device to the network, C_{pen} is the cost of the penalties when the BESS fails to deliver the service, C_{deg} are the degradation costs associated with operating the BESS and π_{bid} and π_{FCR} are respectively the price bid by the aggregator on the market and the market price of the FCR service.

CAPACITY REVENUES, R_{CAP}

The revenues obtained from offering the capacity is the product of the volume of the bid by its price:

$$R_{\mathrm{cap}} = \sum_{t} P_{\mathrm{bid,t}} * \pi_{\mathrm{FCR,t}} \tag{5.3}$$

where $P_{bid,t}$ is the power offered as a bid during the one-hour time period t and $\pi_{FCR,\,t}$ is the FCR-N market price for that same time period.

The active power to be bid was calculated in equation (5.1), but in general, it can be expressed as:

$$P_{\text{bid,max}} = \min\left(P_{\text{Max}}, \frac{0.5 * (SoC_{\text{Max}} - SoC_{min})}{0.5\text{ h} * 100} * E_{\text{BESS}}\right) \tag{5.4}$$

where SoC_{min} and SoC_{Max} are the lowest and highest state of charge available for operation (expressed in percent), E_{BESS} is the total energy that can be stored in the battery and P_{Max} is the maximum rated power of the battery converter. The 0.5 in the numerator and the 0.5 h in the denominator are due to the regulation for providing the service which states that the provision must be symmetrical up and down, and that it has to be provided for at least half an hour. It does not apply in our case, but if the power rating (P_{Max}) of the battery was inferior to the value computed here, the battery could not offer more than its rated power.

REVENUES FROM ENERGY PROVISION, R_E

The revenues obtained from purchasing and selling energy comes from the difference of prices between purchasing and selling energy. The activity of the BESS is not bid on the day ahead or intra-day markets, thus it purchases and sells energy at the up-and down-regulation prices:

$$R_{\text{E}} = \sum_{\text{t}} \pi_{\text{reg,t}} \sum_{\text{m=1}}^{60} E_{\text{in/out,m}} \tag{5.5}$$

where $\pi_{\text{reg, t}}$ is the up- or down-regulation price for the hour t, depending on the sign of the following sum. $E_{\text{in/out, m}}$ is the energy exchanged by the BESS during each minute m of the hour t.

There are two cases for the exchanges of energy. The first one is when the BESS is providing the FCR service. The second one is when the BESS is attempting to bring its SoC to a level that should allow it, in the future, to operate more effectively.

When the BESS provides FCR-N, the energy it is expected to deliver must follow the curve illustrated in Figure 51 (referred to here as “droop curve”). In practice, the assets need to follow the curve as fast as possible. In order to ease the long term calculation, the frequency has been averaged over periods of one minute. Thus, the expected average energy to be provided for a minute is based on the droop curve as follows:

$$E_{\text{exp,m}} = \frac{P_{\text{droop,m}}}{60} \tag{5.6}$$

where $E_{\text{exp, m}}$ is the expected energy to be delivered and $P_{\text{droop, m}}$ is the power that should be delivered during minute m according to the average frequency for minute m, following the droop curve. Here and in the following, all of the $E_{**, \text{m}}$ represent the average energy that should be provided during a minute in order to reach the expected change in power. Similarly as hourly average energy is referred to in terms of kWh/h, in this case the unit is kWh/min.

On one hand where the BESS is close to being full or empty, the desirable energy will not be available and the expected energy exchange is bounded as follows:

$$E_{\mathrm{del,m}} = \mathrm{Max}\left(\min\left(E_{\mathrm{exp,m}}, \frac{SoC_{\mathrm{Max}} - SoC}{100} * E_{\mathrm{BESS}}\right), \frac{SoC_{\mathrm{min}} - SoC}{100} * E_{\mathrm{BESS}}\right) \tag{5.7}$$

where *SoC* is the current state of charge (in %), $\frac{SoC_{\mathrm{Max}}-SoC}{100} * E_{\mathrm{BESS}}$ and $\frac{SoC_{\mathrm{min}}-SoC}{100} * E_{\mathrm{BESS}}$ are respectively the amounts of energy that can still be charged to or discharged from the battery without exceeding its SoC limits.

On the other hand, when the BESS is not providing FCR-N, it can either stay idle, in which case there is no energy exchange or it can follow its optimization strategy. As a result of the optimization process, the BESS has some sort of a dead band between values referred to as SoC_m and SoC_M such that, when the *SoC* is between those two values, the BESS remains idle. When outside of the band, it tries to get back towards it as illustrated in Figure 52.

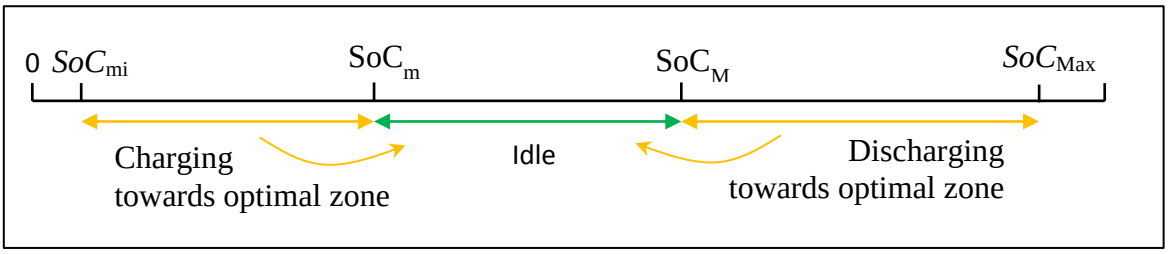

FIGURE 52 – ACTIONS TAKEN BY THE BESS DEPENDING ON ITS STATE OF CHARGE

In mathematical terms, it can be expressed as:

$$E_{\mathrm{opt,m}} = \begin{cases} \frac{P_{\mathrm{max}}}{60} & , if\ SoC < SoC_{\mathrm{m}} \\ 0 & , if\ SoC_{\mathrm{m}} \leq SoC \leq SoC_{\mathrm{M}} \\ -\frac{P_{\mathrm{max}}}{60} & , if\ SoC > SoC_{\mathrm{M}} \end{cases} \tag{5.8}$$

where $E_{\mathrm{opt,\ m}}$ is the energy exchanged when performing the optimization for minute m and P_{max} is the maximum power used to charge and discharge the battery.

In the model, for each minute m, the battery can only be either providing FCR-N (equation (5.7)) or running its SoC optimization (equation (5.8)). In that way, the energy exchanged viewed from the network side is the following:

$$E_{\mathrm{in/out,m}} = \begin{cases} E_{\mathrm{del,m}} & , \text{when providing FCR} - \text{N} \\ E_{\mathrm{opt,m}} & , \text{when running the optimization} \end{cases} \tag{5.9}$$

where $E_{\mathrm{in/out,\ m}}$ is the energy exchanged with the network by the BESS during minute m.

On the BESS side, in order to assess the impact the exchange has on the state of the battery and keep track of its status in the model, we need to include the effect of the efficiency of the BESS system:

$$\Delta E_{\mathrm{m}} = \begin{cases} E_{\mathrm{in/out,m}} \,/\, \eta_{\mathrm{c}}\,, & \text{if } E_{\mathrm{exp}} > 0 \\ E_{\mathrm{in/out,m}} * \eta_{\mathrm{d}}\,, & \text{if } E_{\mathrm{exp}} < 0 \end{cases} \tag{5.10}$$

where ΔE_m is the exchange of energy seen by the BESS during minute m and η_c and η_d are the charging and discharging efficiencies respectively.

TARIFF COSTS, C_{TRF}

The BESS is connected to the distribution grid and thus the aggregator needs to pay a grid tariff, calculated as follows:

$$C_{\mathrm{trf,m}} = \mathrm{BC} + \pi_{trf} * P_{3,m} + (\pi_E + T) * E_m \tag{5.11}$$

where in Helsinki, Finland, for MV customers, BC is a basic charge of 217 € per month, π_{trf} is the power charge, 3.68 €/kW, P_m is the highest hourly average power in the month m. π_E is the energy charge, 1.75 and 0.78 €/kWh in winter days and other times, respectively, T is the electricity tax, 0.872 €/kWh and E_m is the energy consumption of the BESS during a month m. These values were the ones charged at the time of the optimization and reporting. They are of course expected to vary with time.

CAPACITY PENALTIES, C_{PEN}

The BESS has to pay penalties when it has agreed to provide FCR services, but is not able to do so. For the minutes during which E_{del} is different from E_{exp}, the aggregator still receives the payment for E_{del}, but not for the quantity between E_{exp} and E_{del} and has to pay the penalty for the full amount between E_{bid} (P_{bid}/60) and E_{del}. Indeed, in case of failure to deliver, the TSO sees it as an inability to provide the full amount of the offered bid, although the requested energy was lower. This can be expressed as:

$$C_{pen} = \sum_{t} \left(\sum_{m=1}^{60} \left(E_{exp,m} - E_{del,m}\right) * \pi_{FCR,t} + \left(\frac{P_{bid,t}}{60} * \pi_{pen,t}\right)\right) \tag{5.12}$$

where $\pi_{pen,\,t}$ is the penalty price for failure to deliver the service during the hour t.

DEGRADATION COSTS, C_{DEG}

The performance parameters of batteries are degrading according to idling time keeping different SOC levels and charging/discharging cycles, referring calendar ageing and cycle ageing, respectively. Therefore, the degradation costs are composed of two terms. The first is degradation of the battery system over time, which takes place continuously, but is dependent on the state of charge. The second term is a cycling degradation, taking place when the batteries are charged and discharged.

Although the degradation model of the Lithium batteries may change slightly based on their chemistries, the assumption is made that the following methods are accurate enough for demonstrator's purposes. An accelerated ageing test model for Lithium batteries is developed in [33] and the degradation model for the battery used in frequency regulation is developed in [34].

The percentage of calendar capacity fade (C_{cal}) can be calculated as follows:

$$C_{\mathrm{cal}} = 0.1723 * \sum_{\mathrm{i}} e^{0.007388 * SoC_{\mathrm{i}}} * m_i^{0.8} \tag{5.13}$$

where SoC_i represents the SoC level and m_i represents the total time, expressed in months, that battery keep the specific SoC and zero output power. To calculate (5.13), it is enough to find periods having zero output power and divide them to i different SoC level by methods like *histcounts* in MATLAB.

The percentage of cycle capacity fade (C_{cyc}) can be calculated as follows:

$$C_{\mathrm{cal}} = 0.021 * \sum_{\mathrm{i}} e^{-0.01943 * SoC_{\mathrm{k}}} * cd_{\mathrm{k}}^{0.7162} * nc_{\mathrm{k}}^{0.5} \tag{5.14}$$

where nc_k is the number of cycle with having cycle depth equal to cd_k and SoC_k represents the average SoC level of that cycle depth. In order to calculate (5.14), the *rainflow* counts method for fatigue analysis, implemented in MATLAB, can be used.

The battery lifetime is defined as the time it loses a certain percentage of its capacity, called end-of-life (EOL) and considered usually equal to 20%. Assuming salvation value for battery equal to 60% of initial capital cost (ICC) and zero interest rate, the degradation cost (C_d) of the battery for the studied time becomes:

$$C_{\mathrm{d}} = 0{,}4 * ICC * \frac{C_{\mathrm{cal}} + C_{cyc}}{EOL} \tag{5.15}$$

OPTIMIZATION ALGORITHM

The optimization per se is performed in Matlab, using the fmincon function. fmincon is a nonlinear solver using the interior-point method in order to find the optimum solution to a problem. It was chosen because of past experiences with it and the fact that, for this particular optimization problem, the computing time was not much of a factor (this tool does not interact continuously with the operation of the system), so finding the best solver in terms of time performance was not a priority. In this case, the solver is run using the following parameters:

$$\min_{SoC_{\mathrm{m}}, SoC_{\mathrm{M}}} R(\pi_{\mathrm{bid}}, SoC_{\mathrm{m}}, SoC_{\mathrm{M}}) \ \ such\ that\ 0 \leq SoC_{\mathrm{m}} \leq SoC_{\mathrm{M}} \leq 100 \tag{5.16}$$

5.1.4 TEST CASES FOR THE OPTIMIZATION

The test cases use the same optimization algorithm and it is run over 4 years of data (2015-2018). The used historical data of the BESS is owned by Helen and it was given to VTT for the purposes of optimization and forecasting analyses during the EU-SysFlex project. The data considered is the price of FCR services for each hour and the frequency for each second, averaged over one-minute time periods in preprocessing. The difference between the test cases comes from times when the battery is set to provide FCR, to remain idle or to actively try to bring its SoC back to a better state.

Some of the relevant data for market prices and frequency are showed in Table 9, Table 10 and Figure 53. The market data (Table 9) gives an idea of the type of values expected on the FCR-N market, on the day-ahead pool market as well as of the up- and down-regulation prices. It shows the average, standard deviation as well as minimum and maximum values for each market. It can be noticed that the FCR-N capacity and penalty fee (both values are the same currently in the Finnish markets) has a value that is significant when added or removed from the pool market prices. The up and down regulation prices are designed to discourage imbalances. They are thus respectively always higher or lower than the spot price.

The frequency data (Table 10 and Figure 53) shows how often the system is in situations of under- or over-frequency and of how long those events last. This is relevant because the battery capacity is, by design, limited to events lasting for a maximum of 30 minutes (or up to an hour if the battery was either full or empty during an up- or down-regulation event respectively.

TABLE 9 – RELEVANT MARKET STATISTICS FOR THE NORDIC SYNCHRONOUS SYSTEM FROM 2015 TO 2019

Market prices	Mean	Std	Min	Max
FCR-N Capacity fee/penalty (€/MW,h)	20.36	20.22	0	500
Pool market (€/MWh)	36.14	15.03	0	255.02
Down-Regulation (€/MWh)	31.75	20.13	-1000	249.97
Up-Regulation (€/MWh)	41.04	39.62	0.32	3000

TABLE 10 – RELEVANT FREQUENCY STATISTICS FOR THE NORDIC SYNCHRONOUS SYSTEM FROM 2015 - 2019

		Under-Frq	Dead-band	Over-Frq
Time Share (%)		40.4	19.8	39.8
Event Duration (Min)	Mean	5.73	1.76	5.77
	Standard Deviation	12.86	2.89	12.92
	Longest Event	304	900	265

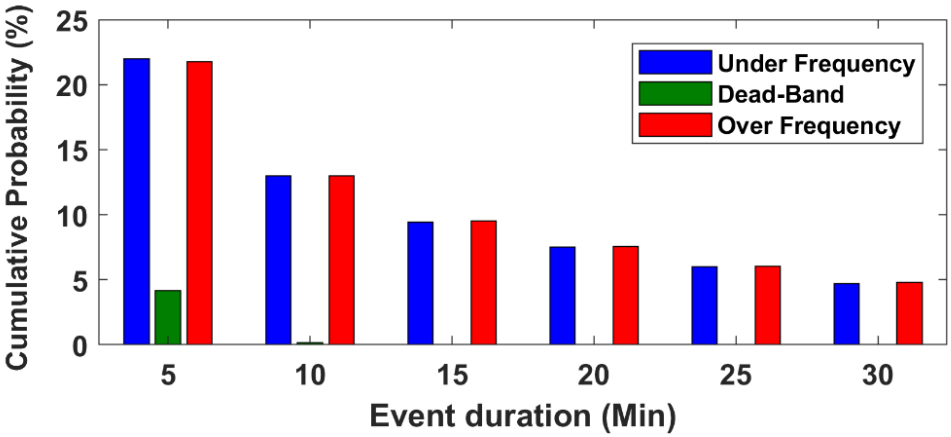

FIGURE 53 – CUMULATIVE PROBABILITY OF EVENTS HAVING A DURATION LONGER THAN A SPECIFIC TIME

Method 1: Dead band optimization

In the first scenario, the BESS is attempting to optimize its SoC during the times when the frequency is in the dead band allowed by the TSO. For the provision of FCR-N, the providers are not required to actually respond to variations smaller than ±0,05Hz. However, it should be noted that the regulation of FCR-N does not currently allow the resource owners to explicitly recover their assets during the times when the frequency is in the dead-band.

Method 2: Price-based recovery

In this scenario, the bidding price is chosen so that, based on historical data, the revenues from the BESS are increased by bringing the SoC back to a more favorable state during the times when the market price is low.

Method 3: High Power SoC recovery

In this scenario, the BESS charges or discharges more power than bid in the day-ahead market at times when the frequency deviation is more than 0.1 Hz. In other words, the BESS follows the dash-line in Figure 51.

5.1.5 EXAMPLARY SIMULATIVE RESULTS FROM BESS OPTIMIZATION

Table 11 shows the results of the optimization based on the 4-year period data between 2015 and 2018 for the three scenarios presented above, where method 1 refers to dead-band optimization, method 2 is the price-based recovery and method 3 is the high-power recovery.

Method 1, i.e. the dead-band optimization, gives the best results for the BESS. It should be noted however that the regulation does not currently allow the resource owners to explicitly recover their assets during the times when the frequency is in the dead-band. The exercise here was more to show that it could be done and that the algorithm was working on a first scenario.

Method 2, i.e. the price-based recovery, shows an increase in total profit of about 6.7%.

TABLE 11 – RESULTS FOR THE OPTIMIZATION OF THE BESS (AVERAGE ANNUAL PROFIT DURING THE FOUR YEAR TIME PERIOD)

	No Recovery	Method 1	Method 2	Method 3	Methods 2 & 3
π_{bid} (€)	0	1	4.46	0	4.73
SoC_m (%)	-	41.14	56.65	14.82	55.60
SoC_M (%)	-	66.92	84.69	83.89	79.20
R_{cap} (k€)	79.19	91.17	80.02	79.26	80.07
C_{pen} (k€)	-17.80	-5.92	-16.97	-17.85	-16.92
R_e (k€)	-0.62	-0.98	0.15	-0.66	0.15
C_{trf} (k€)	-17.59	-16.29	-17.20	-17.51	-17.47
C_{deg} (k€)	-1.20	-1.09	-1.20	-1.20	-1.20
Profit (k€)	**41.98**	**67.00**	**44.80**	**42.03**	**44.58**

In addition, an example of the BESS operation during a cold winter day is given in the following. Figure 54 shows the frequency observed during that day in the Nordic synchronous system. Figure 55 shows, for the different methods, how much power the BESS is injecting or taking from the grid. And Figure 56 shows how the SoC of the BESS changes during the day based on those exchanges.

Figure 55 shows that after each frequency event when the frequency goes back to the dead-band, method 1 starts to inject power in the reverse direction of the last frequency event to recover the SOC. While this behavior helps the BESS to avoid penalty, it recreates pressure on the system immediately after frequency restoration. Therefore, the new technical requirements forbid this recovery method.

On January 7th at hours 2-6, 8-9, and 12-21, the FCR price was lower than 4.46 € (the optimum bid price determined in method 2); therefore, method 2 did not provide FCR-N for these hours. However, since the SoC was in the optimum range, between 56.65% and 84.69% (Table 11, column 4), the BESS, using method 2, did not perform SoC recovery either. During hour 7, the frequency is higher than 50.1 Hz for some minute that could activate method 3. However, since the BESS in that time has SOC in the optimum range, between 14.82 and 83.89 (Table 11, column 5), there will be no SOC recovery in method 3 and its behavior is similar to method 0, in this case.

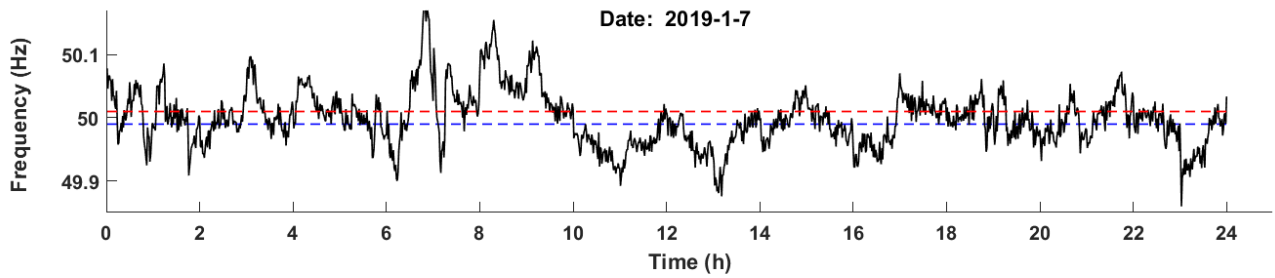

FIGURE 54 – THE FREQUENCY OF THE NORDIC SYNCHRONOUS SYSTEM ON JANUARY 7, 2019

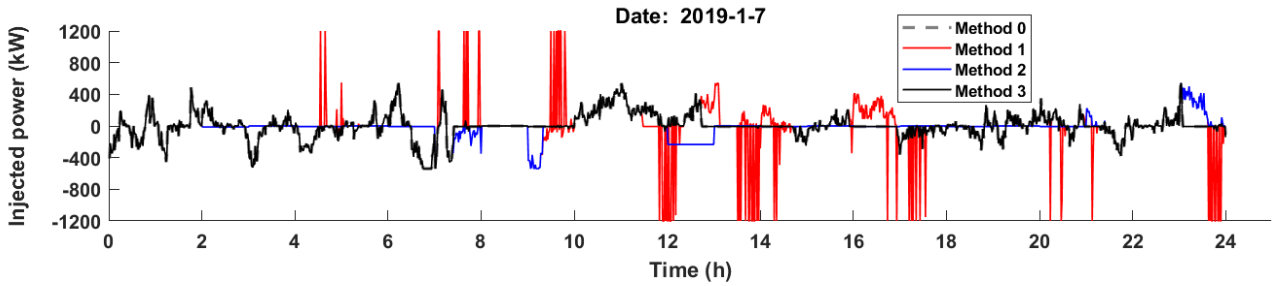

FIGURE 55 – THE INJECTED POWER USED FOR RECOVERY BY THE BESS ON JANUARY 7 2019

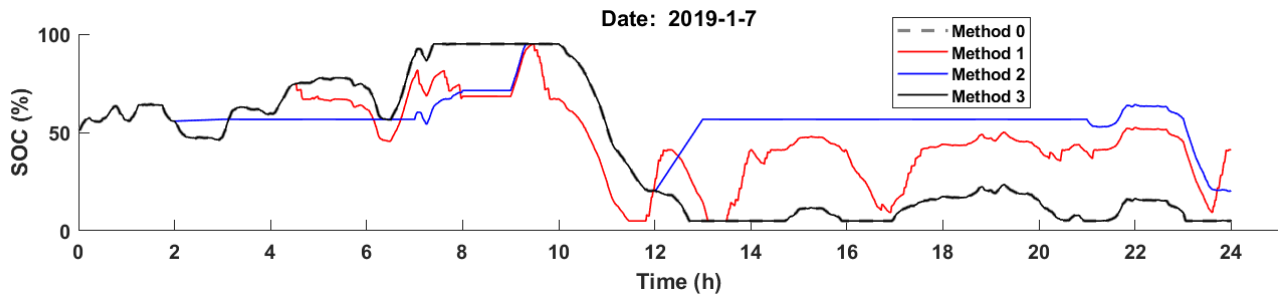

FIGURE 56 – THE SOC OF THE BESS INSTALLED IN HELSINKI AREA ON JANUARY 7 2019

5.1.6 CONCLUSIONS AND OUTLOOK FOR THE BESS

The optimization of the BESS based on the historical frequency data and the modelled behavior of the battery system allows the operator to set a price on the provision of FCR-N services. In opposition with conventional resources where the price is set by the operating costs, in this case, the price is determined so that the BESS is allowed to recover during the low-priced hours and provide more frequency services during the higher priced hours. It could be argued that putting the BESS in recovery mode by paying the imbalance fees negates the benefits of offering the frequency service in the first place. However, it can be answered that the result is a shift from utilizing more cost-intensive resources to cost-effective ones. In addition, in the future, it would be possible for the aggregator, during those hours, to use other resources (such as demand-response units, flexible generators, or even the EV described hereafter) to compensate for the BESS recovery power.

5.2 OPTIMIZATION OF THE EV PUBLIC CHARGING STATIONS

Helen Ltd., as an aggregator, operates a set of EV charging stations in the region of Helsinki. It was identified that they could provide frequency services by adapting the charging rate for the connected vehicles. The first step was to analyze the data about the usage of the stations. The number of stations still being limited and the fact that they are all public charging stations, the data analyses failed to identify any other correlations to the power intake of the set of stations than the time of day. In other words, factors such as the weekday, the temperature or the time of year does not seem to impact the usage of the stations in the available data.

The second step was to forecast the available power that the stations could provide. As mentioned earlier, it boiled down providing estimates of the stations' usage depending on the time of day. As detailed in EU-SysFlex deliverable D6.2 *"Forecast: Data, Methods and Processing. A common description"*, the results of the forecasting work was in the form of cumulative density functions (CDF), giving the probability, in %, for each time of the day, that at least a certain amounts of flexibility would be available. The forecasting tool gives different estimates for FCR-N and FCR-D because the first has to provide flexibility up and down in a symmetric way while the second can provide only up-regulation by decreasing the power consumed. A third hypothesis was to provide FCR-D first and use whatever power was left to provide FCR-N.

5.2.1 NEED FOR THE OPTIMIZATION TOOL

The optimization tool starts with the CDF curves calculated by the forecasting tool. Its objective is to determine how much power the aggregator should bid on the markets. In order to maximize the revenues from providing the service, the optimization algorithm has to find the balance between the increased revenues due to bidding and providing higher amounts of frequency products with the cost of being charged penalties for failing to provide the promised services.

Another result of the optimization process is that, by running it against historical data or against possible future scenarios, the aggregator could estimate the value they could extract from providing the service. That value can then be used to decide the willingness to participate by the aggregator itself, but also, by sharing the revenues, could users be convinced to participate in ways that would increase the potential. This is out of the scope of this demonstrator, but the expected potential value could be used in order to offer a monetary reward to EV users that would agree to collect their car not fully charged when it would otherwise be or to notify the aggregator of their expected charging time before connecting their car.

5.2.2 OVERVIEW OF THE OPTIMIZATION FUNCTIONALITIES

Table 12 gives an overview of the optimization that is run for the EV charging stations

TABLE 12 – BRIEF OVERVIEW OF THE OPTIMIZATION FUNCTIONALITIES

Optimization	Finnish Demonstrator - EVCS
Voltage Level	0.4 kV
Interconnection between:	Aggregator and TSO
Objective	Maximize revenue
Boundaries	Available power for up-regulation or for symmetrical regulation as per the existing CDF
Constraints	State of Charge: $0 < SoC < 100\%$ At the end of each charging period: $SoC > SoC_{exp}$ where SoC_{exp} is the minimum expected SoC for the user when the EV is picked up.
Solver / Methods	Stochastic optimization
Algorithms	First derivative test
Programming Language	Matlab
Data Model	Custom
Aimed Accuracy	Not applicable
Risks	The accuracy of the forecast of the CDF for the EVCS usage would not be sufficient to offer reliable enough results. The same optimization could lead to better results with a better forecast based on more extensive input data.

5.2.3 TECHNICAL DESCRIPTION OF THE OPTIMIZATION TOOL

The aim of the optimization is to find the balance between the increased revenues due to bidding and providing higher amounts of frequency products with the cost of being charged penalties for failing to provide the promised services. In the first case, the flexibility promised is remunerated at the market price. In the second case, the flexibility provided is still rewarded at the same price, but the energy that was promised and not delivered is charged at the penalty price.

The profit for the flexibility provider (PR) can thus be calculated as follows:

$$PR(F,t) = \begin{cases} F\pi_f & f \geq F \\ f\pi_f - (F-f)\pi_{-f} & f < F \end{cases}, \tag{5.17}$$

where F is the amount of flexibility promised for the time t; f is the actual amount of FCR that is provided in real-time, estimated using the Probability Density Function (PDF) compiled from historical EVCS usage and, as shown below, at the root of the CDF; π_f is the remuneration amount in €/MWh; and π_{-f} is the penalty of not providing the promised FCR.

Therefore, the expected profit (PR_{ex}) for the flexibility provider from participating in the reserve market will be:

$$PR_{ex}(F,t) = PDF(f \geq F,t)\,F\,\pi_f + \int_0^F \left(f\pi_f - (F-f)\pi_{-f}\right) PDF(f,t)\,df\ , \tag{5.18}$$

while

$$PDF(f \geq F,t) = 1 - \int_0^F PDF(f,t)\,df\ , \tag{5.19}$$

where CDF is the Cumulative Density Function as described previously and calculated in deliverable D6.2 *"Forecast: Data, Methods and Processing. A common description"* and shown in Figure 57. The CDF have been estimated for FCR-N, FCR-D and FCR-Dn (FCR-D bids after some capacity has already been bid for FCR-N) for the different times of day. These are based on the expected numbers, times, power intakes and durations of charging events for the day. A strategy has been developed to allow the different charging events to provide the flexibilities required for FCR-N and FCR-D and then sum them up.

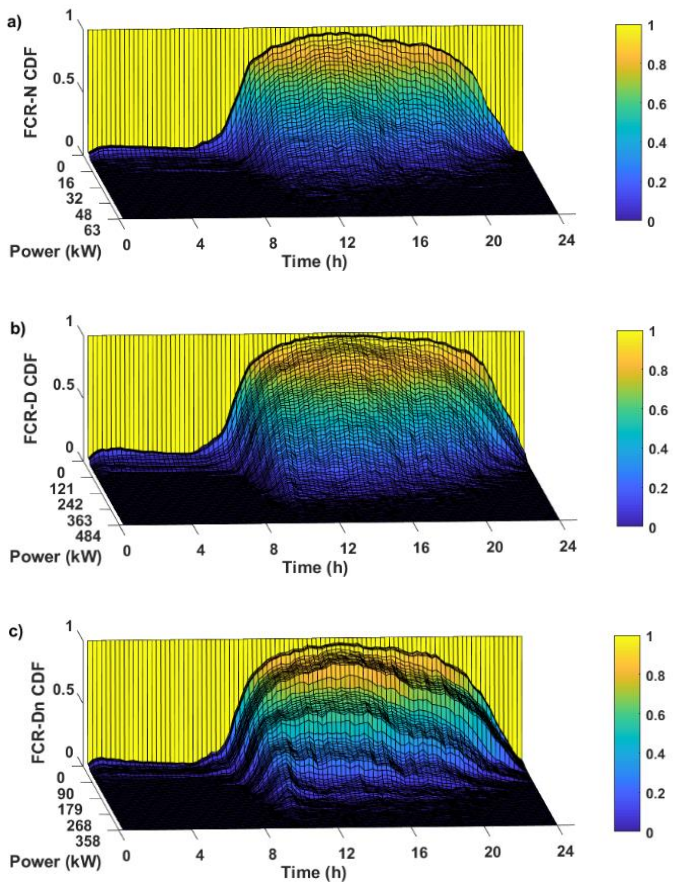

FIGURE 57 – POWER CUMULATIVE DENSITY FUNCTION (CDF) PROVIDED BY EVCSAT DIFFERENT TIMES OF DAY FOR A) FCR-N, B) FCR-D, AND C) FCR-DN

In order to maximize the expected income, F must be selected so that $\partial PR_{ex}/\partial F = 0$. Therefore, the optimum FCR value (F_{op}) can be calculated from (5.18) and (5.19 using Leibniz's rule as follows:

$$\frac{\partial PR_{ex}\left(F_{op},t\right)}{\partial F_{op}} = \\ = \pi_f - \pi_f \,\mathrm{CDF}(F_{op},t) - \pi_{-f}\,\mathrm{CDF}(F_{op},t) = 0, \tag{5.20}$$

$$\mathrm{CDF}(F_{op},t) = \frac{\pi_f}{\pi_f + \pi_{-f}}. \tag{5.21}$$

In other words, the flexibility provider should participate in the reserve flexibility market with a power of F_{op}, which satisfies (5.21). In the current Finnish reserve market regulations, $\pi_f = \pi_{-f}$; therefore, the maximum expected income is achieved by bidding the median of the FCR distribution. At this stage, the flexibility providers could decide which market, e.g. FCR-N, FCR-D, or a combination of them, presents the highest expected profit by calculating (5.21) for the available markets.

5.2.4 TEST CASES FOR THE OPTIMIZATION

The test case analyzed for the EVCS optimization is to run the algorithm against past market and EVCS utilization data. The market data is available from the TSO's open data platform [35], including the capacity prices for FCR-N and FCR-D, as well as the energy and prices used and applied for each time period.

The FCR-N and FCR-D prices vary highly from one day to the next, but an example of them is illustrated in Figure 58.

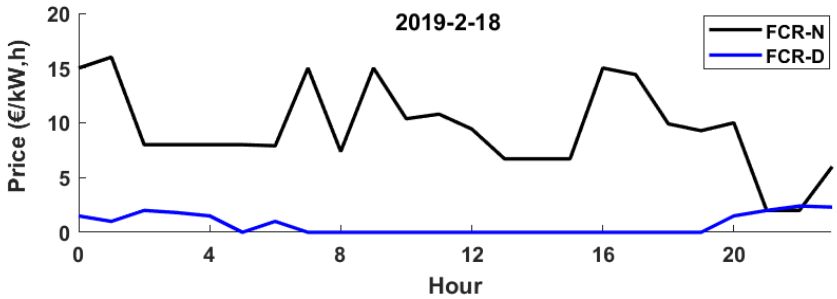

FIGURE 58 – FCR-N AND FCR-D PRICES IN FINLAND FOR FAB. 18TH, 2019

5.2.5 EXAMPLARY SIMULATIVE RESULTS FROM THE EV CHARGING STATIONS

As shown in Figure 57, the capacity that could be used for flexibility by the EVCS will be almost zero during the night. This is because of the fact that people use public charging stations mostly during day times. The data used in this analysis was provided by Helen and it contained the data of Helen's public charging stations in Helsinki. Therefore, private charging stations are excluded since EV owners charge their cars at home, during nights. The maximum expected FCR-N of these EVCS is about 12 kW happening at 2:00 p.m., while the maximum expected

FCR-D is about 143 kW happening at the same time. Looking at an expected profile of FCR-Dn shows that EVs can still provide a considerable amount of FCR-D after providing FCR-N. The maximum FCR capacity calculated here for public EVCS in the Helsinki area is not significant in comparison to the total needs for Finland (140 MW FCR-N and 260 MW FCR-D [36]). This is due to the fact that the numbers of vehicles and stations in the Helsinki area are still very low. Based on the historical data until September 2018, the available capacity has been calculated for the month of October 2018.

Table 13 presents the average daily profit which would have been obtained by providing FCR services, including the incomes for capacity and the penalty at times when the delivery would not have been possible. The profit is calculated in three categories: FCR-N, FCR-D, or as a combination of FCR-N and FCR-Dn. Although FCR-N has a larger remuneration per capacity, the profit of providing FCR-N is less than FCR-D because EV cannot provide large down-regulation compared to up-regulation reserves.

Table 13 shows that providing a combination of FCR-N and FCR-Dn is the most profitable choice. However, providing just FCR-D may be a more wise choice for public EVs. In order to achieve the maximum FCR-D, the EVs should start to charge the battery immediately with the maximum power, which is the most desirable way for a public charging station. In addition, because the departure time is not deterministic, charging the EV by Pav in order to have some FCR-N capacity will lead to a lower than expected state of charge in case of an early departure.

Furthermore, in FCR-D the reserve is provided whenever the frequency is less than 49.9 Hz, while the FCR-N must provide reserve whenever the frequency is out of the dead band of (49.99, 50.01) Hz. Analysis of the frequency records for the Nordic power [35], shows that FCR-D providers must activate their flexibility less than 1% of the time while FCR-N providers need to activate their resources about 80% of the time.

Table 13 compares the profit resulting from the proposed methods with an ideal estimation where the profile forecasting was assumed perfect and the measured data was substituted to the estimations. This comparison shows that the methodology presented here allows extracting about 62% of the ideal available profits. While a perfect forecast and estimation will remain impossible, the uncertainty would be reduced if the data included more EV charging events.

In addition, the table shows the average profit for each charging event and per kWh of energy used for EV charging. This table states that the income for combined FCR-N and FCR-Dn per kWh of energy is about 2 euro cents (1.9 – 2.8), which is about half of the average energy cost in Finland (about 4.6 euro cents in Oct 2018 [“Nordpool Data,” https://www.nordpoolgroup.com/Market-data1/#/nordic/table, accessed August 2018]).

TABLE 13 – THE AVERAGE DAILY PROFIT (EURO) FOR PROVIDING FCR DURING OCTOBER 2018

		FCR-N	FCR-D	D+N *
Proposed Method	Absolute	3.846	9.452	10.99
	Per event	0.057	0.148	0.170
	Per kWh	0.006	0.017	0.019
Ideal estimate	Absolute	5.608	16.48	17.09
	Per event	0.080	0.238	0.247
	Per kWh	0.009	0.027	0.028

* The combination of FCR-N and FCR-Dn

5.2.6 CONCLUSIONS AND OUTLOOK FOR THE EV CHARGING STATIONS

The provision of FCR-N services by EV charging stations does not produce many revenues. In addition, it requires the vehicles to be charged at a rate below their maximum charging power, thus making it very likely that the users will not find a vehicle fully charged when they pick it up.

FCR-D has a better potential and is more practical for the users. It is therefore the recommended mode of operation. The density curves obtained for the provision of FCR-D actually represent the potential for up-regulation, or a reduction in consumption.

5.3 CONCLUSIONS AND OUTLOOK FOR THE FINNISH DEMONSTRATOR

The optimization of the BESS and of the EV charging station gives bids to be placed on the markets for FCR-N (and FCR-D for the EV charging stations). Only active power of these assets has been optimized. In the demonstration, the industrial sized BESS has also flexibility resource of reactive power. Applying reactive power of this BESS for DSO's needs does not at all compete with the use of active power of this special asset.

The behavior of the system frequency is, by nature, extremely difficult to forecast day-ahead. It results from the market actors suffering deviations between their planned production and consumption on one hand, and the exchanges actually realized. Assuming that the frequency deviation could be forecasted would come down to saying that those actors' exchanges could be forecasted better. If that was the case, those actors would already have better forecasts or some other actors would already take advantage of the situation to make some easy profits (successfully bidding the market imbalances would result in incomes without needing to actually produce or consume any power). The fact that no actor does that currently would tend to show that either forecasting the imbalances is impossible, or that it is at the very least extremely complicated.

For that reason, the optimization in the Finnish demonstrator is based on the historical behavior of the markets, i.e. "How would the assets have performed over the past considered time period if it had been given these specific settings?" and then attempt to optimize the settings.

The optimization of the BESS shows good results (about a 6.6% increase in revenues) with the price-based strategy in which the BESS pays the imbalance prices in order to optimize its SoC at times when the FCR-N prices are low.

The EVs show little profit when participating to the FCR markets and the number of events with the FCR-D market are limited over a year. In addition, the participation to the FCR-N market is not very well suited to the normal operation of EVs (needing to charge at a power lower than the rated power, thus, by default, charging the vehicles slower than possible).

6. GENERAL CONCLUSION AND OUTLOOK

This deliverable presents the grid optimization approaches and optimization tools adopted or developed within the three demonstrators of WP6. Furthermore, it gives preliminary results achieved from these optimizations for relevant test cases and scenarios.

The objective of these optimizations is to explore the new operating conditions the networks have to face, in presence of distributed assets flexibility exploitation aimed at proving ancillary services to the TSO. The general need of testing new operating scenarios in order to "analyze the opportunities arising from decentralized flexibility resources connected to the distribution grids to serve the needs of the overall power system" is in common with all the demonstrators.

The fulfillment of the main objectives associated with the demonstrators is ensured with the tools that were developed by the involved partners. Within the frame of the project, based on the individual need of the system operators, directly linked to their grid structure and voltage level, several tools have been developed which can be used to provide ancillary services from distributed flexibility resources. These services have to be in accordance with the requirements of DSOs and TSOs. Thus, they need an improved coordination between the involved system operators using RES's active and reactive power flexibilities. However, the ways pursued to address this need are different and reflect the specific features and background of each demonstrator.

Within the German Demonstrator, the optimizations are carried out taking into account an extra-high voltage grid and a high-voltage distribution network. Two different optimization tools (NETOPT and PQ Maps) with different complementary application functionalities were developed within the German demonstrator. The focus has been on managing distributed energy resources (DER) connected to high-voltage (HV) grids in order to provide suitable active and reactive power (P-Q) flexibilities to the high-voltage grids of a DSO themselves as well as the extra-high-voltage (EHV) grids of a TSO. Contrary to the actual approach, where the TSO solves its grid problems without considering requirements in the distribution grid, it could be shown that the German demonstrator enables a more reliable and efficient operation of both grids. This goal was addressed by generating suitable congestion-free P and Q flexibilities from the control center optimization tool and PQ Maps in combination with network equivalents, which can be accessed by the TSO as well as by improving communication between DSOs and TSOs. Due to this, the approach corresponds to a completely new operational method. However, the PQ Maps do not provide insights on the combination of set-points to reach a specific PQ point available on the flexibility areas. The algorithm only ensures that there is at least one combination of flexibility activations that allow to reach that PQ point. The optimization tool NETOPT works exactly on this part. It computes the resources set-points that optimize the current network operation considering a specific objective function. It has to be ensured that both approaches calculate realistic flexibilities within future applications, such as the planned field test wherein all operational constraints have to be taken into account by both tools.

The optimization tool implemented in the Italian demonstrator is based on a multi-period Mixed Integer Non-Linear Programming (MINLP) model; the algorithm is designed to reduce computational efforts, exploiting non-linearity and integrality decoupling, in order to perform reasonably fast OPF calculations even for networks with a

large number of nodes and in presence of intertemporal energy balance constraints. These features make it suitable for the analysis of distribution networks with a sensible presence of flexible resources and battery storage units and, in other words, it is an effective tool for guaranteeing an optimal state of distribution network.

New functionalities have been added to the core algorithm for exploiting this tool in the context of the EU-SysFlex project. The introduction of power exchange constraints in the primary substation node (slack node) allows modeling the constrained profile of active and reactive power flows resulting from a specific request from the TSO. Flexibility aggregation/disaggregation allows to calculate the correct set-points for flexible resources based on a suitable allocation of flexibility range, addressing the needs of both distribution and transmission networks and thus supporting the coordination between TSO and DSO. The allocation of flexibility is carried out within the optimization process, exploiting other two newly developed functionalities: reactive power capability calculation and active power parametric curve calculation. The integration of these functionalities in a single algorithm allows a more efficient calculation process, guaranteeing also that the consequent flexibility activations respect the network constraints, avoiding the need to run another optimization process after the flexibility selection from the TSO. The resulting optimization tool is capable to carry out the functionalities described in the SUCs presented in D6.1, adequately fitting in the business process defined for the Italian demonstrator.

Preliminary simulations of network scenarios with different shares of controllable resources allowed to test the capabilities of the optimization tool and to carry out specific analysis for assessing the jointly exploitation, and corresponding limits of OLTCs, STATCOMs and distributed flexible resources of different types. This analysis returned valuable knowledge in preparation for the field tests of Task 6.4: the achieved results could be used as a reference framework for preparing the structure of the test to carry out within the physical demonstrator.

Within the Finnish demonstrator, the optimization focuses on optimizing the active power bids of a BESS and of EV charging stations. The provision of reactive power by the BESS inverters for the DSO's needs is not considered, as it does not compete with the use of active power of this specific asset. The optimization of the BESS shows about 7% increased income compared to a system without it. The optimization of the EVs shows little profit, with the existing stations and EV users, when participating to the FCR markets.

The optimization approaches and the corresponding results were reviewed from a holistic point of view, analyzing how they contribute to the Work Package 6 objectives: supporting or fulfil specific request from TSOs by analyzing that the flexibility range for different operating conditions is suitable for the envisioned TSO needs while keeping valid grid conditions for the distribution network. Furthermore, considering the single theoretical grid infrastructure presented in D6.6, both German and Italian optimization approaches could be jointly exploited, sharing outputs and feedbacks, allowing performing optimization analysis on a larger scale with a reasonable accuracy.

7. REFERENCES

[1] ENTSO-E, CEDEC, GEODE, EURELECTRIC and EDSO for Smart Grids. (2016, July). TSO-DSO data management report. ENTSO-E, CEDEC, GEODE, EURELECTRIC and EDSO for Smart Grids.

[2] DIgSILENT, PowerFactory, DIgSILENT GmbH, Gomaringen, 2016. Available: http://www.digsilent.de

[3] Integral, FGH e.V., Forschungsgemeinschaft für Elektrische Anlagen und Stromwirtschaft e.V., Mannheim, Available: http://www.fgh.rwth-aachen.de/www/cms/front_content.php?idcat=34

[4] R. D. Zimmerman und C. E. Murillo-Sanchez, „Matpower 6.0: User's Manual“, Power Systems Engineering Research Center (PSerc), Dez. 2016

[5] J. Hoffmann und U. Brunner, *Matlab und Tools: Für die Simulation dynamischer Systeme*. München: Addison-Wesley, 2002

[6] L. Thurner, A. Scheidler, F. Schäfer et al, pandapower - an Open Source Python Tool for Convenient Modeling, Analysis and Optimization of Electric Power Systems, IEEE Transactions on Power Systems, 2018.

[7] R. Fourer, D. M. Gay und B. W. Kernighan, „A Modeling Language for Mathematical Programming“, *Management Science*, Jg. 36, Nr. 5, S. 519–554, 1990

[8] Anaconda Distribution, Available: https://www.anaconda.com/distribution/Python

[9] R. H. Byrd, J. Nocedal, and R. A. Waltz, “Knitro: An Integrated Package for Nonlinear Optimization,” in Nonconvex Optimization and Its Applications, vol. 83, Large-Scale Nonlinear Optimization, G. Pillo and M. Roma, Eds., Boston, MA: Springer Science+Business Media Inc, 2006, pp. 35–59

[10] D. S. Stock, „Entwicklung eines flexiblen Optimierungswerkzeuges zur nichtlinearen mathematischen Mehrzieloptimierung in der Netzführung und Netzplanung“. Zugl. Dissertation, Leibniz Universität Hannover; 2019

[11] G. Pillo und M. Roma, Hg., Large-scale nonlinear optimization. Springer, 2006

[12] R. A. Waltz, J. L. Morales, J. Nocedal und D. Orban, „An interior algorithm for nonlinear optimization that combines line search and trust region steps“, Math. Program., Jg. 107, Nr. 3, S. 391–408, 2006

[13] R. H. Byrd, M. E. Hribar und J. Nocedal, „An interior point algorithm for large scale nonlinear programming“, *SIAM Journal on Optimization*, S. 9, 1999

[14] R. H. Byrd, N. I. M. Gould, J. Nocedal und R. A. Waltz, „On the Convergence of Successive Linear-Quadratic Programming Algorithms“, *SIAM J. Optim.*, Jg. 16, Nr. 2, S. 471–489, 2005

[15] R. H. Byrd, N. I.M. Gould, J. Nocedal und R. A. Waltz, „An algorithm for nonlinear optimization using linear programming and equality constrained subproblems“, *Math. Program.*, Jg. 100, Nr. 1, 2003

[16] A. Sillaber, Leitfaden zur Verteilnetzplanung und Systemgestaltung: Entwicklung dezentraler Elektrizitätssysteme. Wiesbaden: Springer Vieweg, 2016

[17] VDE e.V. Forum Netztechnik/Netzbetrieb, „Planungsgrundsätze für 110-kV-Netze: VDE-AR-N 4121“, VDE, Berlin

[18] H.-C. G. Maurer, Integrierte Grundsatz- und Ausbauplanung für Hochspannungsnetze. Zugl.: Aachen, Techn. Hochsch., Diss., 1. Aufl. Aachen: Klinkenberg, 2004

[19] Verband der Netzbetreiber - VDN - e.V. beim VDEW, „TransmissionCode 2007: Netz- und Systemregeln der deutschen Übertragungsnetzbetreiber“, Berlin, Aug. 2007

[20] V. H. Quintana, G. L. Torres and J. Medina-Palomo, “Interior-point methods and their applications to power systems: a classification of publications and software codes,” in IEEE Trans. on Power Systems, vol.15, no. 1, pp. 170-176, 2000

[21] B. Jacob, G. Guennebaud et al., Eigen: a C++ template library for linear algebra and related numerical algorithms. [Online] http://eigen.tuxfamily.org/index.php?title=Main_Page#Overview

[22] V. Miranda and N. Fonseca, “EPSO – Best-of-Two-Worlds Meta-Heuristic Applied to Power System Problems”, in Proc. of the 2002 Congress on Evolutionary Computation (CEC'02), Honolulu, USA, 2002

[23] V. Miranda, H. Keko and A. Jaramillo. (2007) EPSO: Evolutionary Particle Swarms. In: Jain L.C., Palade V., Srinivasan D. (eds) Advances in Evolutionary Computing for System Design. Studies in Computational Intelligence, vol 66. Springer, Berlin, Heidelberg

[24] R.D. Zimmerman, C.E. Murillo-Sánchez and R.J. Thomas, “MATPOWER: Steady-State Operations, Planning and Analysis Tools for Power Systems Research and Education,” in IEEE Trans. on Power Systems, vol. 26, no. 1, pp. 12-19, 2011

[25] W. F. Tinney and C. E. Hart, “Power Flow Solution by Newton’s Method,” in IEEE Trans. on Power Apparatus and Systems, vol. PAS-86, no. 11, pp. 1449–1460, 1967

[26] C. Grigg et al., “The IEEE Reliability Test System 1996. A report prepared by the reliability test system task force of the application of probability methods subcommittee,” in IEEE Trans. on Power Systems, vol. 14, no. 3, pp. 1010-1020, 1999

[27] C. Barrows et al., Reliability Test System - Grid Modernization Lab Consortium, (2017), GitHub repository. [Online] https://github.com/GridMod/RTS-GMLC

[28] D. Moneta, C. Carlini, G. Viganò, D. Stein and L. Consiglio, "Voltage control of active MV networks integrating RES and storage units: Advanced algorithm and lab tests," *IEEE PES Innovative Smart Grid Technologies, Europe*, Istanbul, 2014, pp. 1-6

[29] Norme CEI 0-16 e 0-21, “Reference technical rules for the connection of active and passive consumers to the HV and MV electrical networks of distribution Company”, April 2019, https://www.ceinorme.it/it/norme-cei-0-16-e-0-21.html

[30] M. Rossi, G. Viganò, D. Moneta, M. T. Vespucci and P. Pisciella, "Fast estimation of equivalent capability for active distribution networks," in *CIRED - Open Access Proceedings Journal*, vol. 2017, no. 1, pp. 1763-1767, 10 2017

[31] EU-SysFlex project, 2018. http://eu-sysflex.com/documents/

[32] Fingrid Oyj., ”The technical requirements and the prequafilication process of Frequency Containment Reserves (FCR)”, [Online], Available: https://www.fingrid.fi/globalassets/dokumentit/en/electricity-market/reserves/appendix3---technical-requirements-and-prequalification-process-of-fcr.pdf

[33] Stroe, D.-I., Swierczynski, M., Stan, A.-I., Teodorescu, R., Andreasen, S.J.: “Accelerated Lifetime Testing Methodology for Lifetime Estimation of Lithium-Ion Batteries Used in Augmented Wind Power Plants”IEEE Trans. Ind. Appl., 2014, 50, (6), pp. 4006–4017

[34] Stroe, D.-I., Swierczynski, M., Stroe, A.-I., Laerke, R., Kjaer, P.C., Teodorescu, R.: “Degradation Behavior of Lithium-Ion Batteries Based on Lifetime Models and Field Measured Frequency Regulation Mission Profile”IEEE Trans. Ind. Appl., 2016, 52, (6), pp. 5009–5018

[35] Fingrid open data: https://data.fingrid.fi/en/

[36] Fingrid Oyj., "Application instructions for the maintenance of frequency controlled reserves", [Online], 2018, Available: https://www.fingrid.fi/globalassets/dokumentit/en/electricity-market/supply-security-of-electricity/taajuusohjattujen-reservien-yllapidon-sovellusohje-1.1.2018_eng.pdf

8. COPYRIGHT

This project has received funding from the European Union's Horizon 2020 research and innovation programme under EC-GA No 773505.